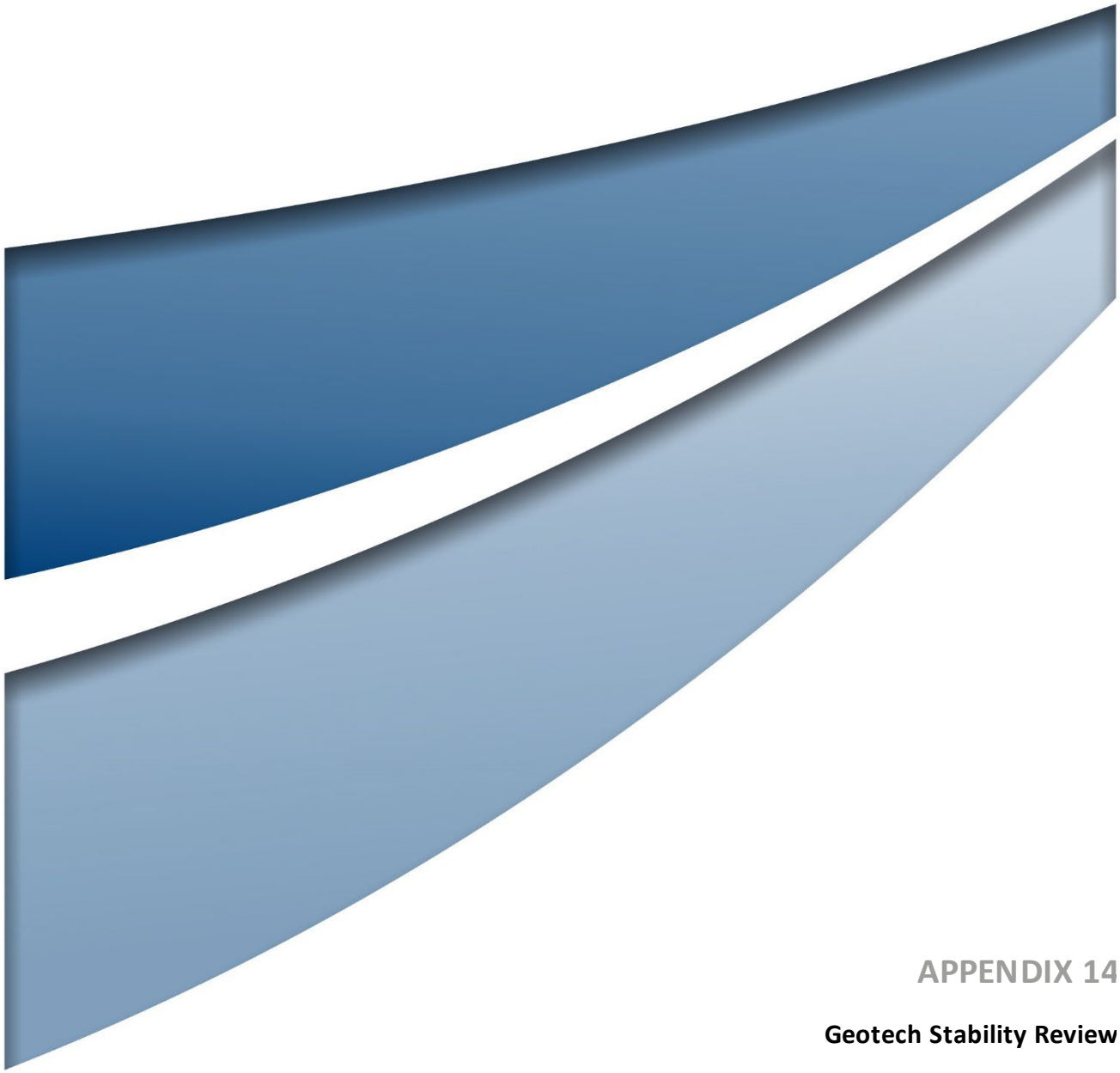

APPENDIX 14

Geotech Stability Review

Stone Ridge Quarry

Geotechnical Stability Review

Australian Resource Development Group Pty Limited

26 May 2023

The Power of Commitment

GHD Pty Ltd | ABN 39 008 488 373
GHD Tower, Level 3, 24 Honeysuckle Drive
Newcastle, New South Wales 2300, Australia
T +61 2 4979 9999 | **F** +61 2 9475 0725 | **E** ntlmail@ghd.com | **ghd.com**

Document status

Status Code	Revision	Author	Reviewer		Approved for issue		
			Name	Signature	Name	Signature	Date
S4	0	T Mok	S Narendranathan		A Sneddon		25/10/22
S4	1	T Mok	S Narendranathan		A Sneddon		01/11/22
S4	2	T Mok	S Narendranathan		A Sneddon		10/11/22
S4	3	T Mok	S Narendranathan		A Sneddon		26/05/23

Executive summary

This Geotechnical Stability Review report presents the geotechnical stability performance of the proposed Stone Ridge Quarry and has been prepared as part of the Environmental Impact Assessment (EIS) requirements to obtain approval for a Development Application that satisfies the Secretary's Environmental Assessment Requirements (SEARs).

This report is subject to, and must be read in conjunction with, the limitations set out in section 1.4 and the assumptions and qualifications contained throughout the Report.

This report relied on geological reference material, drilling campaign logs, surface topography, and past reports related to the proposed Stone Ridge Quarry Project, as provided by the Client.

This geotechnical assessment evaluates the long-term stability of the proposed quarry batters and considers both kinematically (structurally) controlled and rock mass controlled (overall) stability. The stability analyses are supported by geological reference material, drilling campaign logs, surface topography, and past reports related to the proposed Stone Ridge Quarry Project, as provided by the Client.

The kinematic assessment takes into consideration the orientation of the quarry walls relative to the mapped geological structures as per the available drilling data and was undertaken to assess and inform the minimum batter-berm configuration of the quarry. Stability analyses have also been undertaken to assess the overall long-term stability of slopes with additional sensitivity assessments undertaken to assess the stability implications of seismic events, elevated phreatic conditions and the influence of final pit lake level.

The proposed pit geometry analysed for the geotechnical assessment is as follows:

– The total depth of extraction is expected to be approximately 95 m below the current surface level of approximately +78 m AHD, with the proposed floor and sump at -2 m AHD and -17 m AHD respectively.
– Individual benches are to be formed at 15 m high with bench widths of 20 to 30 m.
– A nominal face angles of 70 degrees for individual benches.

A summary of the key outcomes of the stability assessment is as follows:

Kinematic Analyses

Planar Sliding

– Under expected conditions, north, east and south walls i.e., excavations within the northern, eastern and southern domain, are comparatively more sensitive to planar sliding than the western wall.
– The minimum calculated bench width with respect to critical sets and weathering grade was calculated (to the nearest metre) to be 16 m.
– In general, the FoS increases and the PoF decreases where the degree of weathering decreases.
– Note that potentially larger volumes are calculated along the east wall.

Tetrahedral Wedge Sliding

– Under expected conditions, south and west walls were calculated to be comparatively more sensitive (PoF > 50%) to tetrahedral wedge sliding compared to other walls.
– The minimum calculated bench width with respect to critical sets and weathering grade was calculated (to the nearest metre) to be 13 m.
– In general, the FoS increases and the PoF decreases where the degree of weathering decreases.
– The volume of instability was calculated to be of limited scale/volume where good blasting and scaling practices are employed.

Rock Toppling

– Where the spacing of toppling joints occurs in the range of 0.8 m to 0.85 m or less, the likelihood of toppling becomes notably higher as the calculated FoS falls below 1.2 for all stratigraphic units.

A minimum bench width of 16 m is required to ensure there is adequate catch capacity to retain potentially dislodged material to a single bench. The proposed Stone Ridge Quarry pit design incorporates 20 to 30 m benches at the individual bench scale, which satisfies the minimum bench width requirements.

Slope Stability Analyses

– Under 'expected' conditions The stability performance at individual batters and overall slope scales satisfy the nominated DAC for stability Sections S1, S2 and S3 .

Seismic Loading

– Under a 1:500 year seismic loading event, the stability performance was calculated to satisfy the design performance objectives.

Elevated Phreatic Conditions

– A reduction in the slope stability performance was calculated under 'worst case' fully saturated conditions compared to 'expected' condtions.
    - At the overall slope scale the stability performance was calculated to be above unity (FoS > 1) for all stability sections.

Influence of Final Pit Lake Level

– The stability performance of rehabilitated slopes, incorporating a recovered pit lake, along Sections S1, S2 and S3 were calculated to satisfy the Design Acceptance Criteria associated to the "Serious Consequence of Failure" category when considering the overall slope scale.

Potential Erodibility of Terminal Slopes

As part of the geotechnical assessment, preliminary erodibility assessments were carried out for the proposed rehabilitation concept. Key outcomes of the erosion assessment is as follows:

– The erosion potential of the excavated batters is considered 'Very Low' (< 150 t/ha/yr – Criterion 1) and satisfies the Commonwealth (2016) (Criterion 2) guidelines after ~20 months of perennial grass coverage.
– The susceptibility to erosion within these units is largely controlled by the topographic factor and ability to apply cover. Erosion in these areas is expected to be ongoing which is likely to result in some minor sloughing of the excavated face. It is anticipated that in the long-term, erosion of these faces would not pose a significant geotechnical risk.

In summary, under 'expected' conditions, the proposed slope configuration is sufficient for catching and retaining potential dislodged material of structurally controlled deposits at Stone Ridge Quarry. Furthermore, the proposed slope design geometry is sufficient for maintaining stability performance at overall slope scale for the critical sections analysed, with Factors of Safety greater than 1.5 calculated for all stability sections. As such, the proposed slope design geometry is considered suitable for geotechnical stability.

Contents

Table index

Figure index

1. Introduction

1.1 General

GHD has been requested by Australian Resource Development Group Pty Limited (the Client) to undertake a geotechnical stability assessment for the proposed development of the Stone Ridge Quarry (the site), located in Wallaroo State Forest, Balickera, New South Wales. It is understood ARDG is preparing an Environmental Impact Statement (EIS) to the Department of Planning and Environment (DPE) to obtain approval for a Development Application that satisfies the Secretary's Environmental Assessment Requirements (SEARs).

The proposed development relates to a hard rock quarry that is a mixture of igneous and sedimentary rock units. It is understood the proposed development will extract approximately 1.5 million tonnes per annum with an expected quarry life of up to 30 years.

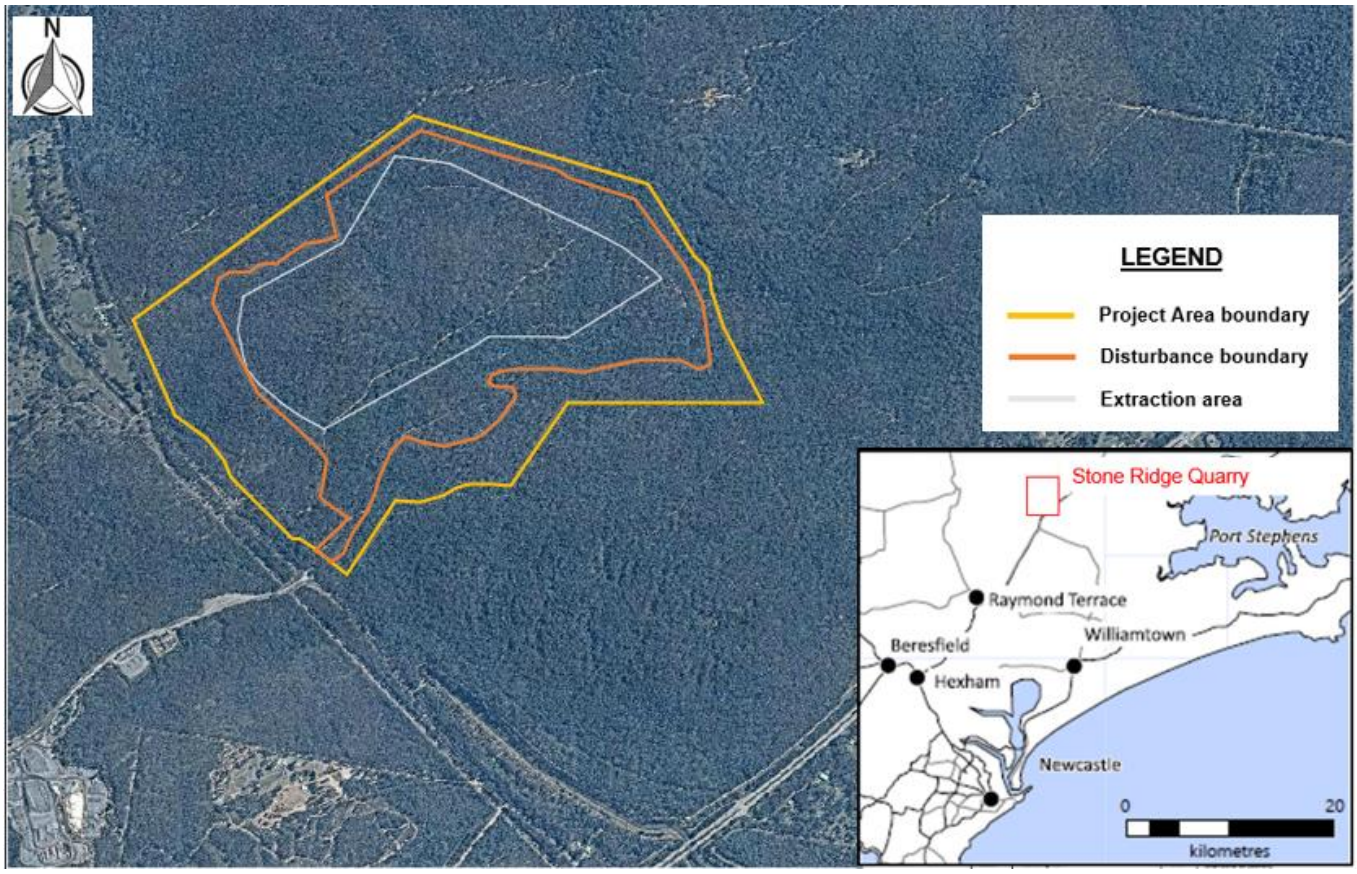

Figure 1.1 Plan View of Stone Ridge Quarry Depicting Proposed Extraction Area

1.2 Client Objectives

GHD understands ARDG's primary objective is to obtain development consent from the Department of Planning and Environment to proceed with development of Stone Ridge Quarry. The Secretary's Environmental Assessment Requirements (SEARs) for the Project require the EIS to include:

– A preliminary geotechnical assessment to identify the likely long-term stability risks and the measures that will be required to minimise potential risks to public safety.
– Potential impacts on landforms (topography) and long-term geotechnical stability of any new landforms.
– Potential impacts on soils and land capability, i.e., including potential erosion.

This geotechnical assessment report has been prepared to address the above aspects of the SEARs.

1.3 Scope of Work

The geotechnical assessment report (this report) includes:

- A summary of the methodology
- Limit equilibrium stability analysis results
- Kinematic assessment from the field mapping
- Soil erodibility assessment results
- An assessment of long-term stability of the proposed rehabilitation
- Recommendations on safe and stable batter profiles / geometries within the overburden (if any) and resource units
- Outline of recommendations as applicable for requirements in relation to slope / batter movement monitoring during profiling works to the proposed design

1.4 Limitations

This report has been prepared by GHD for Australian Resource Development Group Pty Limited and may only be used and relied on by Australian Resource Development Group Pty Limited for the purpose of supporting an Environmental Impact Statement for a State Significant Infrastructure project application.

GHD otherwise disclaims responsibility to any person other than Australian Resource Development Group Pty Limited arising in connection with this report. GHD also excludes implied warranties and conditions, to the extent legally permissible.

The services undertaken by GHD in connection with preparing this report were limited to those specifically detailed in the report and are subject to the scope limitations set out in the report.

The opinions, conclusions and any recommendations in this report are based on conditions encountered and information reviewed at the date of preparation of the report. GHD has no responsibility or obligation to update this report to account for events or changes occurring subsequent to the date that the report was prepared.

The opinions, conclusions and any recommendations in this report are based on assumptions made by GHD described in this report. GHD disclaims liability arising from any of the assumptions being incorrect.

GHD has prepared this report on the bases of information provided by Australian Resource Development Group Pty Limited and others who provided information to GHD (including government authorities), which GHD has not independently verified or checked beyond the agreed scope of work. GHD does not accept liability in connection with such unverified information, including errors and omissions in the report which were caused by errors or omissions in that information.

The opinions, conclusions and any recommendations in this report are based on information obtained from, and testing undertaken at or in connection with, specific sample points. Site conditions at other parts of the site may be different from the site conditions found at the specific sample points.

Investigations undertaken in respect of this report are constrained by the particular site conditions, such as the location of buildings, services and vegetation. As a result, not all relevant site features and conditions may have been identified in this report.

Site conditions (including the presence of hazardous substances and/or site contamination) may change after the date of this Report. GHD does not accept responsibility arising from, or in connection with, any change to the site conditions. GHD is also not responsible for updating this report if the site conditions change.

1.5 Information relied upon

We have relied upon the following sources of information for the assessment detailed in this report. Relevant information was extracted from the following documents:

- Surface Topography in MapInfo and Discover3D
- Drilling campaign, 15 diamond drill holes, extending up to -56 m AHD, DDH 9 to 14 include ATV logs

- Aerial magnetic survey
- Surface geological mapping from the Client
- Geology Reference Material provided by the Client, as follows:
  - Hunter District Water Board (1957). Report on Geology of Balickera Tunnel Site
  - Rattigan (1966). The Balickera Section of the Carboniferous Kuttung Facies, New South Wales
  - Pells Consulting (2015). Balickera Tunnel Remediation
- Laboratory test results on rock core
- JBA (2017) Report titled “State Significant Development Application – Environmental Impact Statement – Eagleton Quarry – Barleigh Ranch Way”
- Australian Resource Development Group Pty Limited (2020). Proposed Stone Ridge Quarry Project – Scoping Report. Wallaroo State Forest No. 781

2. Background

2.1 General

The Site is located to the south-west of the Wallaroo State Forest at Balickera, approximately 25 km north of Newcastle, New South Wales. The location of the site is presented in Figure 2.1.

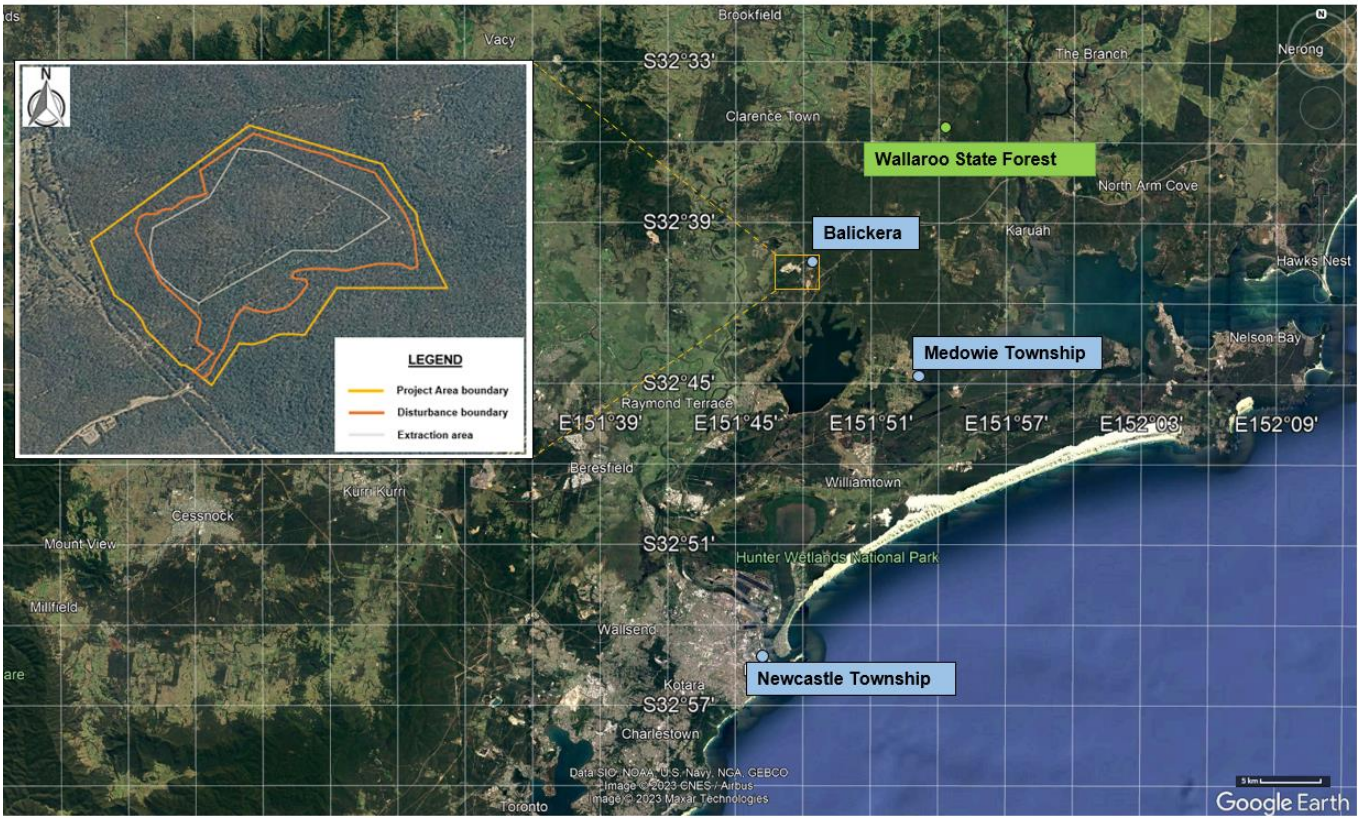

Figure 2.1 Approximate Location of Stone Ridge Quarry

The Stone Ridge Quarry is seeking planning for approval to be operational for up to 30 years and covers an approximate disturbance footprint area of 79 Ha. The primary resource to be extracted is associated with volcanic rocks, predominantly rhyodacite, which is expected to be uniform. The resource is suited to the production of concrete, sealing and asphalt aggregates, gabion, armour rock, ballast, road base and crushed rock products.

Access to the proposed quarry will be via Italia Road (two-lane road used by heavy vehicles) which connects to the Pacific Highway, located to the south and southeast of the project.

The Wallaroo State Forest extends to the north and east of the proposed development, and comprises three separate areas of land, that combined exceed 300 Ha. The Boral Seaham Quarry, located to the southwest, has operated for around 20 years. It is accessed via Italia Road.

The Balickera Channel, an open feature along most of its ~ 2.7 km length, is located to the west and south and transports water from the William's River to Grahamstown Dam. Balickera Tunnel is 1.2 km long.

Around the project area there are three main drainage catchment areas, Nine Mile Creek Catchment, Caswell Creek Catchment and Italia Road Catchment.

Vegetation cover within the proposed development is dominated by dry sclerophyll forest.

2.2 Regional and Local Geology

2.2.1 Regional Setting and Geological History

The first detailed historical geological assessment around the Stone Ridge Balickera area, between Seaham and the Pacific Highway, was undertaken in 1957 and documented in "*Report on Geology of Balickera Tunnel Site*" (Hunter Water Corporation, 1999) . Nine vertical diamond drill holes confirmed that the geology in the area is comprised of a sequence of Carboniferous aged sedimentary and volcanic rocks. This bedded sequence dips in a south easterly direction.

The sequence is represented by a basal sequence of conglomerate, tuff, and sandstone, overlain by volcanic lava flows. The volcanic rocks are overlain by a further sequence of basal conglomerate, sandstone and tuff, overlain by toscanitic lava, followed by interbedded conglomerate and indurated shales. These overlying units characterise the geology between the eastern end of the Balickera Tunnel and the Pacific Highway.

Geological and stratigraphic mapping was conducted in 1966, with the outcomes of the mapping investigation summarised in "*The Balickera Section of the Carboniferous Kuttung Facies, New South Wales*" (Royal Society of New South Wales, 1966). Based on this report, the Carboniferous stratigraphy was interpreted to dip 35 degrees southeast. The geology to the north of the site was characterised by volcanic rocks assigned to the Mosman Swamp Andesites Formation of which is in the lower part of the Gilmore Volcanic Group. The document reported, the Mosman Swamp Andesites Formation was overlain by the Eagleton Volcanics Formation (upper part of Gilmore Volcanic Group) (see Figure 2.2).

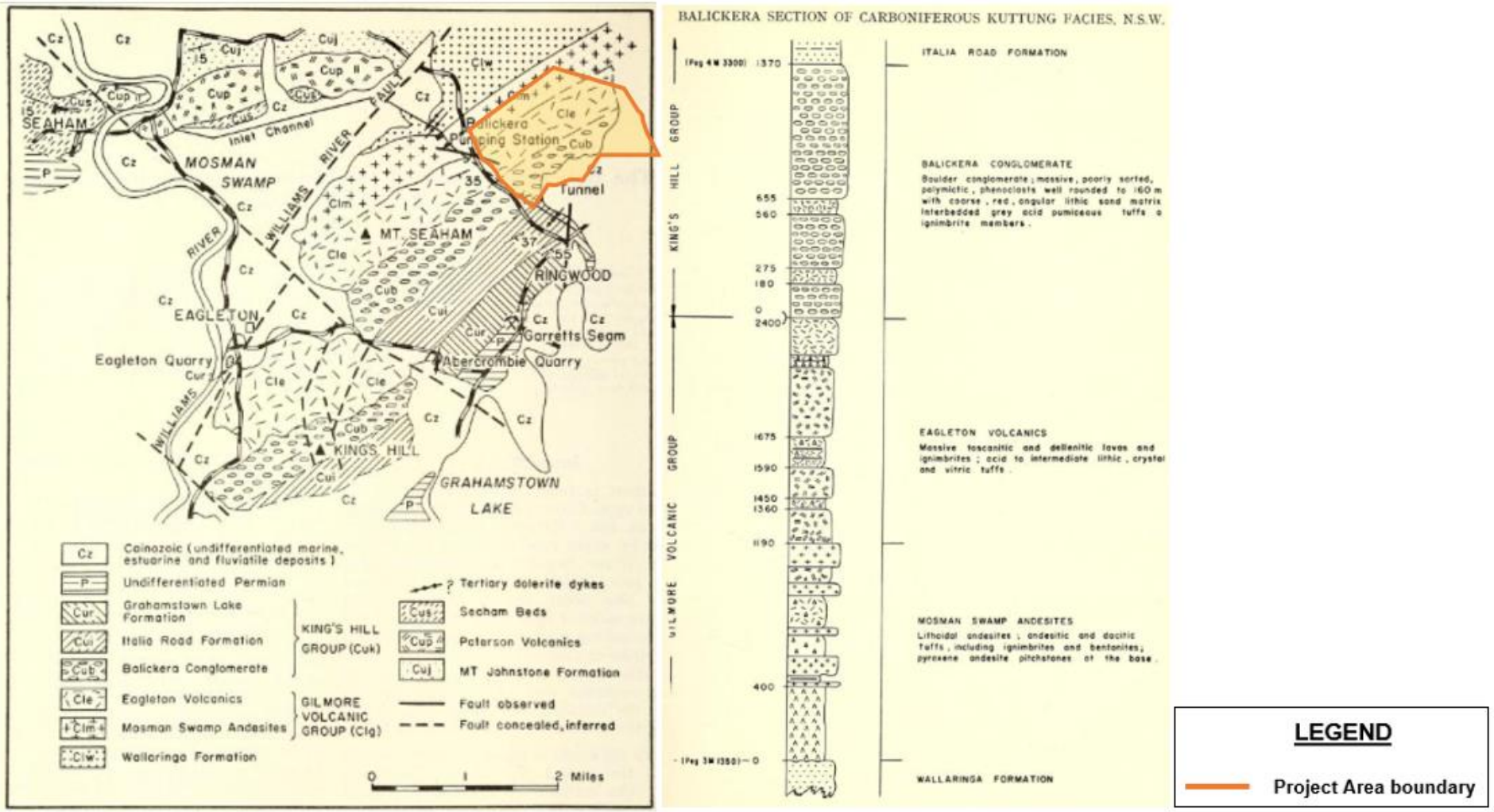

Figure 2.2 ***Geological map of the district about the Balickera excavations and Section through Balickera Conglomerate east of Balickera pumping station. Taken from Balickera Section of Carboniferous Kuttung Facies, (Royal Society of New South Wales, 1999)***

In 1992, a study within the Wallaroo State Forest was commissioned by FCNSW and the findings were summarised in the report "*Geological Study on the Feasibility of Establishing a Hardrock Quarry – Hamburger Hill, Wallaroo State Forest, Bulahdelah District*". As part of this study two diamond holes were drilled on the ridge line. Both diamond holes intersected competent rhyodacite close to surface.

The NSW Seamless Geology dataset presents a revised geological interpretation, with the geology previously assigned by Rattigan (1966) to the Mosman Swamp Andesites incorporated within the Eagleton Volcanics. The geology previously mapped as Balickera Conglomerate has now been assigned to the Mount Johnstone Formation. The lower part of the Mount Johnstone Formation is dominated by conglomerate, whereas the upper part of the formation is characterised by sandstone, shale and carbonaceous shale.

Local Geology

From the Client's report (2020) titled: '*Quarry Resource Assessment Investigations*', it was confirmed that the volcanic rocks encountered, mainly rhyodacite and dacite, comprised part of the Eagleton Volcanics Formation. The resource is uniform, and the overburden is close to non-existent (see Figure 2.3).

Within the area of the project, the Eagleton Volcanics comprise a bedded sequence of rocks that dip approximately 35 degrees to the southeast. Information from the diamond drilling, surface and downhole geophysics and surface mapping carried out from 2016 to 2019, indicated that the dominant and most relevant rocks are rhyodacitic and dacitic rocks. Mapping and petrographic assessment confirmed the existence of five major rock types: rhyodacite, dacite, rhyolitic vitric crystal welded tuff, volcanic breccia and andesitic lithic crystal tuff (see Figure 2.4).

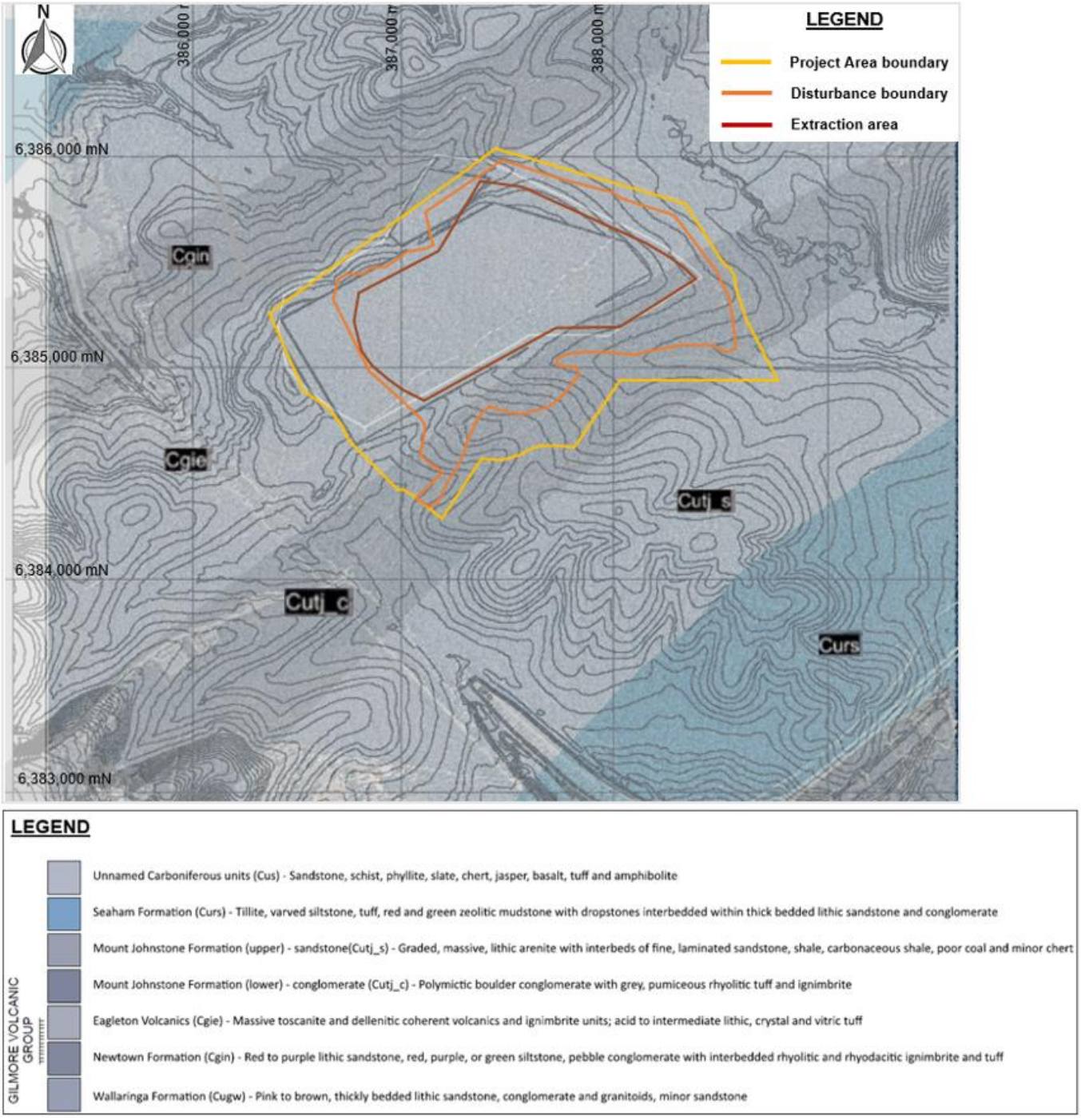

Figure 2.3 Regional Geology mapping

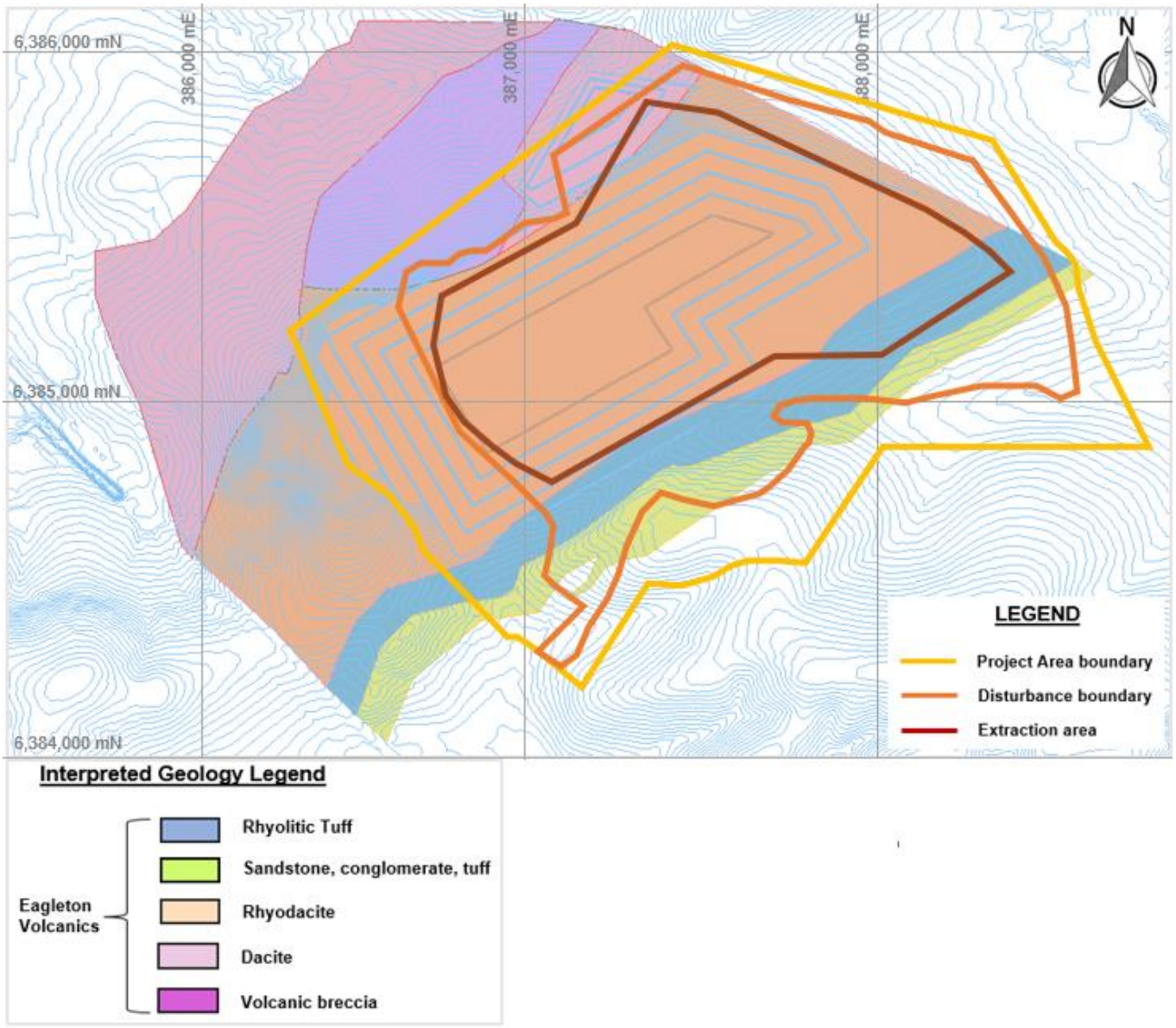

Figure 2.4 Interpreted geology of Stone Ridge Quarry Area (Provided by Australian Resource Development Group)

2.2.2 Outcrop Geology

In March 2017, preliminary geological mapping was carried out to confirm the characteristics of the dominant Eagleton Volcanics rock types based on surface outcrop exposures.

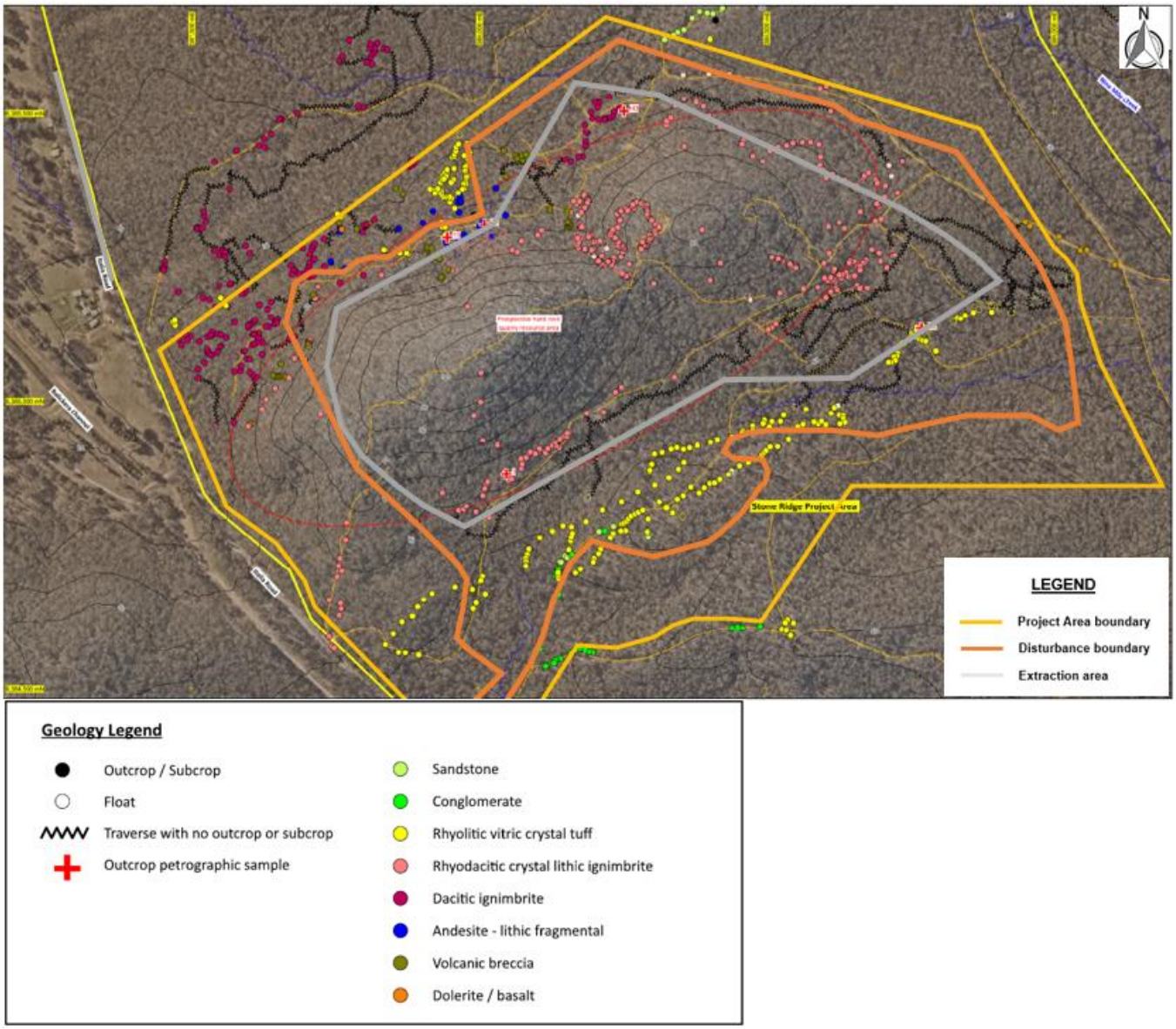

Figure 2.5 Geological Outcrop on Stone Ridge Area (Provided by Australian Resource Development Group)

The study confirmed that the flanks and crest of the site are characterised by extensive outcrop of rhyodacite. This varies from blocky rubble to broad sheet-like areas.

Figure 2.6 Rhyodacite outcrop on Stone Ridge (Provided by Australian Resource Development Group)

Initial outcrop mapping showed that rhyodacite and dacite are the dominant rock types with intermittent outcrops of finer grained volcanic rocks of rhyolite or rhyodacite composition.

In gullies on the northwest slopes of the site, weathered exposures of volcanic breccia were observed. Additionally, a minor sub-crop and float was observed to the northwest flank of the site and was confirmed to be lithic crystal tuff of andesitic composition. This was encountered immediately below the base of rhyodacite.

Figure 2.7 Volcanic Breccia in washout gully on Stone Ridge (Provided by Australian Resource Development Group)

2.2.3 Drilling Campaign

Based on the information provided by the Client, a total of 16 Diamond Drill Holes (DDHs) were drilled by Blacklaws Drilling Pty Ltd in the vicinity of the Site. The geotechnical investigation was conducted in two stages during 2018 and 2019. A summary of the drilling information is provided in Table 2.1, and the locations of the drill holes are presented in plan view in Figure 2.8.

Table 2.1 Drillhole Summary after Blacklaws Drilling Pty Ltd (2018 & 2019)

Bore ID	Easting	Northing	Elevation (mAHD)	Drill Depth (m)	Azimuth (°)	Dip (°)
ARDG-DDH01	388,571	6,385,233	50.5	50.5	320	-60
ARDG-DDH02	388,580	6,385,481	26.4	26.4	315	-60
ARDG-DDH03	388,252	6,385,440	71.8	71.8	315	-60
ARDG-DDH04	388,369	6,385,188	130.4	130.4	330	-60
ARDG-DDH05	388,543	6,385,091	98.9	98.9	317	-60
ARDG-DDH06	388,277	6,384,906	78.2	78.2	322	-60
ARDG-DDH07	387,976	6,385,057	111.2	111.2	322	-60
ARDG-DDH08	387,981	6,385,306	117.3	117.3	322	-60
ARDG-DDH09	388,096	6,384,828	119.8	119.8	332	-57.9
ARDG-DDH10	388,258	6,385,009	120.5	120.5	322	-59.6
ARDG-DDH11	388,360	6,385,068	98.9	98.9	356	-60.6
ARDG-DDH12	388,683	6,385,162	114.3	114.3	315	-60
ARDG-DDH13	388,479	6,385,347	66.2	66.2	357	-60
ARDG-DDH14	388,719	6,385,286	104.2	104.2	360	-60
ARDG-DDH15	388,237	6,385,209	132.2	132.2	360	-60
ARDG-DDH16	388,063	6,385,145	100.0	141.3	346	-60

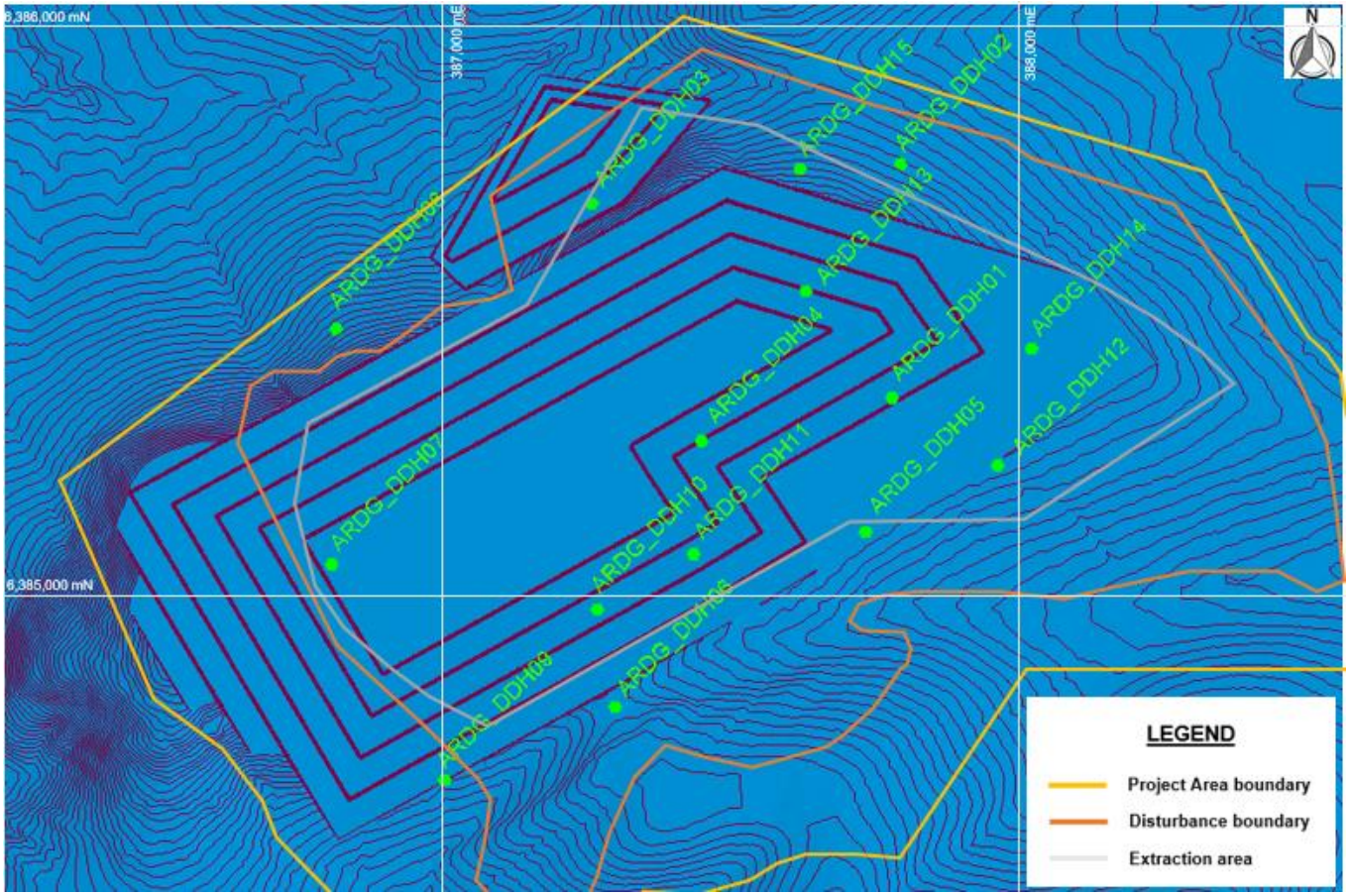

Figure 2.8 Location of Diamond Drill Hole Locations (

All core extracted during drilling was geotechnically logged for the following parameters to facilitate calculation of RMR_{89}, after Bieniawski (1989):

- Core Recovery and Rock Quality Designation (RQD)
- Lithology, degree of weathering, alteration types of strength class
- Defect (structure) type, number of defect sets and orientation information for the respective structure i.e., alpha and beta angles
- Defect plane characteristics (rough, smooth, stepped etc.) and infill type and thickness
- Groundwater conditions

2.2.4 Weathering

The Stone Ridge deposit is comprised predominantly of volcanic rhyodacite from the Eagleton Volcanics Formation, overlain by Quaternary aged soil (overburden/residual soil). The rhyodacite is characterised by varying degrees of weathering clearly demarcated by a weathering horizon. Accordingly, for this assessment, delineation of the stratigraphy has been done sympathetically to the observed weathering horizon using the ISRM (1981) classification, forming the basis for categorising materials with “similar” geotechnical characteristics. The ISRM (1981) classification is summarised in Table 2.2.

Table 2.2 Weathering Grades of Rock Mass after ISRM (1981)

Term	Symbol	Description	Grade
Fresh	FR	No visible sign of rock material weathering; perhaps slight discolouration on major discontinuity surfaces.	I
Slightly Weathered	SW	Discoloration indicates weathering of rock material and discontinuity may be somewhat weaker externally than in its fresh condition.	II
Moderately Weathered	MW	Less than half the rock material is decomposed and or disintegrated to a soil. Fresh or discoloured rock is present either as a continuous framework or as a corestones.	III
Highly Weathered	HW	More than half the rock material is decomposed and/or disintegrated to a soil. Fresh or discoloured rock is present either as a discontinuous framework or as a corestones.	IV
Extremely Weathered	EW	All rock material is decomposed and/or disintegrated to a soil, the original mass structure is still largely intact.	V
Residual Soil	RS	All rock mass fabric is converted to a soil. The mass structure and material fabric are destroyed. There is a large change in volume, but the soil has not been significantly transported	VI

Figure 2.9 graphically depicts the depth of weathering (i.e., the weathering profile) interpreted for each of the DDHs.

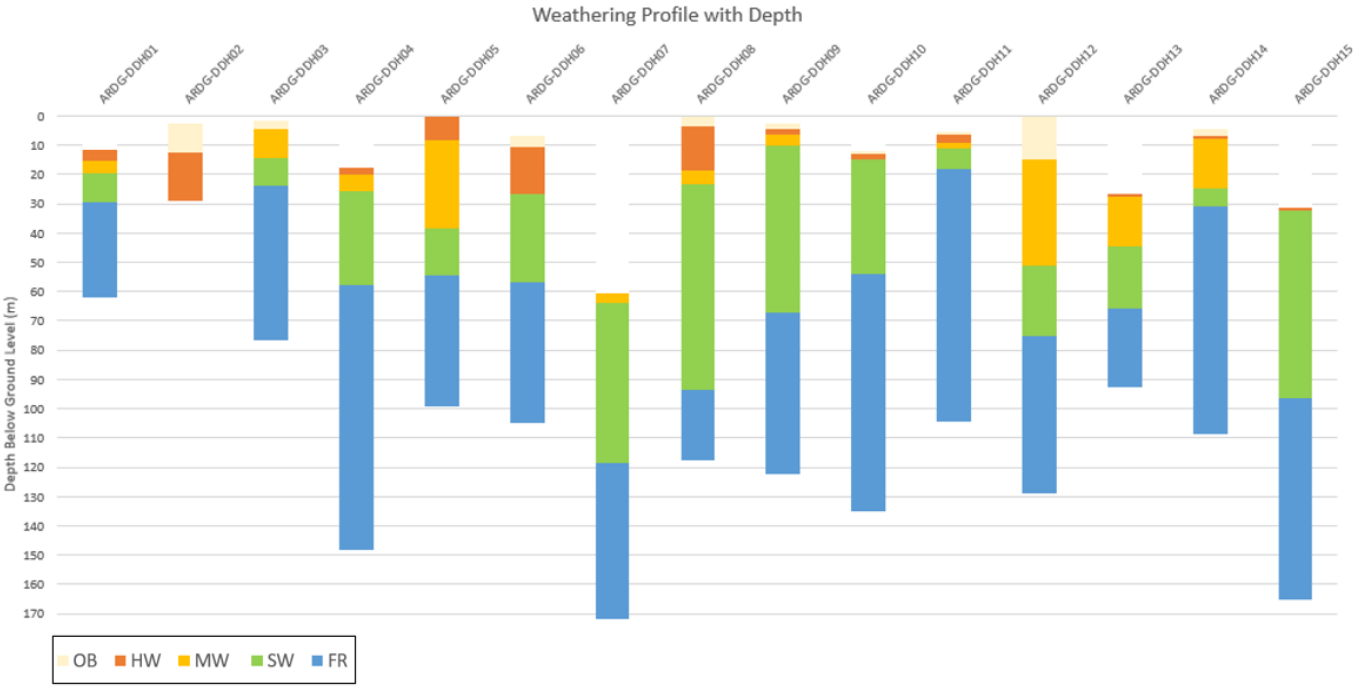

Figure 2.9 Weathering Profile with Depth

The weathering profiles interpreted from the boreholes are plotted as a downhole histogram in Figure 2.10 to Figure 2.24. Further discussion on the weathering profile and the use of weathering information in the development of the geological model is further discussed in Section 4.2 of the report.

Note that at six of the drilling locations, namely ARDG-DDH09 to ARDG-DDH14, Groundsearch Australia Pty was commissioned to undertake downhole geophysical surveys to obtain structural data (i.e., lithotype boundaries, anomalies, and fractures) using Acoustic Televiewer (ATV). The information obtained from this campaign was utilised to determine and interpret the rock mass strengths.

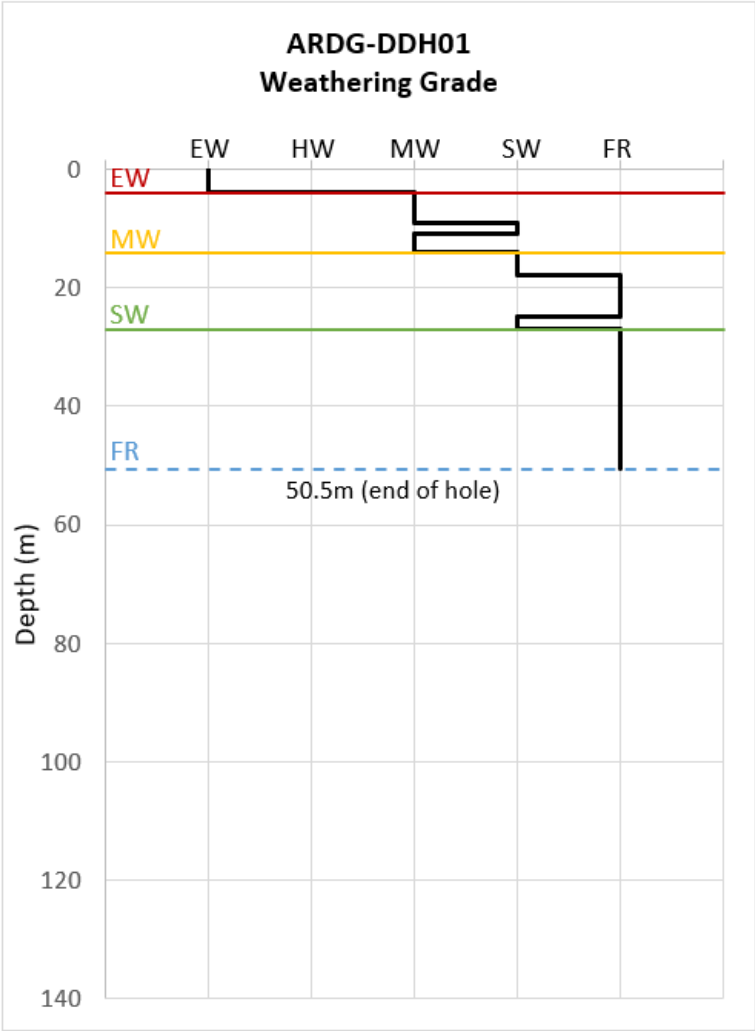

Figure 2.10 Weathering Profile – ARDG-DDH01

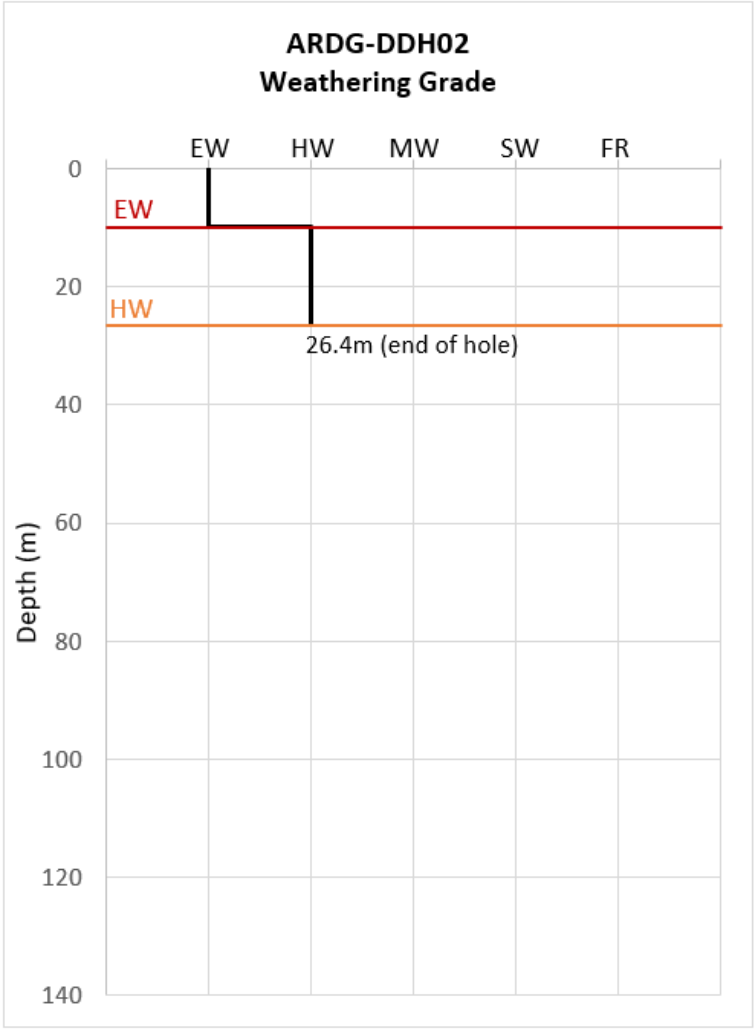

Figure 2.11 Weathering Profile – ARDG-DDH02

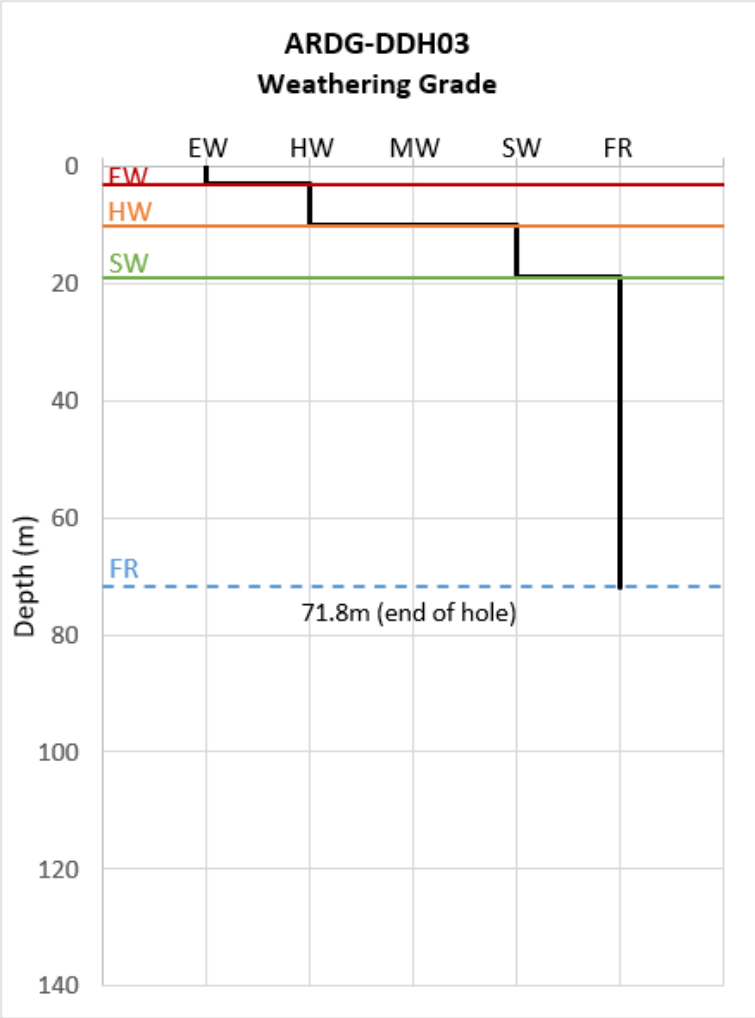

Figure 2.12 Weathering Profile – ARDG-DDH03

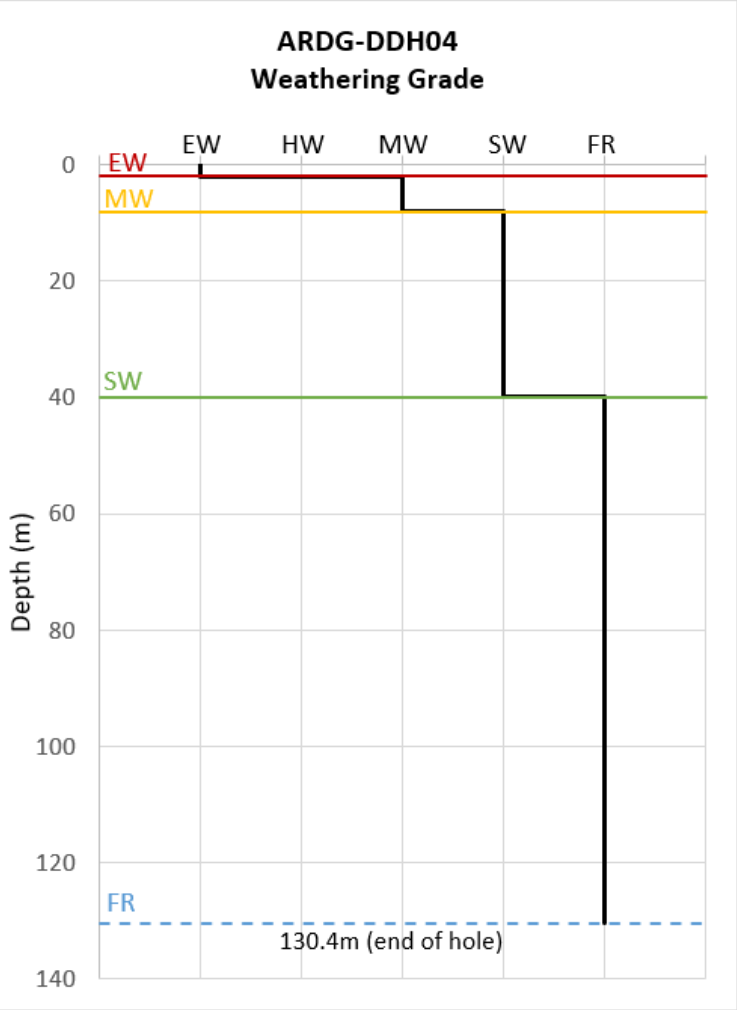

Figure 2.13 Weathering Profile – ARDG-DDH04

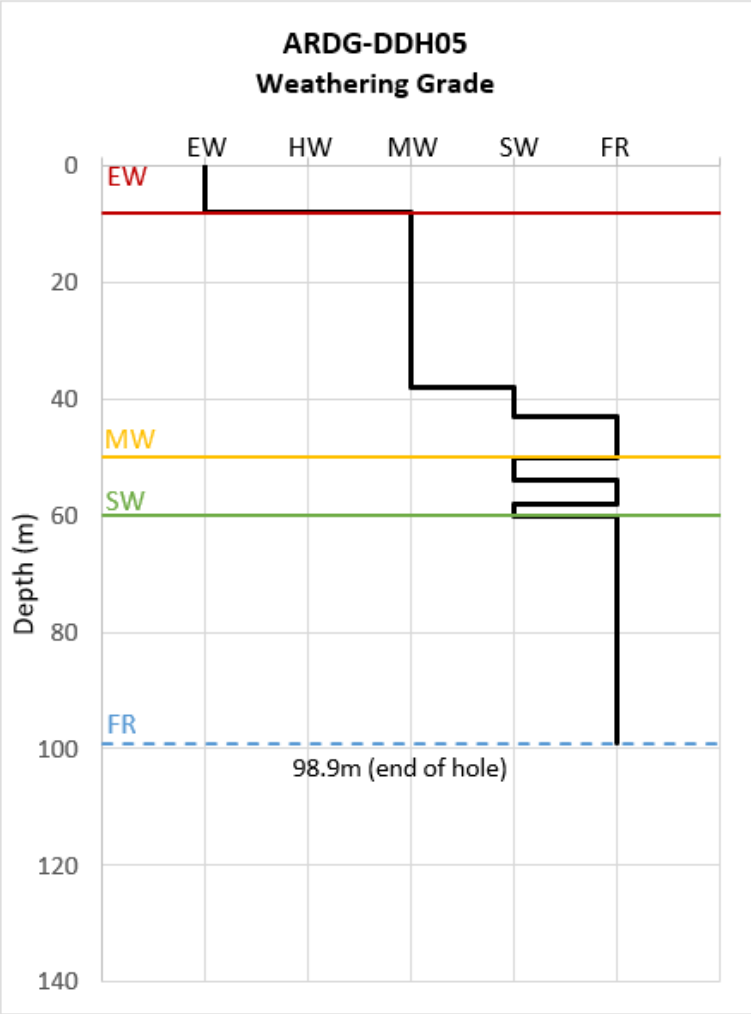

Figure 2.14 Weathering Profile – ARDG-DDH05

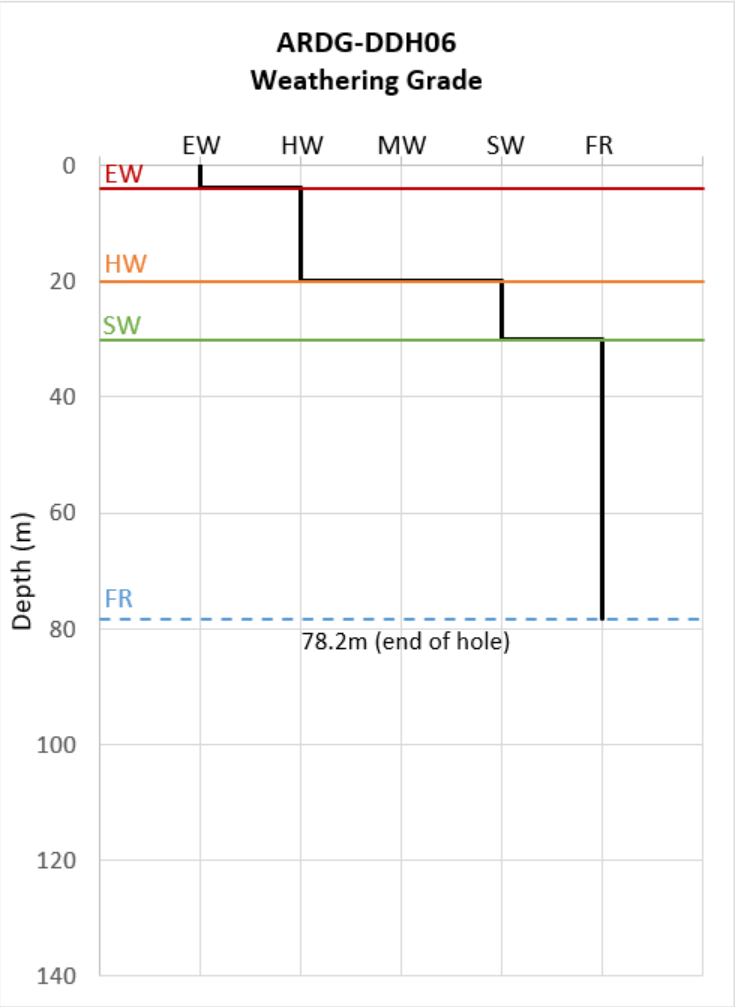

Figure 2.15 Weathering Profile – ARDG-DDH06

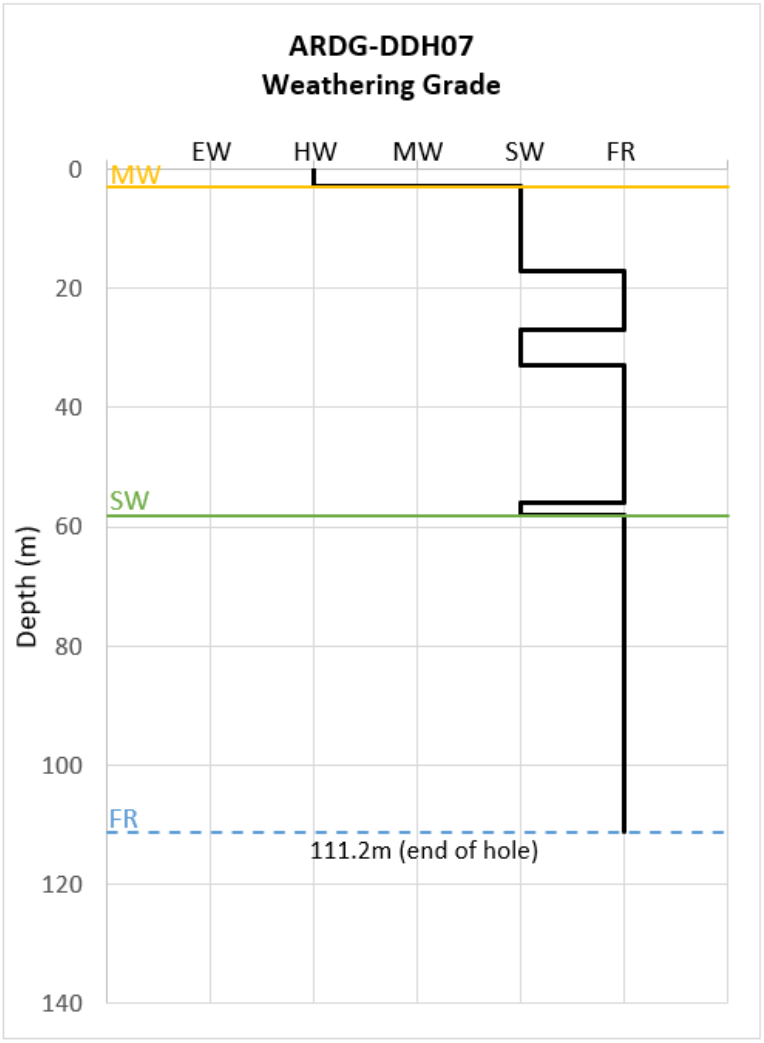

Figure 2.16 Weathering Profile – ARDG-DDH07

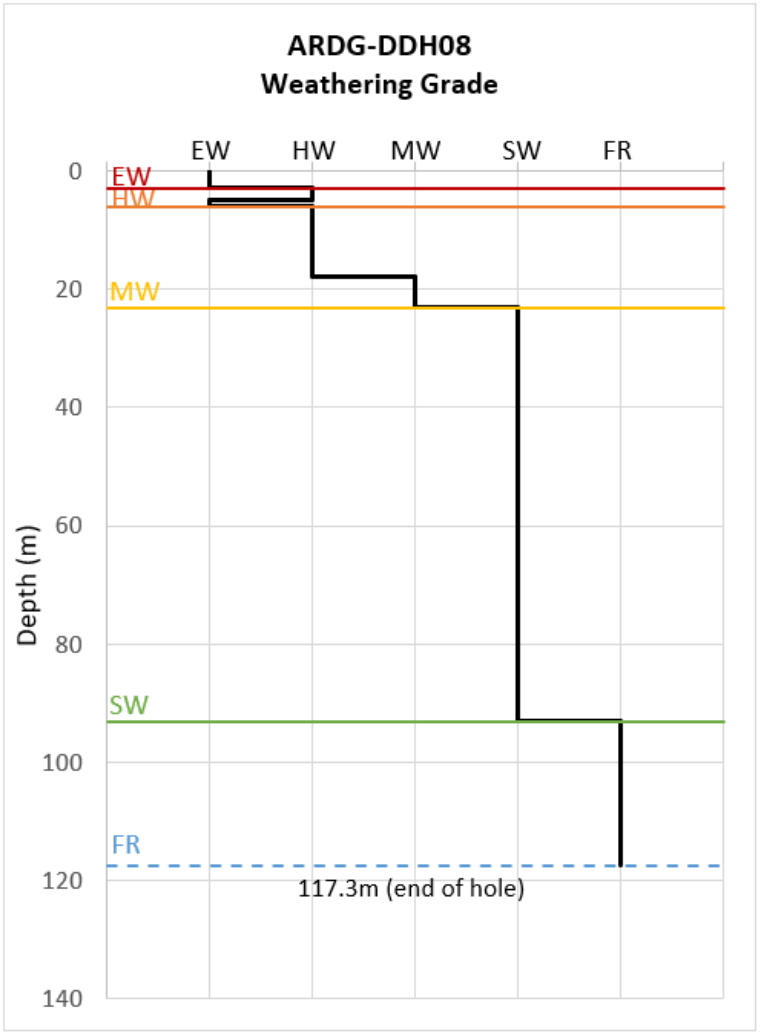

Figure 2.17 Weathering Profile – ARDG-DDH08

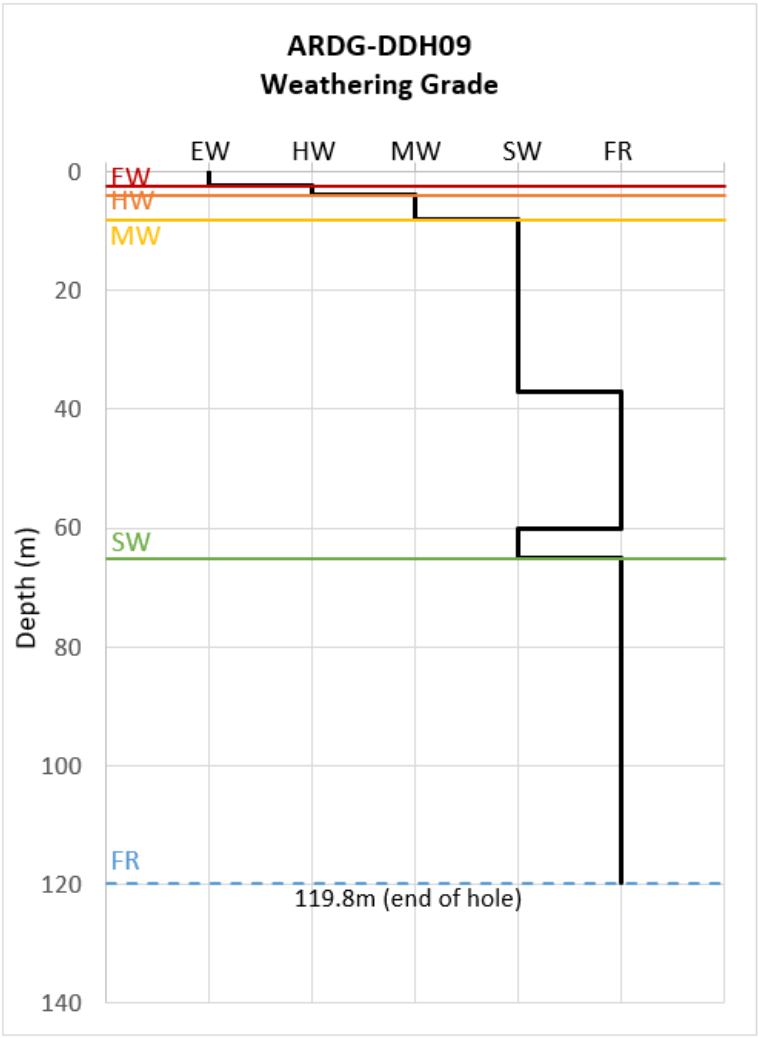

Figure 2.18 Weathering Profile – ARDG-DDH09

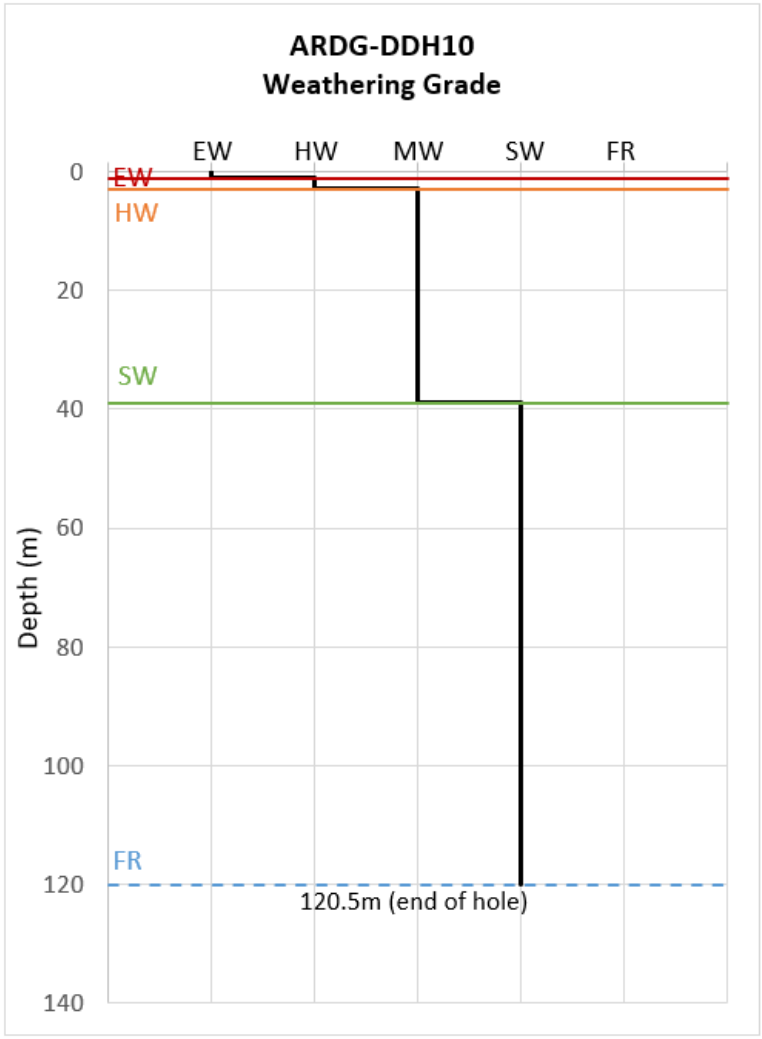

Figure 2.19 Weathering Profile – ARDG-DDH10

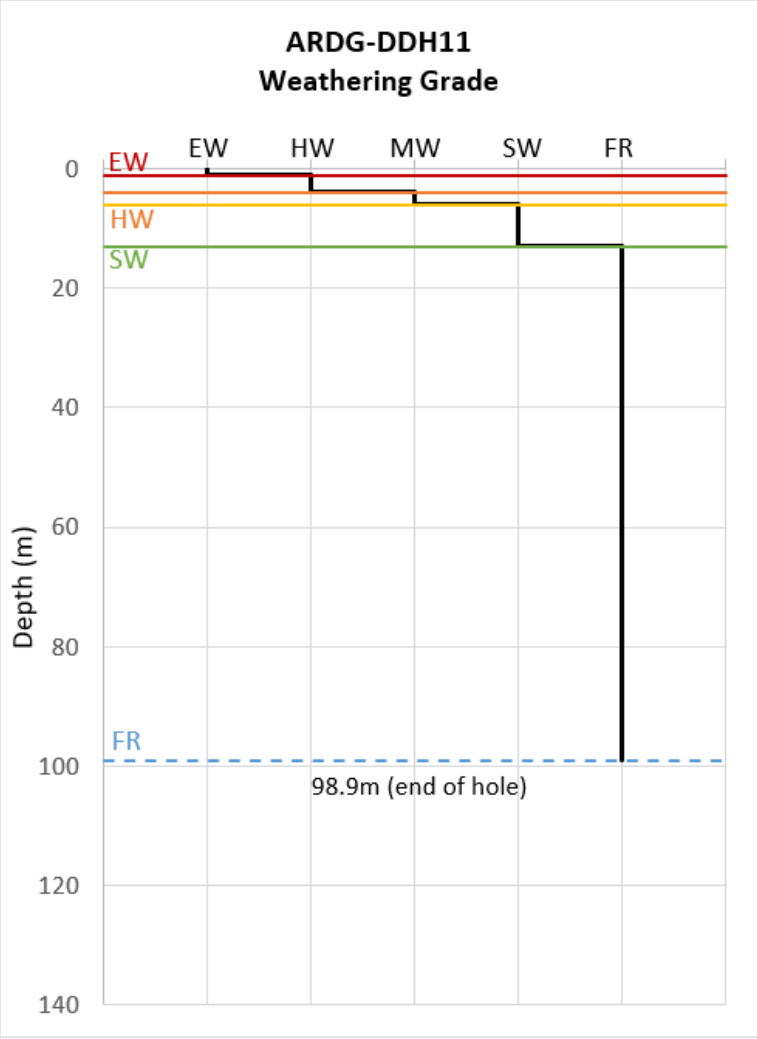

Figure 2.20 Weathering Profile – ARDG-DDH11

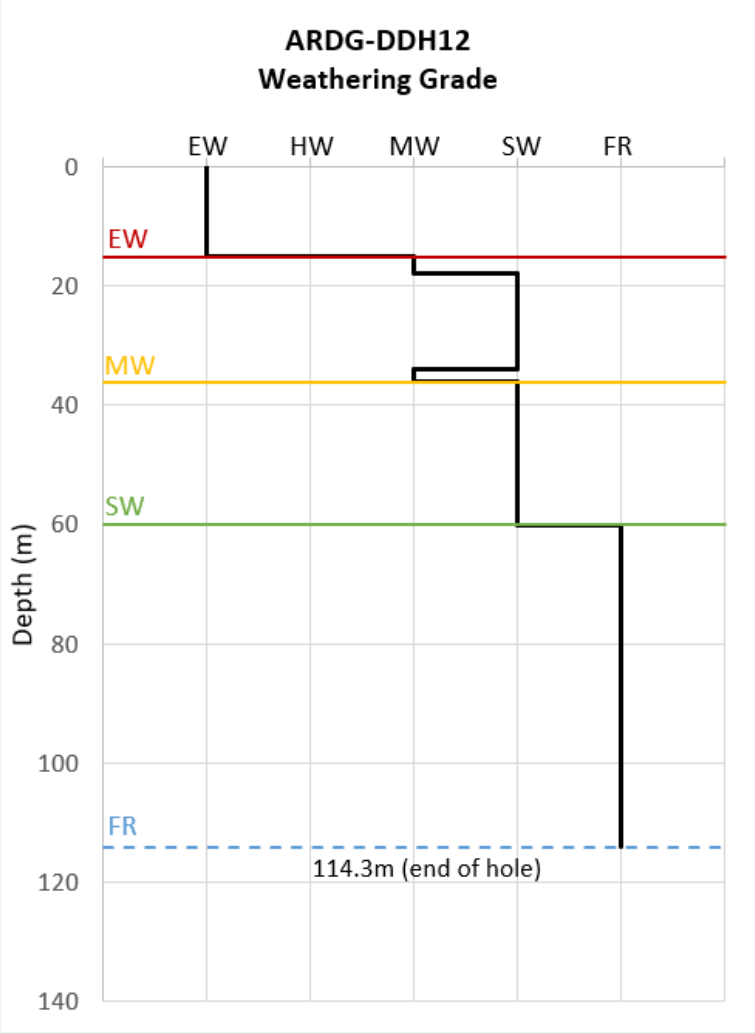

Figure 2.21 Weathering Profile – ARDG-DDH12

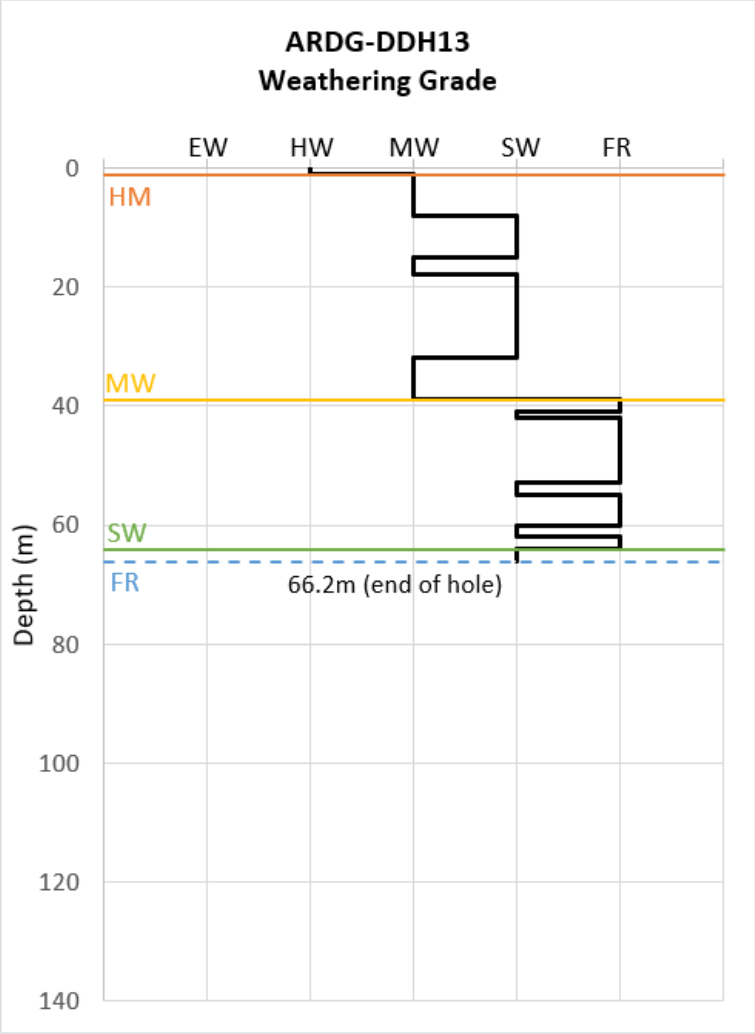

Figure 2.22 Weathering Profile – ARDG-DDH13

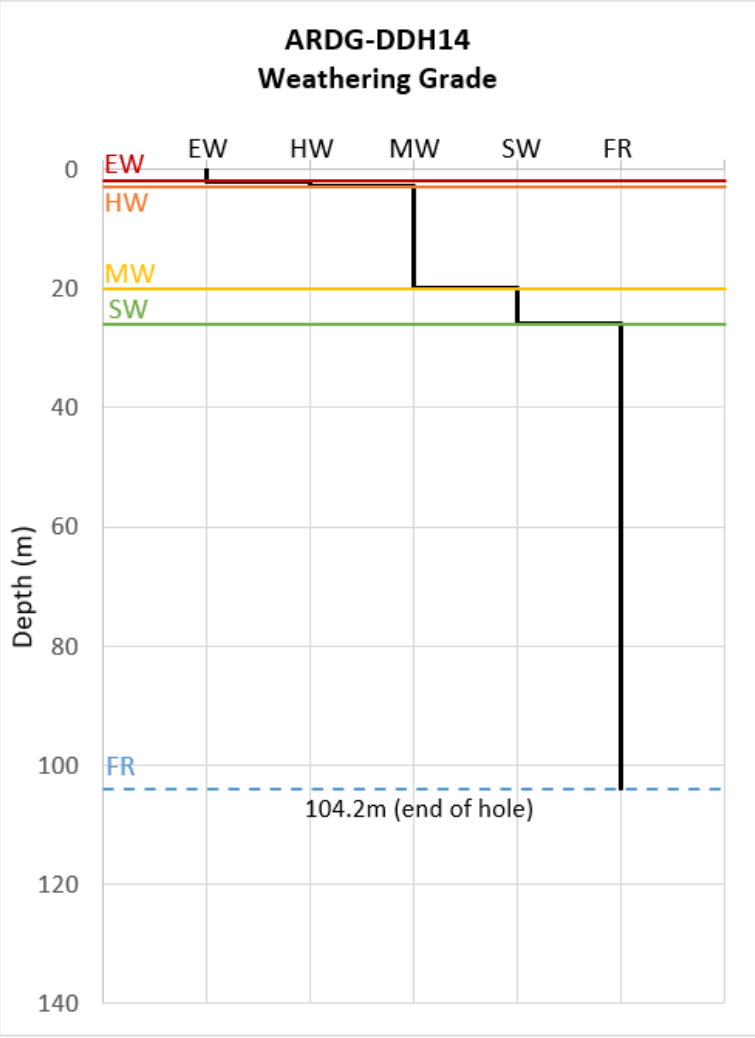

Figure 2.23 Weathering Profile – ARDG-DDH14

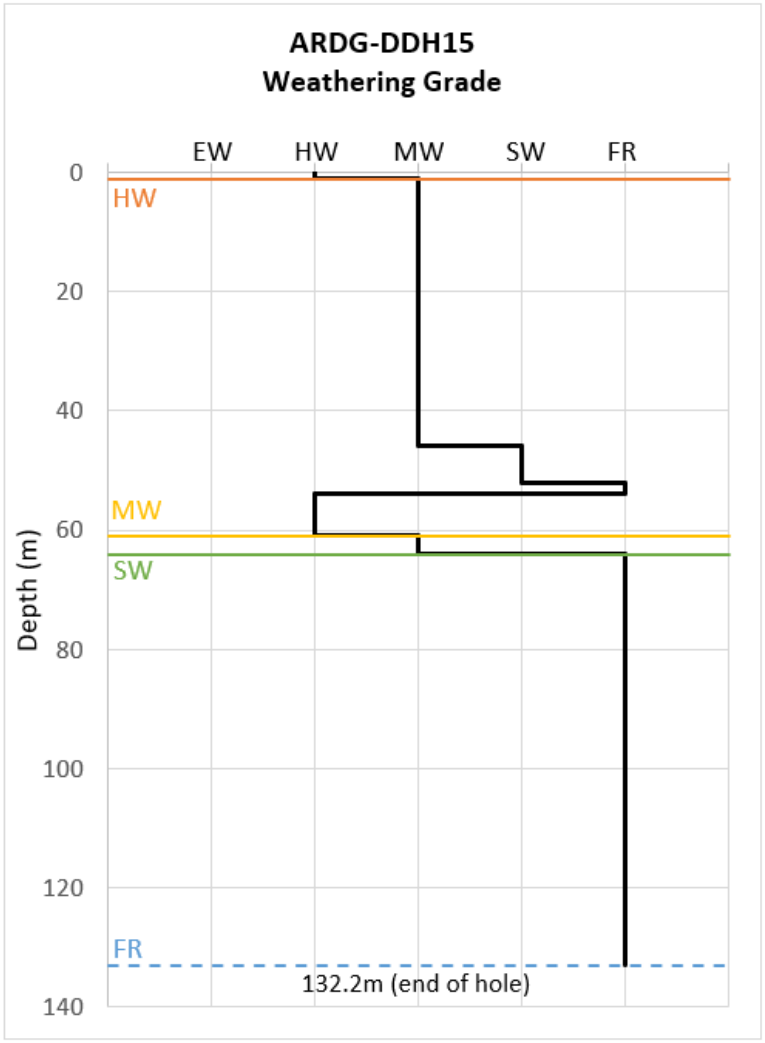

Figure 2.24 Weathering Profile – ARDG-DDH15

2.2.5 Site Stratigraphy

From the drilling campaigns conducted, rhyodacite represented 66% of the total meters drilled and is the dominant unit. The area in the vicinity of the proposed Stone Ridge Quarry consists of two main stratigraphic units (youngest to oldest) as summarised in Table 2.3.

Table 2.3 Stratigraphic Sequence at the Stone Ridge Site

Geological Formation	Colour	Material Type	Lithology Code	Lithological Description
Undifferentiated		Soil	SL	Overburden / Residual Soil
Eagleton Volcanics		Predominantly Rhyodacite	RD	*'Toscanitic, dellentitic and rhyolitic volcaniclastic and pyroclastic rocks with minor intermediate (andesitic or dacitic) tuffs and minor volcanic breccias and tuffaceous sediments'*

Based on the weathering profile interpreted from the drillhole logs, as depicted in Section 2.2.4, it is noted that the upper portion of the proposed Stone Ridge Quarry Pit consists of a highly weathered unit (HW) that extends to 25 m below the surface, followed by a transition zone consisting of moderately to slightly weathered material (MW to SW) which extends to 70 m depth before transitioning to fresh rock.

Five weathering grades were encountered as follows:

– **Unit 1** – Overburden – up to 6 m depth
– **Unit 2** – Highly Weathered (HW) Rhyodacite – up to 25 m depth
– **Unit 3** – Moderately Weathered (MW) Rhyodacite – up to 45 m depth
– **Unit 4** – Slightly Weathered (SW) Rhyodacite – up to 70 m depth
– **Unit 5** – Fresh (FR) Rhyodacite – extending below the quarry floor

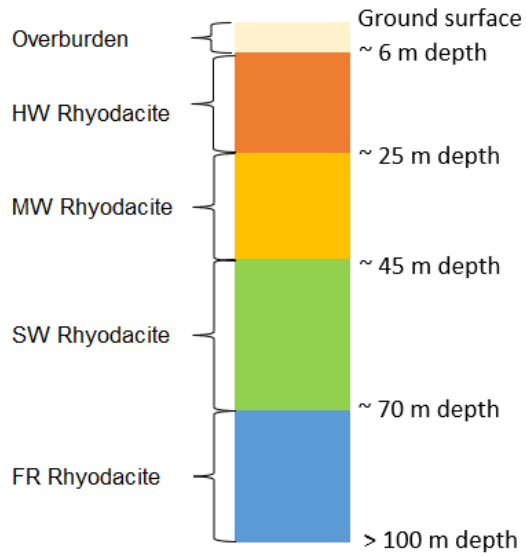

Figure 2.25 Schematic Depicting Typical Stratigraphic Sequence at the Stone Ridge Site

2.2.6 Major Structures

As depicted in Figure 2.26, four fault features have been identified from a detailed ground magnetic survey conducted by Fender Geophysics for Australian Resource Development Group. These have been designated ML1 to ML4. The Central Fault (ML1) crosses along the centre of the site and is orientated in a northwest-southeast direction. The Central Fracture to (ML2) is located parallel to ML1. The Splay Fault (ML3) also crosses the centre of the site and is orientated in a similar direction as above. The Nine Mile Creek Fault (ML4) is located some 100 m east of the site and is not within the proposed extraction pit.

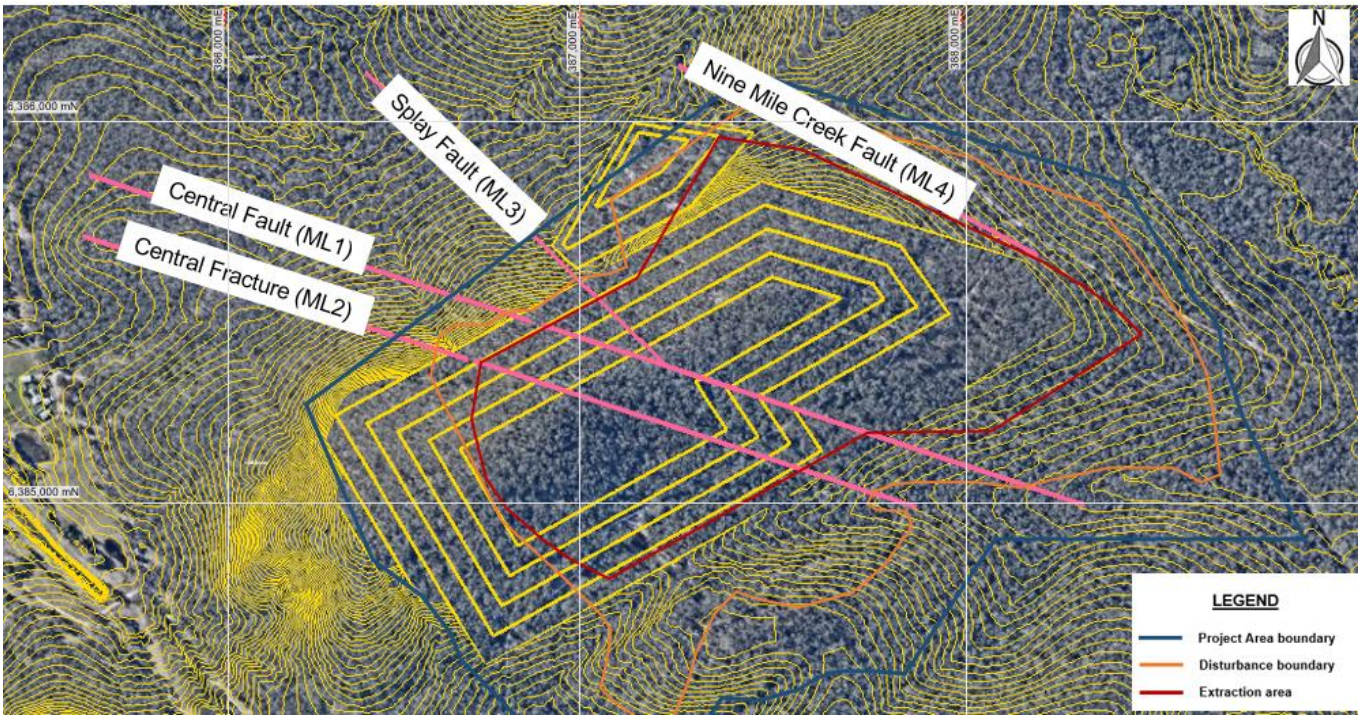

Figure 2.26 Simplified view of known Fault Zones in the vicinity of Stone Ridge Quarry Site

2.2.7 Minor Structures

From the Acoustic Televiewer interpretations for Diamond Drill Holes ARGD-DDH09 to ARGD-DDH14, a total of 660 discontinuities were identified. Stereonet projections and cluster analyses of the discontinuities indicate there are seven (7) major defect sets as summarised in Table 2.4. The corresponding stereographic projection is presented in Figure 2.27.

Table 2.4 Summary of Defect Characteristics

Discontinuity Set	Dip Angle (°)	Dip Direction (°)	Fisher Constant (K)	Description
Set 1	0	263	147.75	Major structural set
Set 2	34	218	38.52	Major structural set
Set 3	55	92	46.54	Major structural set
Set 4	34	37	36.92	Major structural set
Set 5	56	271	50.49	Major structural set
Set 6	45	345	76.04	Major structural set
Set 7	46	164	72.97	Major structural set

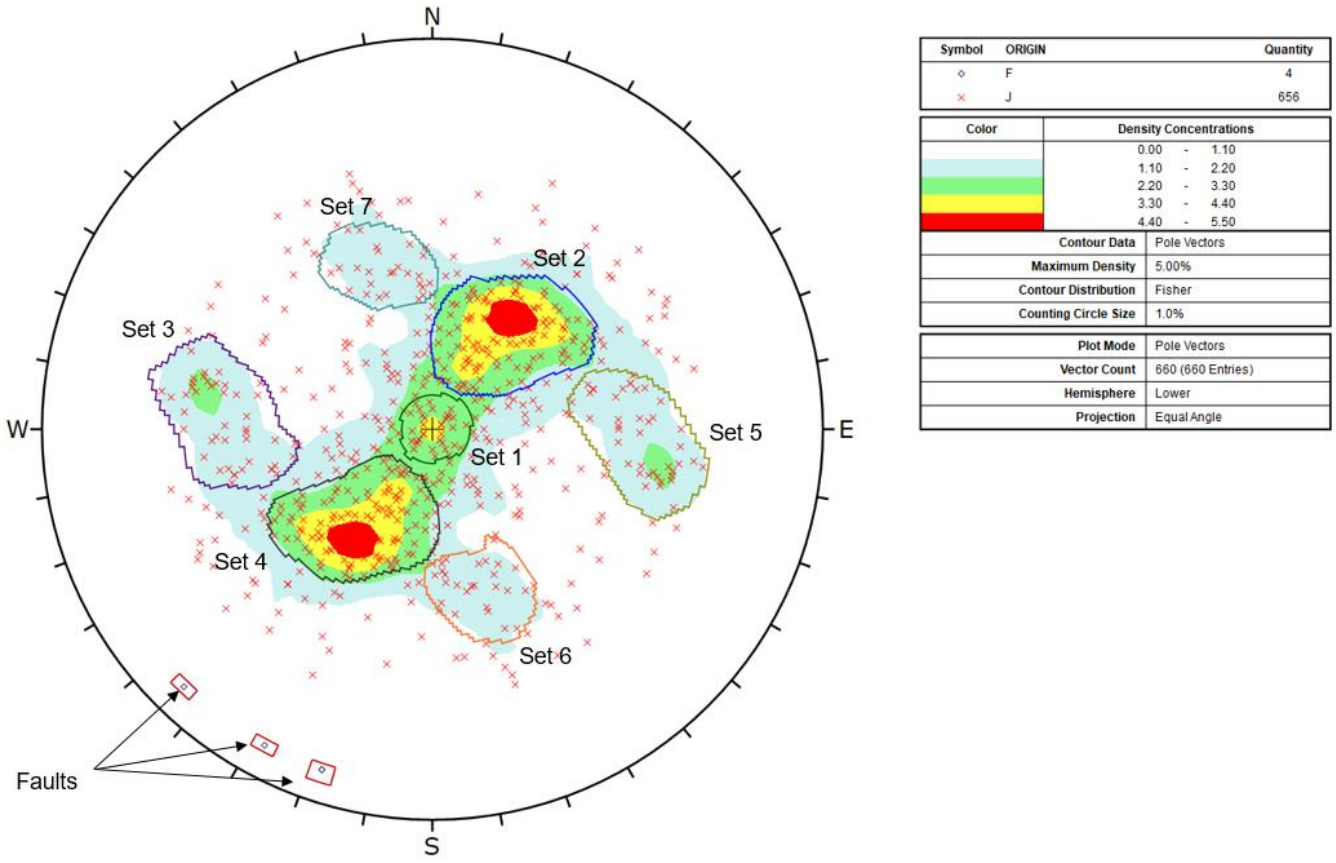

Figure 2.27 Stereographic Projection of Identified Defect Sets

Further discussion of these structures is provided in Section 4.1.1.

2.3 Hydrogeology

According to information provided by the Client, four (ARDG-DDH017 to ARDG-DDH020) and six (ARDG-P01 and ARDG-P06) groundwater monitoring bores were installed in vicinity of the site by Blacklaws Drilling in 2019 and by Precision Drill and Blast in 2020 to 2021 respectively. Summarised in Table 2.5 are the bore survey details and recorded groundwater levels as of 2019 to 2021. The locations of the groundwater observation bores are shown in Figure 2.28.

Table 2.5 Summary of Groundwater Observation Bores after Blacklaws Drilling (2019 and 2020)

Groundwater Bore ID	Elevation (m AHD)	Easting	Northing	Monitored Surface Water Level (m AHD)
ARDG-DDH17	41.5	388,825	6,385,205	23.73
ARDG-DDH18	31.9	388,181	6,385,515	19.17
ARDG-DDH19	36.7	387,692	6,385,205	20.01
ARDG-DDH20	40.0	388,583	6,385,561	22.11
ARDG-P01	29.9	388,942	6,385,528	22.33
ARDG-P02	45.1	388,511	6,385,099	29.02
ARDG-P03	46.6	388,102	6,384,851	24.97
ARDG-P04	34.2	387,771	6,384,708	15.37
ARDG-P05	49.5	387,766	6,384,710	26.13
ARDG-P06	20.1	387,714	6,385,490	12.69

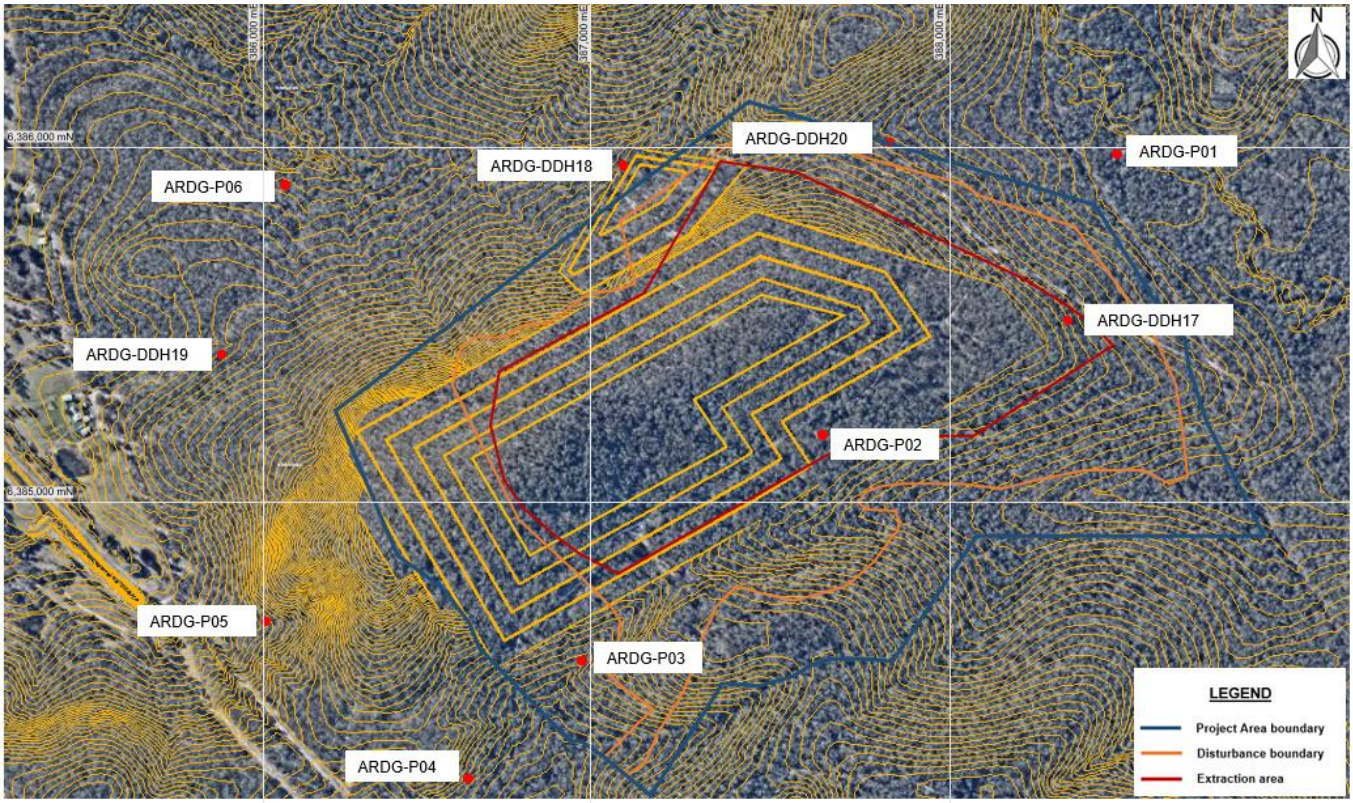

Figure 2.28 Approximate Location of Groundwater Bores in the vicinity of Stone Ridge Quarry

Based on information from these bores, groundwater has been interpreted to occur at an average level of approximately +21.5 m AHD.

2.4 Hydrology

Surface water run-off generated within the extraction footprint is to be channelled down the excavated slopes to a sump located on the quarry floor at approximately -17 m AHD. Water collected in the sump is to be pumped to an upper storage area.

3. Proposed Pit Geometry

The client wishes to extract the resources using a staged approach. The broad parameters associated with the proposed pit geometry after 30 years of extraction are as follows:

– The total depth of extraction is expected to be approximately 95 m below the current surface level of approximately +78 m AHD, with the proposed floor and sump at -2 m AHD and -17 m AHD respectively.
– Individual benches are to be formed at 15 m high with bench widths of 20 to 30 m.
– A nominal face angles of 70 degrees for individual benches.

The depth of overburden and underlying stratigraphy have been modelled as per the weathering profile outlined in Section 2.2.4 and Section 2.2.5.

The location of the proposed stockpile area is depicted in Figure 3.1. Note that the stockpile geometry has not been considered as part of the EIS stage. However, it is anticipated that if the slopes are formed at the angle of repose and good surface water management is implemented, adverse stability conditions are unlikely to manifest.

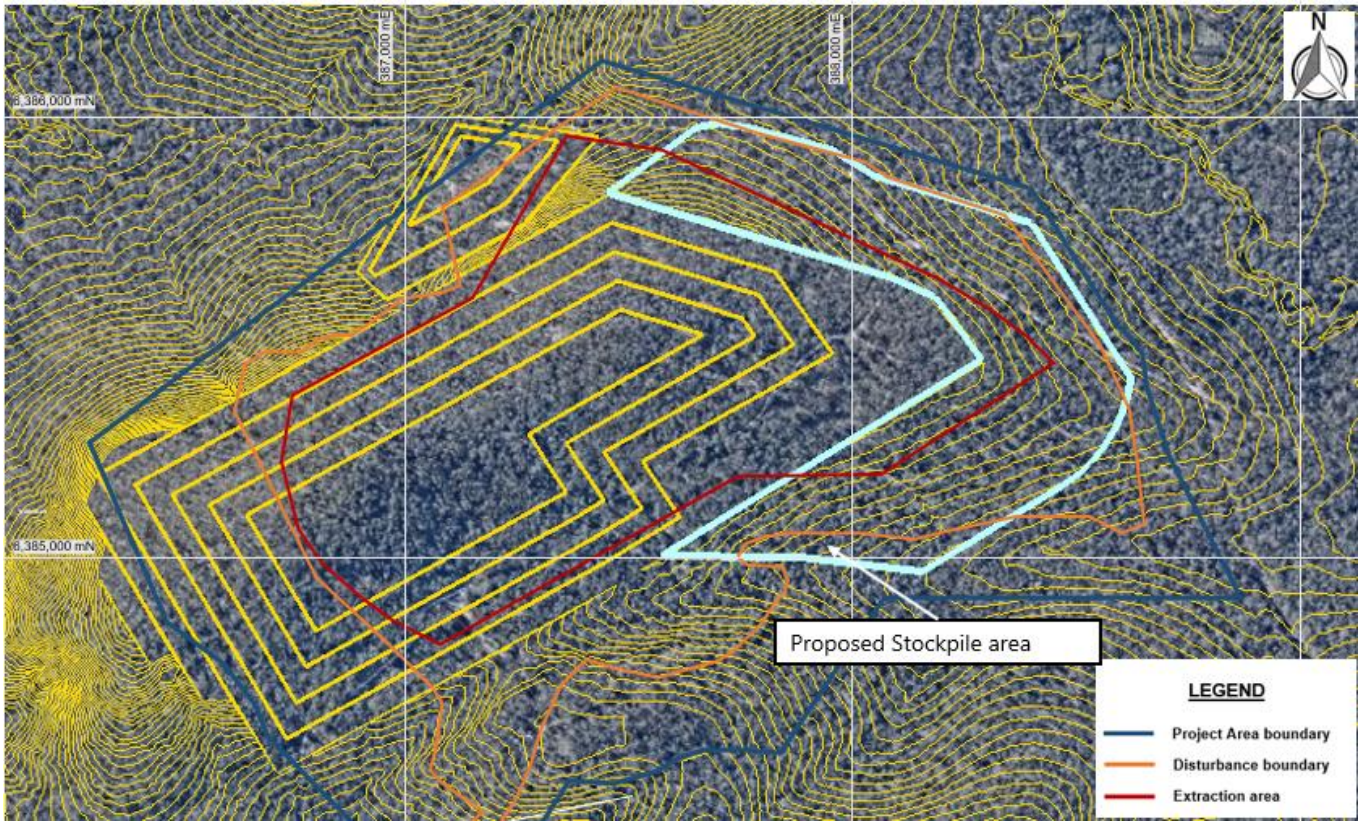

Figure 3.1 Plan view depicting proposed Stockpile area

4. Geotechnical Domain Model

The geotechnical domain model forms the basis for the quarry pit slope design and facilitates segregation of the quarry pit into sectors or zones which have similar geological, structural and material characteristics, thus modes of instability. In principle, geotechnical domaining allows for multiple optimisation techniques to apply, where the slope design is optimised, in terms of safety and economics, for a given sector rather than applying a single slope design across the entire pit. In essence, geotechnical domaining a quarry pit can be used to inform quarry owners/operators where to focus their time and effort.

The geotechnical domain model is compiled from four component models:

– Geological model
– Structural model
– Hydrogeological model, and
– Rock mass (material properties) model

Geotechnical domaining of the Stone Ridge Quarry site has relied upon the philosophy set out by the CSIRO *Guidelines for Open Pit Slope Design* (Read and Stacey, 2009). Outlined in Figure 4.1 are the considerations that are taken into account when formulating site specific geotechnical domains.

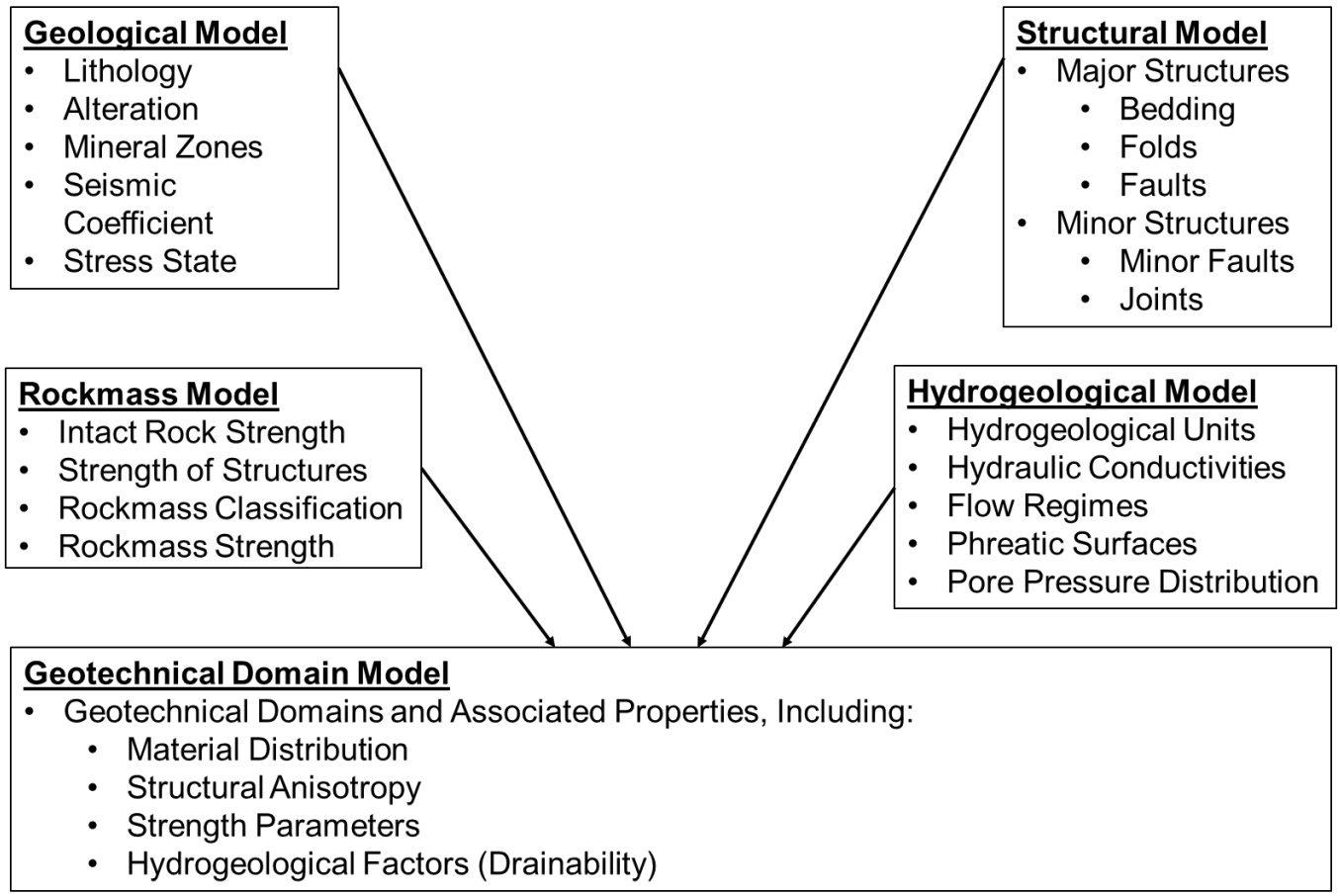

Figure 4.1 Development of Geotechnical Domain Model after Read and Stacey (2009)

4.1 Anticipated Pit Slope Instability Mechanisms

Understanding the scale and mode of instability forms a crucial component of the geotechnical model. Modes of instability can be classified as either kinematic (structural) or rock mass, and in open cut excavations may occur independently or in combination (multi-modal). The following sub-sections outline the instability mechanisms that are likely to be encountered within the Stone Ridge Quarry.

4.1.1 Kinematic (Structural)

Kinematic stability is governed by the characteristics of structural defects (e.g., length of defect) in relation to the orientation and design of corresponding batter geometries. Slopes that contain structural defects are generally susceptible to multiple types of kinematic instability e.g., planar and wedge sliding, however, it is the critical instability mode that will manifest first. The kinematic instability modes likely to be present within Stone Ridge Quarry are likely to manifest as the following:

– Planar sliding
– Tetrahedral wedge sliding
– Block/flexural toppling

It is common practice to identify the critical instability mode, along with secondary instabilities modes using stereonet projections, the interpretation of which is described in more detail below.

4.1.1.1 Interpretation of Stereonet Projections

The orientation i.e., dip angle and dip direction of structural defects (discontinuities) which have been logged / mapped are plotted as lower hemispheric 'poles' relative to a given slope orientation. Multiple poles with similar orientations i.e., poles that are clustered together, may be represented by a singular mean value (set) from which statistical parameters that define the variability in orientations can be derived. An example of a lower hemisphere stereonet projection highlighting the key features is presented in Figure 4.2.

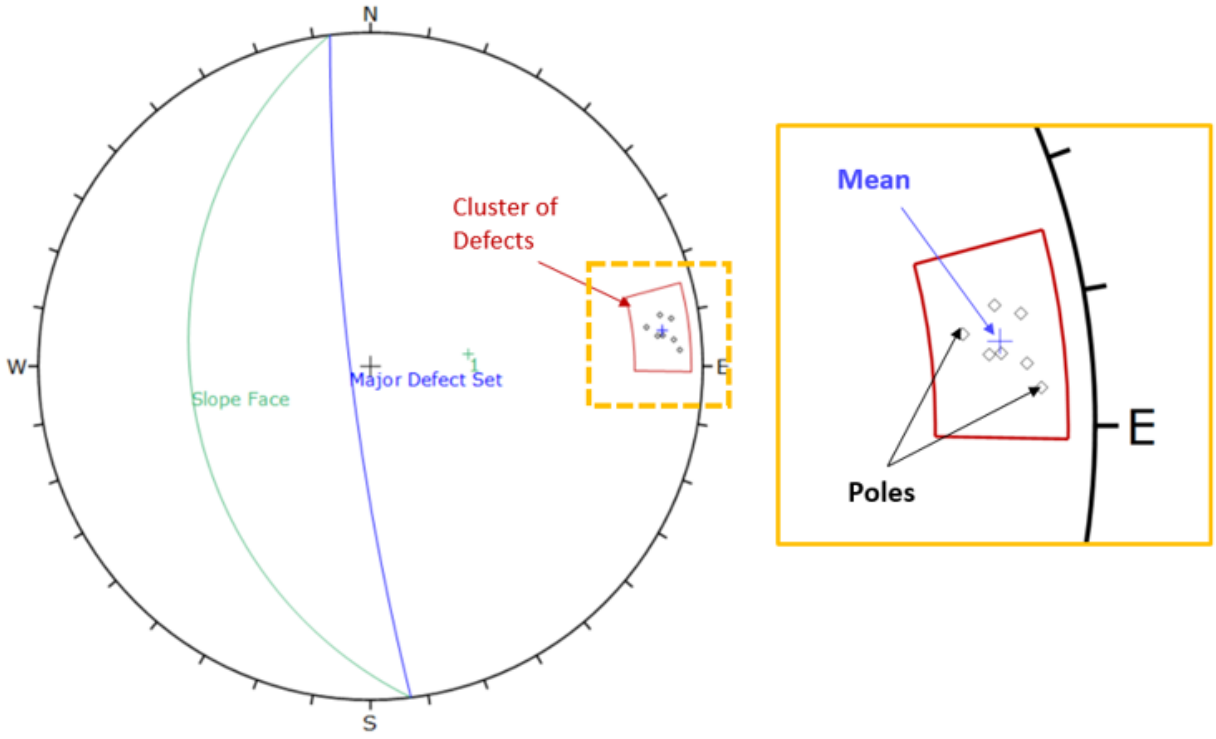

Figure 4.2 Stereonet Depicting Key Features

The Fisher Distribution is commonly used for modelling the distribution of 3-dimensional orientation vectors such as the distribution of defect orientations on a sphere. A Fisher distribution describes the angular distribution of orientations about a mean value and is symmetric about the mean. The Fisher 'K' constant describes the tightness or dispersion of a clustered set, where a larger value implies a tighter cluster and vice versa. The Fisher K constant can be expressed by the following:

$$\theta = \frac{(81°)}{\sqrt{K}}$$

Where:

K = Fisher constant

θ = Angular standard deviation

Rocscience's Dips software used for stereographic analysis automatically calculates the Fisher K constant (or angular standard deviation) for a defined cluster. The Fisher K constant provides a statistical parameter for downstream probabilistic analyses, e.g., assessing the likelihood for planar sliding to occur.

4.1.1.2 Planar Sliding

Planar sliding occurs when structural defects (e.g., bedding planes), which are sub-parallel to the slope face become exposed during mining and 'daylight' in the slope face. Figure 4.3 depicts a kinematically feasible instability where the angle of the instability plane (Ψ_A) dips at a flatter angle than the slope face (Ψ_f) – plane 'A-A' ($\Psi_A < \Psi_f$).

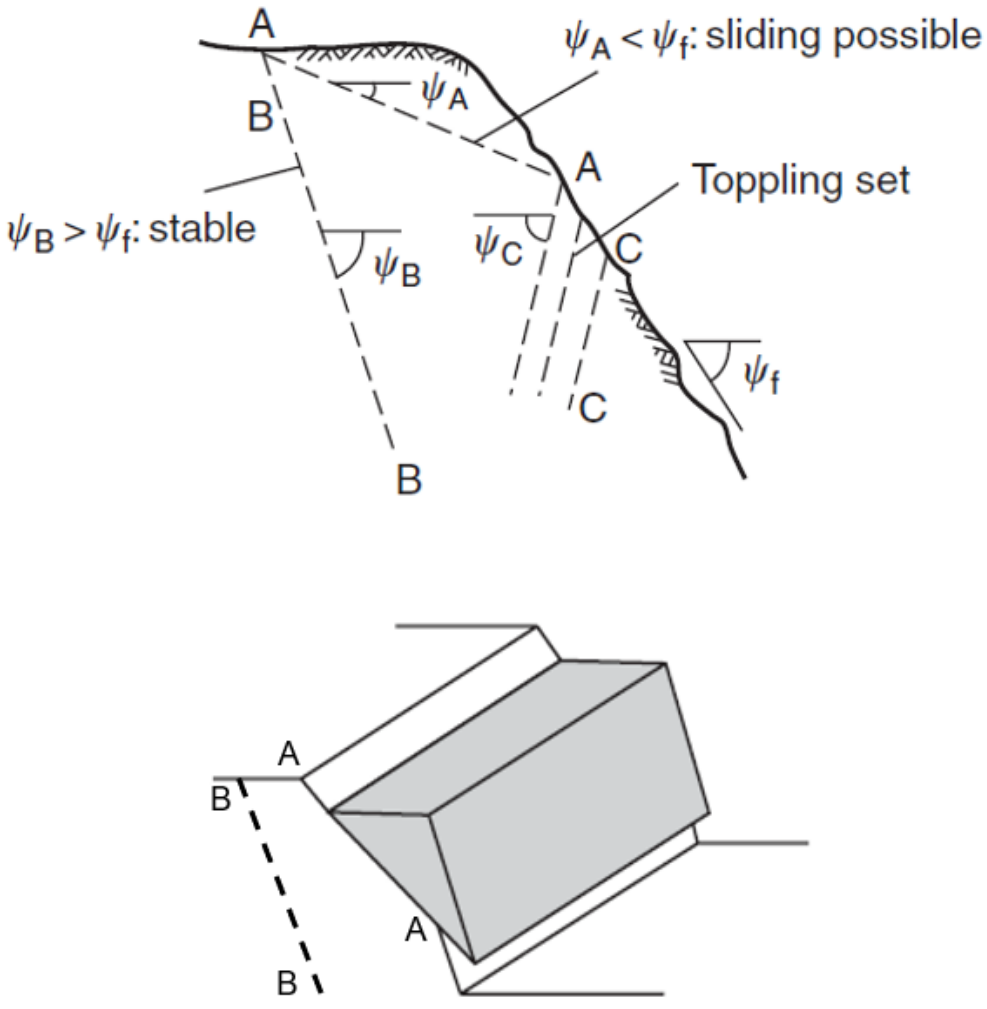

Figure 4.3 Planar Sliding Instability Schematic

Conversely, planar sliding cannot occur when the structural planes e.g., 'B-B' dips at a steeper angle than the slope face ($\Psi_B < \Psi_f$) and does not 'daylight'. Similarly, planes that are not orientated towards the direction of excavation e.g., plane 'C-C', are not feasible for planar sliding to occur. In addition to the orientation of structural defects, there are two mechanical principles that also govern the kinematic feasibility for planar sliding, which are:

1. The dip angle of the structural discontinuity must be greater than the angle of friction of the discontinuity i.e., the mobilised shear resistance, referred to as the friction cone (Φ). As the friction angle of the discontinuity surface diminishes the feasibility for planar sliding increases.
2. The dip direction of the structural discontinuity plane cannot differ from the dip direction of the slope face by more than approximately 20°, because under these conditions there will be an increasing thickness of intact rock at one end of the block, which is sufficient for resisting block movement.

The mechanical principles discussed above are used to define a 'zone of feasibility' on stereonet projections, which are commonly referred to as the 'daylight envelope'. The 'daylight envelope' for planar sliding is highlighted for a 60° (red) and 80° (blue) slope face in Figure 4.4.

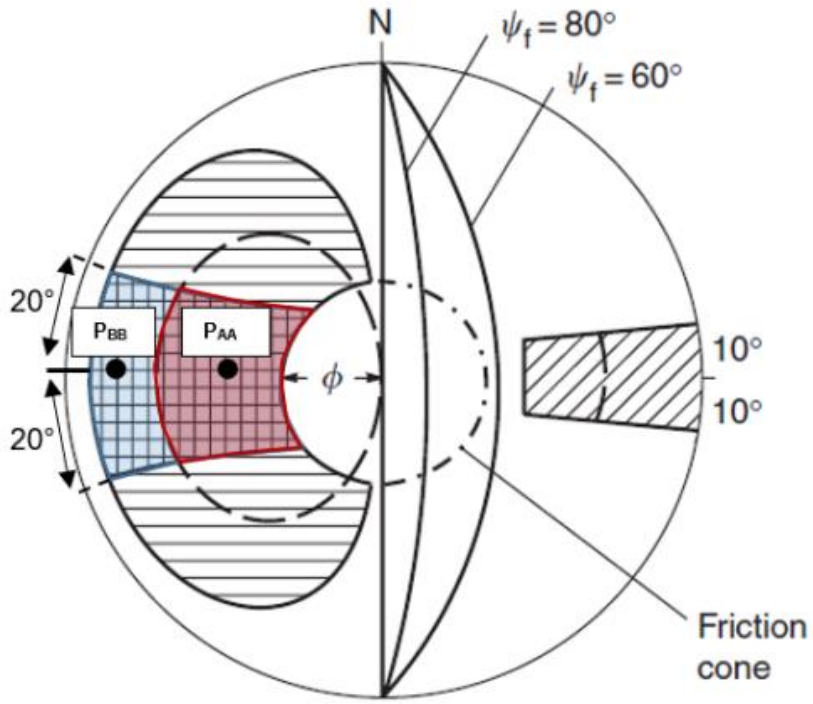

Figure 4.4 Stereographic Projection Depicting Daylight Envelope and Friction Cone – Planar Sliding

The discontinuity plane 'A-A', which was used to depict planar sliding in Figure 4.3 is represented in Figure 4.4 as pole 'PAA'. Pole 'PAA' clearly lies within the daylight envelope for the 60° slope face and therefore planar sliding is feasible. Pole 'PBB', used to represent discontinuity plane 'B-B', lies outside of the daylight envelope for a 60° slope face and therefore planar sliding is rendered infeasible. Both pole 'PAA' and 'PBB' lie within the daylight envelope for an 80° slope face and therefore is susceptible to planar sliding along two discontinuity planes (i.e., in this example the slope becomes more susceptible to planar sliding when increased from 60° to 80°).

4.1.1.3 Tetrahedral Wedge Sliding

From a kinematic perspective, the formation of wedge type instabilities requires a specific occurrence of structural conditions to become kinematically feasible, which include:

– The dip of the discontinuity planes is flatter than the angle of the slope face
– The dip of at least one discontinuity plane is greater than the friction angle of the discontinuity surface
– Two or more planes of discontinuity intersect the slope face

A generalised depiction of tetrahedral wedge sliding is presented in Figure 4.5 along with the corresponding stereographic projection.

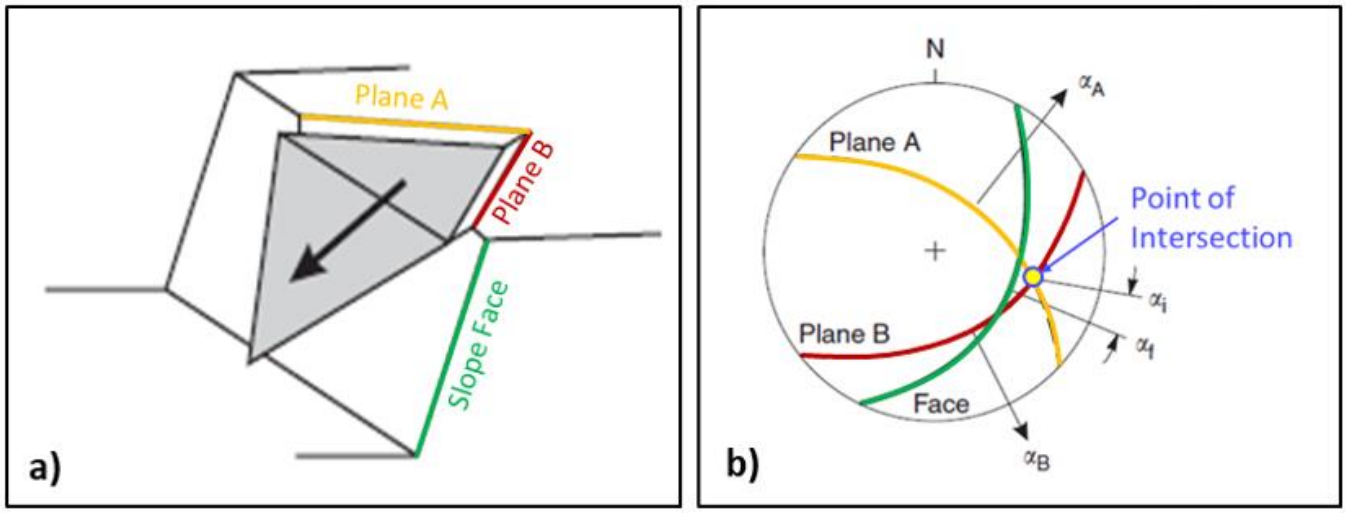

Figure 4.5 Schematic of a) Kinematically Feasible Wedge, and b) Corresponding Stereographic Projection

Given that a wedge is formed by the intersection of at least two discontinuity planes, the direction of sliding (i.e., the daylight envelope), is less restrictive than that of planar failures because there are two planes that form release surfaces. The daylight envelope for wedge formations is the locus of all poles representing lines of intersection whose dip directions lie in the plane of the slope face as shown in Figure 4.6.

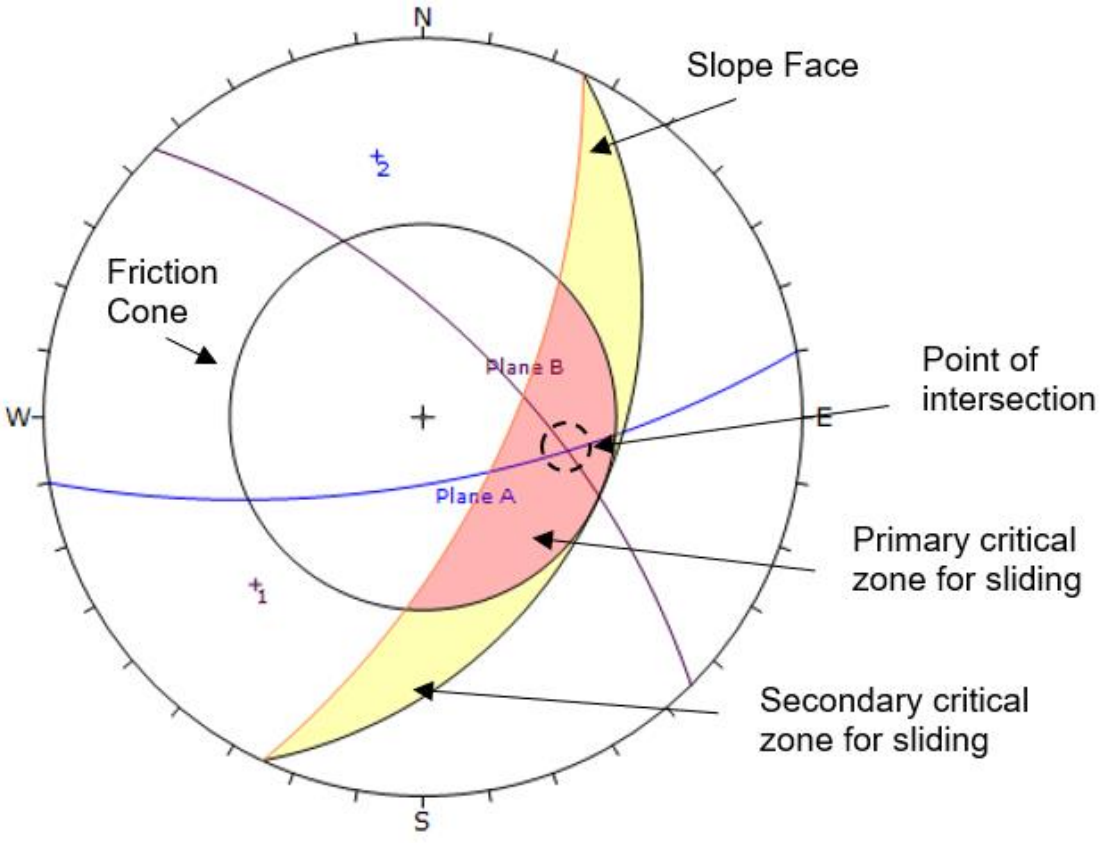

Figure 4.6 Stereographic Projection Depicting Daylight Envelope – Wedge Sliding

As shown in Figure 4.6, there are two daylight envelopes, which are the primary (red) and secondary (yellow) critical zones for wedge sliding. The primary difference between the two zones is that in the primary critical zone of sliding, a wedge may slide along the line of intersection (i.e., along two defect planes, or on one defect plane) while the critical secondary zone represents wedges which slide on only one defect plane, noting that the dip vector for sliding on a single plane must be in the primary critical zone.

4.1.1.4 Toppling

There are several kinds of toppling mechanisms that may result in slope instability, which typically include, but are not limited to:

– Flexural
– Block toppling
– Block-flexural toppling

Each of the above toppling mechanisms are pictorially presented in Figure 4.7.

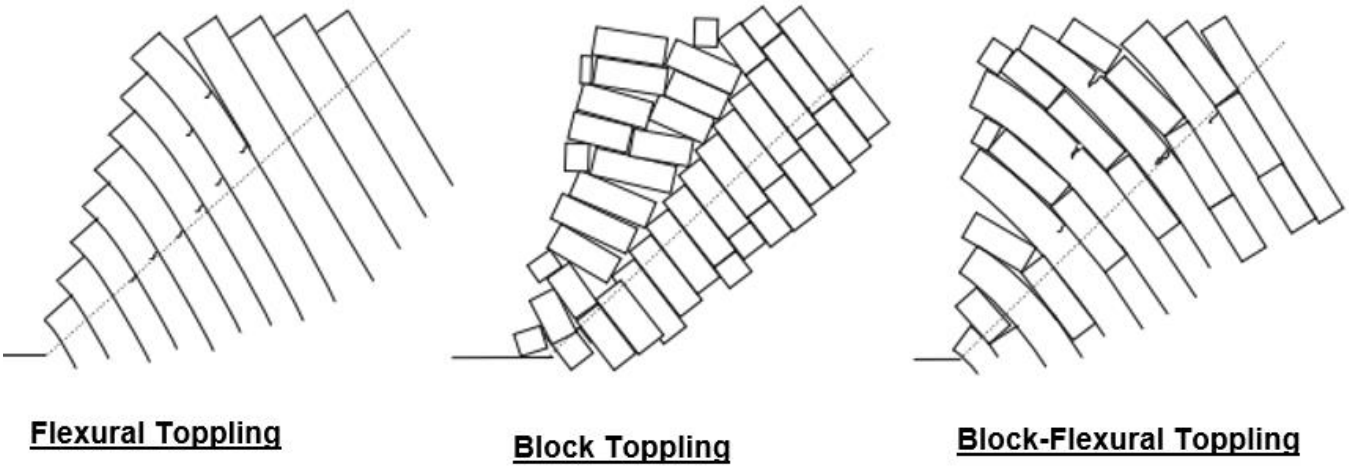

Figure 4.7 Schematic of Primary Toppling Mechanisms

4.1.1.4.1 Flexural Toppling

Rocks with a pervasive fabric (e.g., bedding planes, or a preferred discontinuity system), orientated to present a rock slope with semi-continuous cantilever beams have the potential to result in a flexural toppling type instability. In such instances, columns formed by sub-vertical structures break in flexure as they bend forward, where characteristics of the defect system and intact rock mass strength govern the potential for toppling to occur. According to Goodman (1980), blocks cannot topple if they cannot slide with respect to one another, and for a slip to occur, the discontinuity system must have a dip angle that is less than a line inclined at an angle equivalent to the friction angle above the slope, which is termed the 'slip limit'. Additionally, flexural toppling cannot occur when the dip direction of the discontinuity system differs from the slope orientation by more approximately 10° to 15°. A daylight envelope showing the zone for which the flexural toppling mechanism is feasible is presented in Figure 4.8.

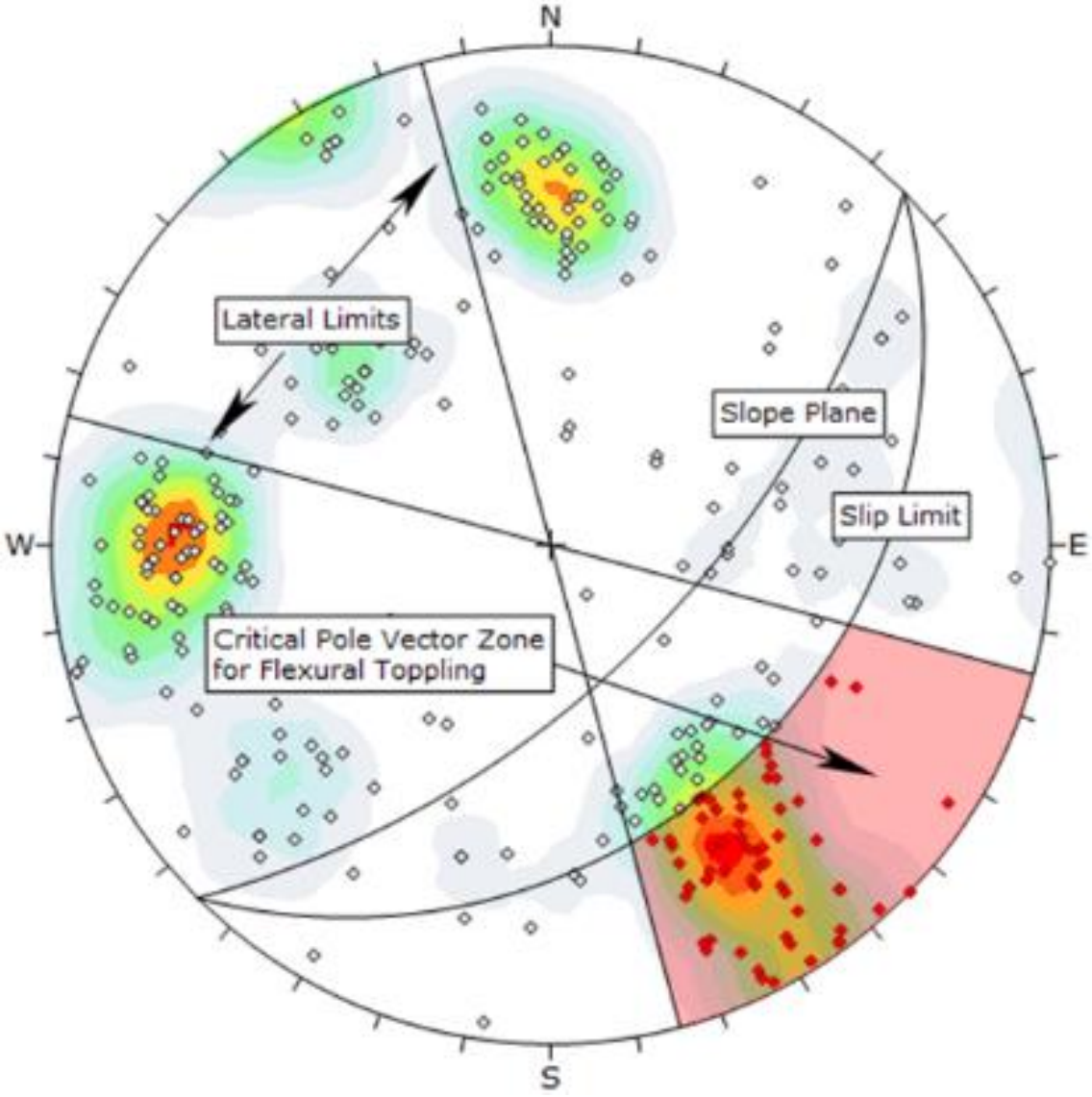

Figure 4.8 Stereographic Projection Depicting Daylight Envelope – Flexural Toppling

4.1.1.4.2 Block Toppling

Block toppling occurs where rock columns created by sub-vertical defect systems, are intersected by cross-cutting defect systems. At the toe of the slope where the columns are shorter, load from upper (and larger) columns thrust toe columns forward permitting further toppling. In order for block toppling to be kinematically feasible, two discontinuity systems must intersect such that the intersection line dips into the slope and can form discrete toppling blocks, and a third discontinuity system (e.g., cross cutting plane), that acts as a release plane or release and sliding plane. Similar, to flexural toppling, the feasibility of block toppling requires the dip direction of intersecting discontinuity systems to occur within approximately 10° to 15° of the slope dip direction. A daylight envelope showing the zone for which block toppling is feasible is presented in Figure 4.9.

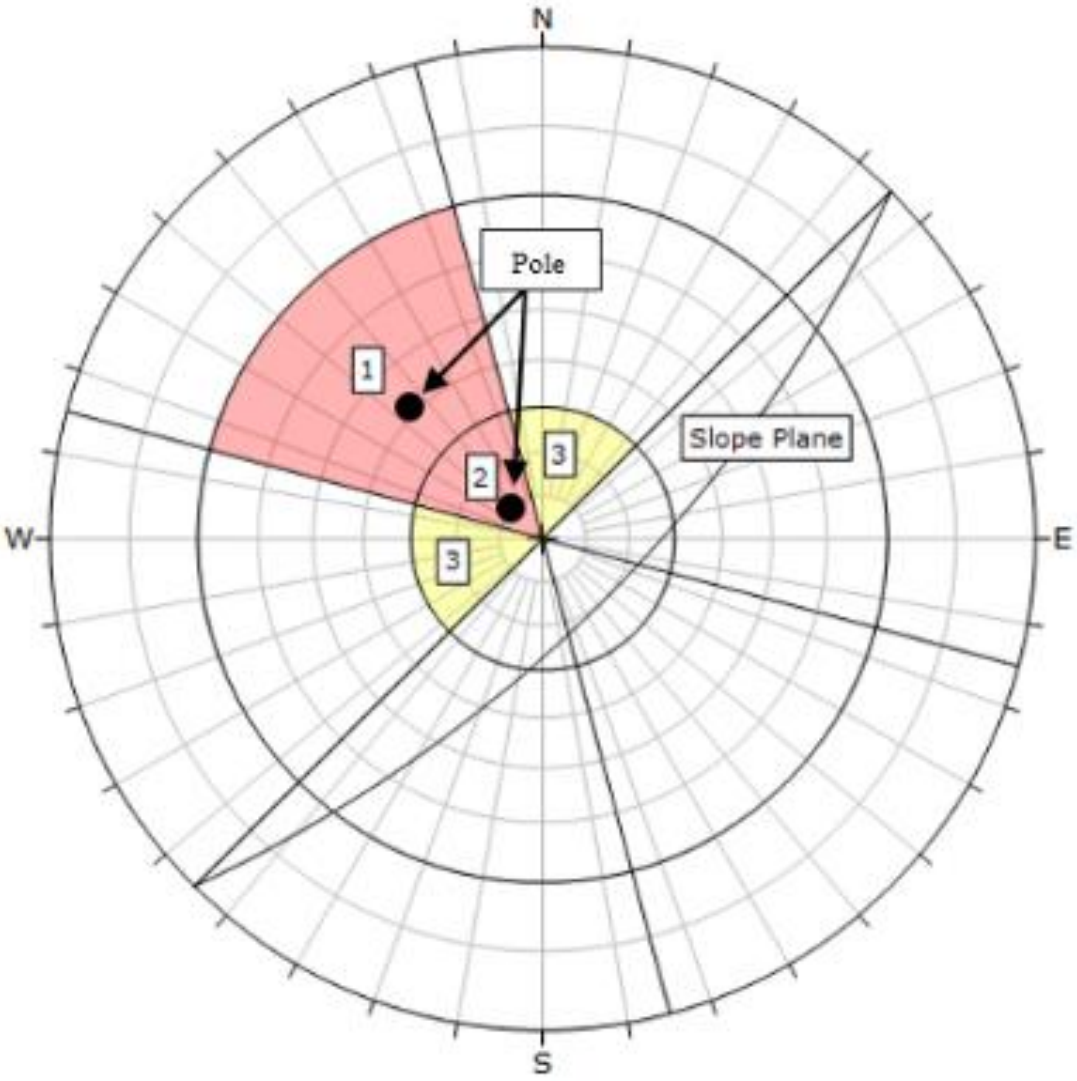

Figure 4.9 Stereographic Projection Depicting Daylight Envelope – Block Toppling

As shown in Figure 4.9, there are three critical zones that make up the daylight envelope. Critical zones 1 and 2, highlighted in red, represent the feasibility of direct block toppling. Critical zones marked 3, highlighted in yellow, represent the feasibility of oblique block toppling. Any poles which fall into the combined region of zones 2 and 3 represent cross-cutting planes that act as release planes, however, do not permit sliding as the dip angle of the defect plane is less than the mobilised shear resistance. On the other hand, poles that fall into zone 1 represent release planes for which sliding can occur, where a combined sliding and toppling mechanism may manifest.

4.1.1.4.3 Block Flexural Toppling

The two mechanisms presented above, flexural toppling and block toppling, are idealistic mechanisms which are seldom observed in practice. The block-flexural toppling mechanisms is a combination of flexural and block toppling instability modes. In block-flexural toppling, some blocks fail due to tensile bending stress, and some separate from the cross-cutting defect system, at which point all blocks topple together. The block-flexural toppling model accounts for irregularities in the persistence and orientation of cross-cutting joints that serve as release or release and sliding planes. Whilst block-flexural toppling is more readily observed in practice, most methods of toppling assessment do not consider block-flexural toppling and only consider the above idealistic conditions.

4.1.2 Rock Mass Instability

Rock mass stability is governed by the characteristics of both intact rock mass and structural discontinuities. Where kinematic mechanisms typically control the stability at the bench to inter-ramp scale, rock mass mechanisms control the stability at the inter-ramp and global scales. Assessment of the rock mass stability is an essential step in the design process, to check that the rock mass can sustain the proposed design over the full height of the slope. Rock mass models such as the Generalised Hoek Brown Criterion, assume that a rock mass is comprised of an isotropic clump of intact rock pieces separated by closely spaced joints for which there is no preferred failure direction. Rock mass that has a pervasive fabric e.g., bedding planes, the strength of the rock mass may be notably lower in the direction of the discontinuity system.

4.1.3 Circular/Rotational Instability

Circular/rotational instability typically occurs in highly disturbed and/or weathered material that typically does not have any remnant structure (see Figure 4.10).

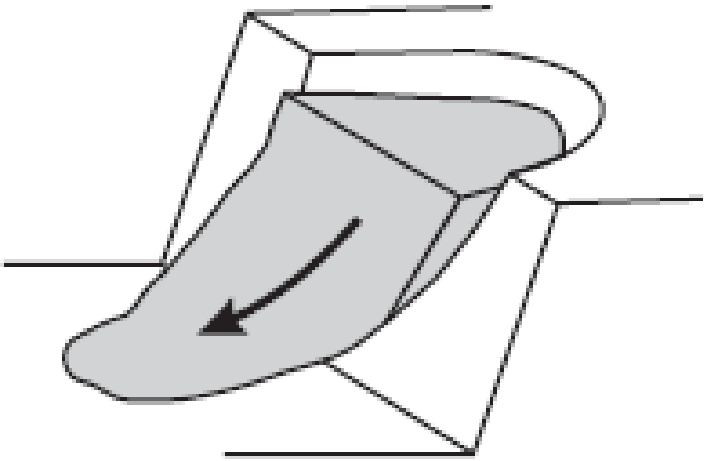

Figure 4.10 Schematic of a Circular Instability

Circular instability is dependent upon the shear strength characteristic of the highly weathered material and the slope angle of the cut face. Circular instability occurring as potential instability mechanism within the residual soil and soft rock units where there is no discernible structure present. Mobilisation of a circular failure is likely to be contained to bench scale instability.

4.1.4 Structural Analyses

A fundamental component of the structural model and thus the geotechnical domain model is the orientation characteristics of critical defect structures relative to pit walls. Presented in Figure 4.11 is a stereonet projection depicting defect orientations mapped at the Stone Ridge Quarry Site.

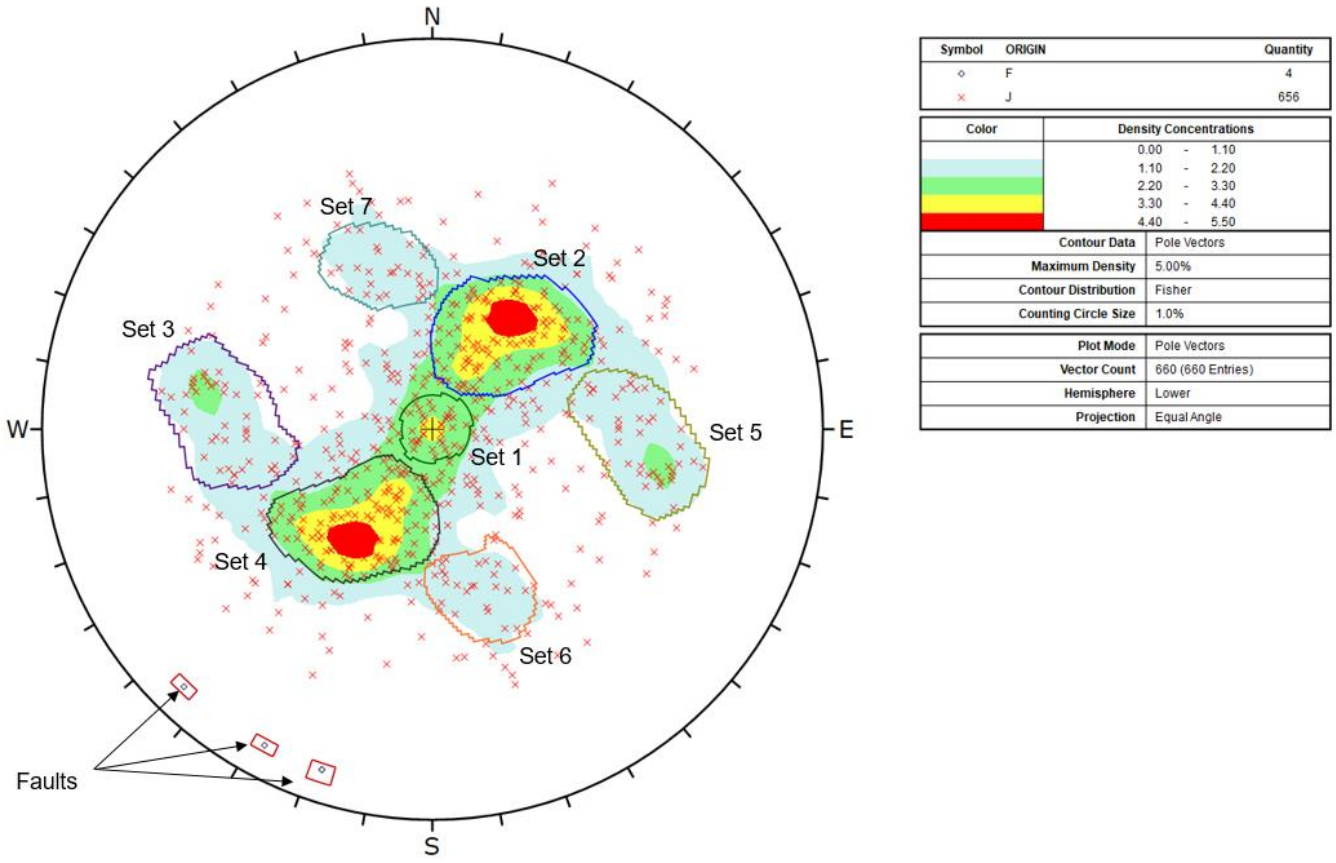

Figure 4.11 Stereonet Projection Depicting Mapped Defect Plane Orientations

Summarised in Table 4.1 and Table 4.2 are the defect set and fault characteristics respectively.

Table 4.1 Summary of Defect Set Orientation Characteristics

Discontinuity Set	Dip Angle (°)	Dip Direction (°)	Fisher Constant (K)	Description
Set 1	0	263	147.75	Major structural set
Set 2	34	218	38.52	Major structural set
Set 3	55	92	46.54	Major structural set
Set 4	34	37	36.92	Major structural set
Set 5	56	271	50.49	Major structural set
Set 6	45	345	76.04	Major structural set
Set 7	46	164	72.97	Major structural set

Table 4.2 Summary of Fault Characteristics

Fault	Dip Angle (°)	Dip Direction (°)
Central Fault	85	18
Central Fracture	85	18
Splay Fault	85	28
Nine Mile Creek Fault	85	44

4.2 Interpretation of Material Strength Properties

As outlined in Section 2.2.4, five (5) stratigraphic units have been observed within the Stone Ridge Quarry site. To adequately define the strength characteristics of each unit, a suitable strength criterion should be selected in sympathy to the rock mass characteristics (Hoek and Brown, 2019). Where there is discernible structure within a rock mass, adoption of the Mohr Coulomb criterion can result in an overestimation in the rock mass strength compared to if the Generalised Hoek Brown (GHB) criterion is adopted, particularly under low normal stresses (or confinement) (Hoek, 1994). Each strength criterion requires unique strength parameters to derive shear strength characteristic curves i.e., the relationship between normal stress and shear stress. Summarised in Table 4.3 is the strength criterion type along with the strength parameters required for each material type.

Table 4.3 Summary of Strength Criterion and Parameters by Material Type

Unit	Criterion	Required Strength Parameters
1	Mohr Coulomb	Cohesion (c') and Friction Angle (ϕ')
2 - 5	Generalised Hoek-Brown	Uniaxial Compressive Strength (σ_c), Geological Strength Index (GSI), Material Constant (m_i) and Disturbance Factor (D)

For each material type and associated strength criterion, strength parameters were obtained through available data. Each criterion and the material parameters adopted for downstream stability analyses are discussed further in the following subsections.

4.2.1 Rock Mass Strength and Soil Model(s)

In this section the methodology by which the interpretation of rock mass and associated defect plane strengths, as well as soil strengths is presented. The geotechnical core drilling logs and photo information was used for interpretation.

The approach by which characteristic strength behaviour for each of the observed stratigraphic units is discussed further in the following subsection. It is the characteristic strength behaviour which forms the basis of the rock mass and soil mass model.

4.2.2 Derivation of Rock Mass Strengths

The above sources of information were subjected to data reduction and engineering interpretation to calculate the Rock Mass Rating (RMR_{89}) for each stratigraphic unit. The RMR_{89} parameter Bieniawski (1989), is a geomechanical classification tool that is related to intact rock strength, geological defects and is calculated for discrete intervals of rock mass. The RMR_{89} parameter forms the basis for interpreting material strength parameters after Hoek and Brown (1997), report titled '*Practical Estimates of Rock Mass Strength*'.

4.2.2.1 Methodology

The RMR_{89} parameter is calculated by attributing a series of weighted factors to the constituent components for a given interval of rock (see Table 4.4). To achieve this, the following information is required:

– Core Recovery and Rock Quality Designation (RQD)
– Lithology, degree of weathering, alteration types of strength class
– Defect (structure) type, number of defect sets and orientation information for the respective structure i.e., alpha and beta angles
– Defect plane characteristics (rough, smooth, stepped etc.) and infill type and thickness
– Groundwater conditions

The above information was adequately captured during the 2018 and 2019 drilling campaigns which were carried out for the Stone Ridge Quarry site.

Table 4.4 RMR_{89} Weighting Factors of Bieniawski (1989)

A. Classification Parameters and their Ratings									
Parameter			Range of Values						
1	Strength of intact rock material	Point Load Strength Index	> 10 MPa	4-10 MPa	2-4 MPa	1-2 MPa	For this low range unixiaxial compressive test is preffered		
		Uniaxial Compressive Strength	> 250 MPa	100 - 250 MPa	50 - 100 MPa	25 - 50 MPa	5-25 MPa	1-5 Mpa	< 1 MPa
	Rating		15	12	7	4	2	1	0
2	Drill Core Quality (RQD)		90% - 100%	75% - 90%	50% to 75%	25% to 50%	< 25%		
	Rating		20	17	13	8	3		
3	Spacing of Discontinuities		> 2 m	0.6 - 2 m	200 - 600 mm	60 - 200 mm	< 60 mm		
	Rating		20	15	10	8			
4	Condition of Discontinuities (see E)		Very Rough Surfaces Not Continuous No Seperation Unweathered Wall Rock	Slightly Rough Surfaces Seperation < 1 mm Slightly Weathered Walls	Slightly Rough Surfaces Seperation < 1 mm Highly Weathered Walls	Slickensided Surfaces or Gouge < 5mm Thick or Seperation 1-5 mm Continuous	Soft Gouge > 5mm Thick or Seperation > 5 mm Continuous		
	Rating		30	25	20	10	0		
5	Groundwater	Inflow per 10m tnnel length (l/m)	None	<10	10 -25	25 - 125	> 125		
		(Joint Water Pressure)/ Major principal σ	0	< 0.1	0.1 - 0.2	0.2 - 0.5	> 0.5		
		General Conditions	Completley Dry	Damp	Wet	Dripping	Flowing		
	Rating		15	10	7	4	0		
B. Rating Adjustment for Discontinuity Orientations									
Strike and Dip Orientations			Very Favourable	Favourable	Fair	Unfavourable	Very Unfavourable		
Ratings		Tunnels and Mines	0	-2	-5	-10	-12		
		Foundations	0	-2	-7	-15	-25		
		Slopes	0	-5	-25	-50			
C. Rock Mass Classes Determined From Total Ratings									
Ratings			81 - 100	61 - 80	41 - 60	21 - 40	< 21		
Class Number			I	II	III	IV	V		
Description			Very Good Rock	Good Rock	Fair Rock	Poor Rock	Very Poor Rock		
D. Meaning of Rock Classes									
Class Number			I	II	III	IV	V		
Average Stand-up Time			20 Years for 15 m Span	1 Year for 10 m Span	1 Week for 5 m Span	10 Hours for 2.5 m Span	30 Mins for 1 m Span		
Cohesion of Rock Mass (kPa)			> 400	300 - 400	200 - 300	100 - 200	< 100		
Friction Angle of Rock Mass (deg)			> 45	35 - 45	25 - 35	15 - 25	< 15		
E. Guidelines for Classifcation of Discontinuity conditions									
Discontinuity Length (Persistance) Rating			< 1 m 6	1 - 3 m 4	3 - 10 m 2	10 - 20 m 1	> 20 m 0		
Seperation (Aperature) Rating			None 6	< 0.1 mm 5	0.1 - 1.0 mm 4	1 - 5 mm 1	> 5 mm 0		
Roughness Rating			Very Rough 6	Rough 5	Slightly Rough 3	Smooth 1	Slickensided 0		
Infilling (Gouge) Rating			None 6	Hard Filling < 5 mm 4	Hard Filling > 5 mm 2	Soft Filling < 2mm 2	Soft Filling > 2mm 0		
Weathering Rating			Unweathered 6	Slightly Weathered 5	Moderatley Weathered 3	Highly Weathered 1	Decomposed 0		

RMR_{89} values were calculated for each interval rock mass logged as part of the geotechnical drilling campaigns as outlined in Section 2.2. Subsequent to the calculation of RMR_{89}, a data reduction process was undertaken to segregate the data and form groups of materials that share similar characteristics (e.g., rock mass quality). RMR_{89} data was segregated by:

– Lithology type e.g., rhyodacite
– Degree of weathering e.g., highly weathered to fresh rock

4.2.2.2 Statistical Analyses

As is the case with any data set, one must consider the distribution of values when determining characteristic inputs for the purposes of downstream stability modelling. Accordingly, for each RMR_{89} grouping frequency distribution functions were produced. By way of example, a frequency distribution chart is presented in Figure 4.12 and Figure 4.13 based on the lithology types and weathering grades encountered.

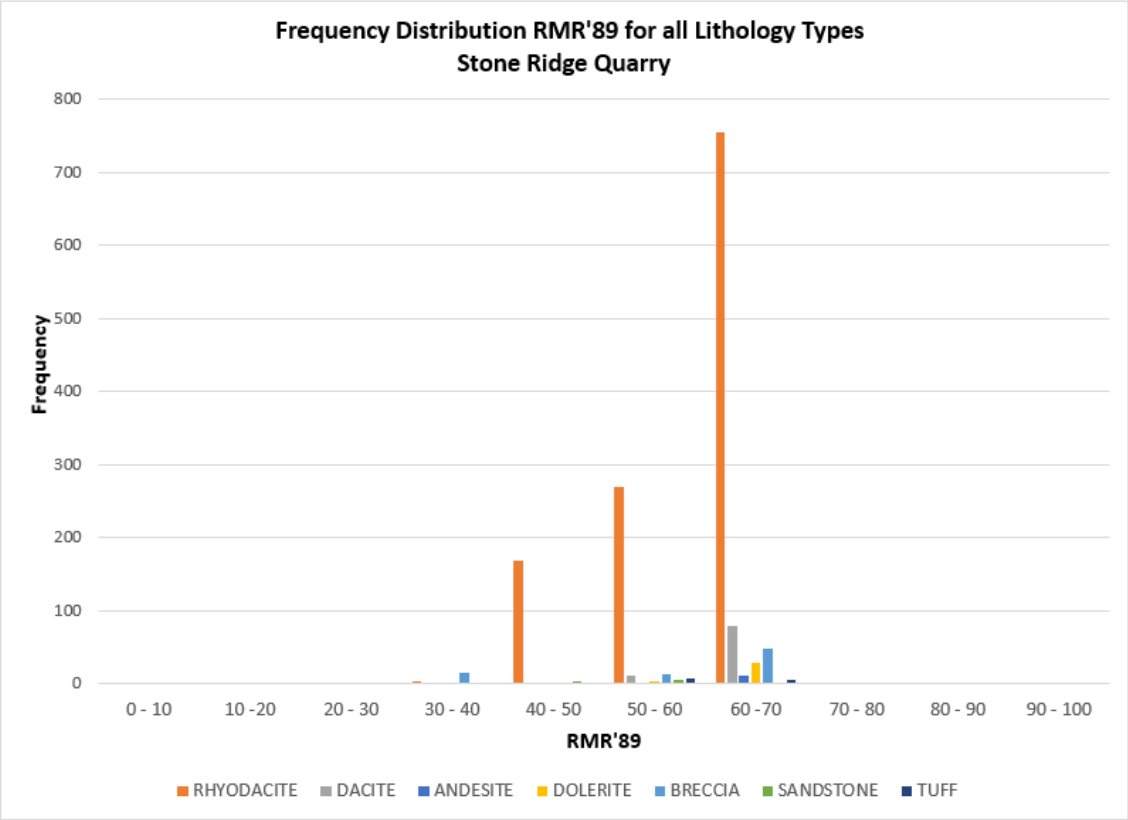

Figure 4.12 Example Frequency Distribution of RMR_{89} – for lithology types - Stone Ridge Quarry

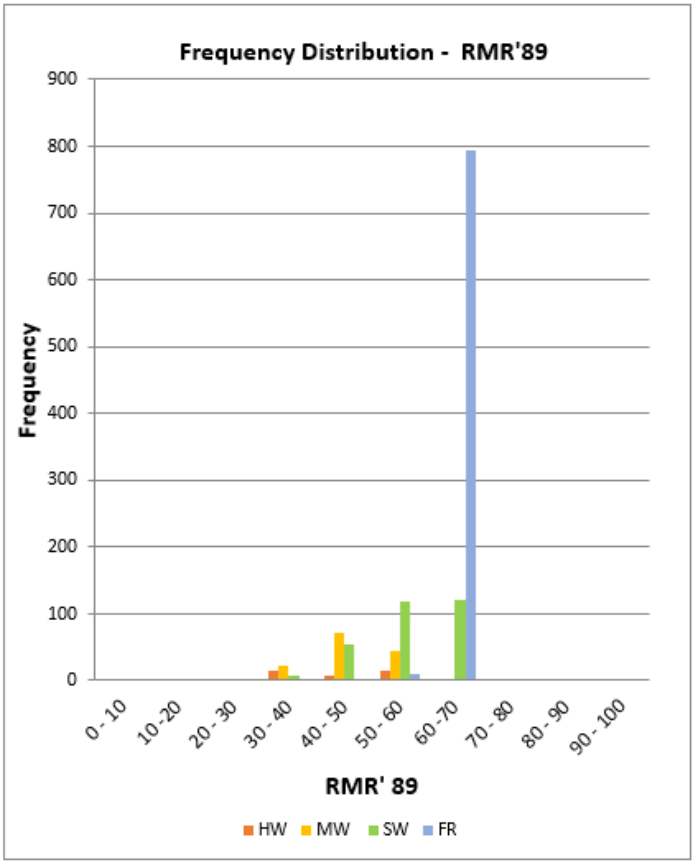

Statistical Parameter (RMR'89)	Weathering Grade			
	HW	*MW*	*SW*	*FR*
Mean	43.9	48.9	56.8	67.0
Standard Error	1.2	0.5	0.3	0.1
Median	44	50	59	68
Modal Class	40 - 50	40 - 50	50 - 60	60 - 70
Standard Deviation	7.1	5.6	6.0	2.1
Range	17	17	29	12
Minimum	34	40	35	56
Maximum	51	57	64	68
Sum	1535	6846	17272	53911
Count	35	140	304	805
Perc. 25%	39	45	55	68

Figure 4.13 Example Frequency Distribution of RMR_{89} – for all weathering grades - Stone Ridge Quarry

As shown in Figure 4.12 and Figure 4.13, the frequency distribution of the units is skewed, with the majority of the calculated RMR_{89} values falling in the 40-70 range. Typical descriptive statistical parameters used to describe characteristic values associated with frequency distributions include:

– Mean - average value of the data set
– Median - the number separating the higher half of the data set from the lower half
– Modal Class - the raw data unit (or range) that occurs most often within a data set

For approximately normal distributions, adoption of the mean/median value is typically used for the characteristic value, whereas when the distribution is skewed (left or right) (e.g., log-normal distribution), and/or the standard deviation is large, the modal class value tends to provide a better representation.

Based on the outcomes of the data reduction and statistical analyses, the **blue** RMR_{89} values presented in Table 4.5 were adopted for this assessment. These are aligned with the lower quartile (i.e., 25th percentile) of the respective data sets / distribution curves.

Table 4.5 Summary of Calculated RMR_{89} values

Stratigraphic Unit	Mean RMR	Minimum RMR	Median RMR	Maximum RMR	25th Percentile
HW	44	34	40	51	**39**
MW	49	40	50	57	**45**
SW	57	35	59	64	**55**
FR	67	56	69	68	**68**

4.2.2.3 Interpretation of Strength Functions – Generalised Hoek Brown

For the interpretation of rock mass strength, the GHB criterion was adopted, which was developed specifically for the characterisation of rock masses. RocScience's software package RSData v.1.004 was utilised to derive shear strength functions for the expected stress range. RSData generates a shear-normal function based on the GHB stress envelope, which is described by a set of empirical equations defined by a series of rock mass failure parameters, which are:

– Geological Strength Index (GSI) – describes the relationship between a rocks structure and surface quality, both of which are related to rock strength. According to Hoek *et al.* (1995) the RMR_{89} parameter is empirically related to the GSI parameter as follows:
  - $GSI = RMR_{89}$; $RMR_{89} \leq 23$,
  - $GSI = RMR_{89} - 5$; $RMR_{89} > 23$
– σ_{ci} – Uniaxial Compressive Strength (UCS) – determined utilising the field strength indices from the characteristics of weathering for the respective horizons, according to ISRM (1981). The following UCS values were adopted for the respective units:
  - HW Unit = 25
  - MW Unit = 50
  - SW Unit= 100
  - FR Unit = 175
– m_i – a material constant for intact rock mass which is defined as the ratio between UCS and Uniaxial Tensile Strength. A m_i value of 25 ± 3, was adopted which is based on typical m_i values for rhyolite / dacite. For the different weathering units, the following m_i values were adopted.
  - HW and MW Units = 22
  - SW and FR Units = 28
– *D* – Disturbance factor, which is related to the degree of disturbance to which the rock mass has been subjected during excavation. It varies from 0 for undisturbed in-situ rock masses to 1 for very disturbed. Based on the anticipated extraction method, a D-factor of 0.7 was adopted.

Appearance of rock mass	Description of rock mass	Suggested value of D
	Excellent quality controlled blasting or excavation by Tunnel Boring Machine results in minimal disturbance to the confined rock mass surrounding a tunnel.	D = 0
	Mechanical or hand excavation in poor quality rock masses (no blasting) results in minimal disturbance to the surrounding rock mass. Where squeezing problems result in significant floor heave, disturbance can be severe unless a temporary invert, as shown in the photograph, is placed.	D = 0 D = 0.5 No invert
	Very poor quality blasting in a hard rock tunnel results in severe local damage, extending 2 or 3 m, in the surrounding rock mass.	D = 0.8
	Small scale blasting in civil engineering slopes results in modest rock mass damage, particularly if controlled blasting is used as shown on the left hand side of the photograph. However, stress relief results in some disturbance.	D = 0.7 Good blasting D = 1.0 Poor blasting
	Very large open pit mine slopes suffer significant disturbance due to heavy production blasting and also due to stress relief from overburden removal. In some softer rocks excavation can be carried out by ripping and dozing and the degree of damage to the slopes is less.	D = 1.0 Production blasting D = 0.7 Mechanical excavation

Figure 4.14 Guidelines for Estimating Disturbance (D) Factor After Hoek et al. (2002)

The GHB shear strength function derived for each stratigraphic unit is presented below and the corresponding GHB shear strength parameters summarised and presented in Table 4.6 and Figure 4.15 respectively. It should be noted that most values adopted during this process are based on limited data, and subsequent sampling and testing should be undertaken to verify these parameters.

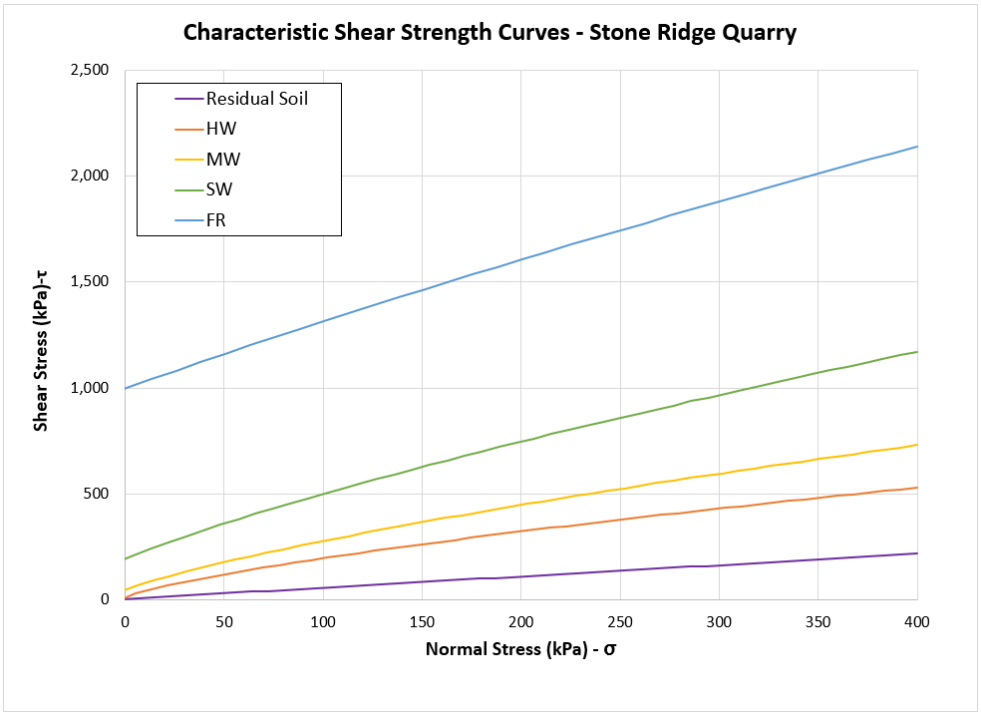

Figure 4.15 Rock Mass Shear Strength Curves – Stone Ridge Quarry

Table 4.6 Summary of GHB Shear Strength Parameters

GHB Parameter	HW	MW	SW	FR
GSI	34	40	50	63
σ_{ci}	25	50	100	175
m_i	22		28	
D	0.7			

4.2.3 Defect Plane Strengths

Shear strength parameters for defect planes have been interpreted using data obtained during the 2019 drilling campaigns. The shear strengths of defect planes were interpreted using the Barton-Bandis (1980) criterion, a non-linear mathematical function specifically derived for modelling the shear strength behaviour of defects in a rock mass. The Barton-Bandis (1980) equation is expressed by the following:

$$\tau = \sigma_n \cdot \tan\left(JRC \cdot \log_{10}\left(\frac{JCS}{\sigma_n}\right) + \phi_b\right)$$

Where:

t = Peak shear strength of a discontinuity

σ_n = Normal stress acting on discontinuity plane

JRC = Joint Roughness Coefficient

JCS = Joint Compressive Strength

ϕ_b = Basic friction angle

4.2.3.1 Joint Compressive Strength (JCS)

The JCS parameter is considered to be the Uniaxial Compressive Strength (UCS) of the rock wall, which is outlined in Table 4.7.

4.2.3.2 Basic Friction Angle (ϕ_b)

The basic friction angle (ϕ_b) parameter is the friction angle of a flat surface (an intrinsic property of the rock mass). A basic friction angle of 30° has been adopted for the Stone Ridge Quarry site, which is based on previous experience in dealing with similar materials.

4.2.3.3 JRC Parameter

The JRC parameter defines the roughness profile of the defect surface which ranges from 0 for smooth, planar, and slickenside surfaces to as much as 20 for rough undulating surfaces. Typical roughness profiles according to Barton and Choubray (1977) and JRC values are presented in Figure 4.16. Based on the information from the drill core logs, a JRC value of 4 was considered for the subsequent stability analyses.

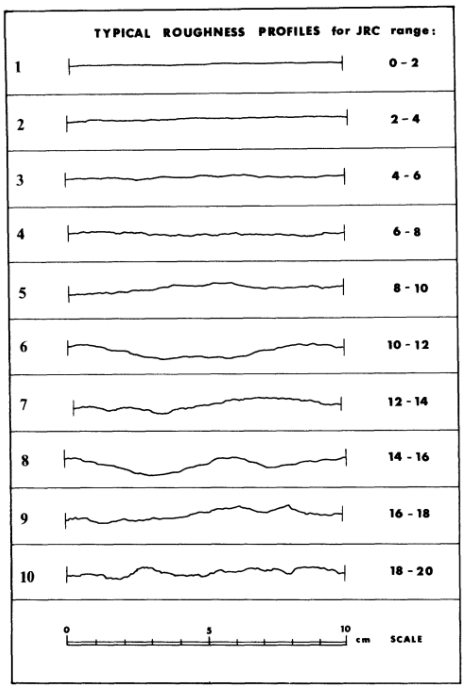

Figure 4.16 Roughness Profiles and Corresponding Range of JRC Values after Barton and Choubey (1977)

4.2.3.4 Barton and Bandis Parameters

Defect plane strengths only apply to rock mass with discernible structure, and therefore defect plane strengths were derived only for Units 2 to 5. Summarised in Table 4.7 are the Barton and Bandis parameters adopted for the Stone Ridge Quarry site.

Table 4.7 Summary of Barton and Bandis Defect Plane Strength Parameters

Unit	Description	Joint Compressive Strength – JCS (MPa)	Basic Friction Angle - ϕ_b (°)	Joint Roughness Coefficient - JRC
2	Highly Weathered (HW)	25	30	4
3	Moderately Weathered (MW)	50		
4	Slightly Weathered (SW)	100		
5	Fresh	175		

4.2.4 Soil Strength

According to the drill core logs, the overburden/residual soil within the Stone Ridge Quarry area is comprised predominantly of clays with minor proportion of silt and sand. Strength parameters for the in-situ overburden unit, were conservatively adopted based on GHD's experiences dealing with similar materials. The material parameters for the soil units are presented in the form of the Mohr Coulomb criterion in Table 4.8.

Table 4.8 Summary of Mohr Coulomb Parameters

Unit	Description	Cohesion – c' (kPa)	Friction Angle - ϕ' (°)
1	Overburden	5	28

4.3 Geotechnical Domain Model

A geotechnical domain model has been derived, which is shown below in Figure 4.17, along with the critical instability mechanisms. Table 4.9 summarises the kinematically feasible instability mechanisms for each of the quarry domains.

Table 4.9 Summary of Kinematically Feasible Instability Mechanisms for Proposed Stone Ridge Quarry Pit

Domain	Dip Direction (°)	Instability Mechanism
North Domain	140	**Primary:** Planar instability **Secondary:** Wedge, rock mass
East Domain	196	**Primary:** Wedge instability **Secondary:** Planar, Toppling, rock mass
South Domain	328	**Primary:** Planar and Wedge instability **Secondary:** Toppling, rock mass and composite instability
West Domain	58	**Primary:** Wedge instability **Secondary:** Toppling, planar, rock mass instability

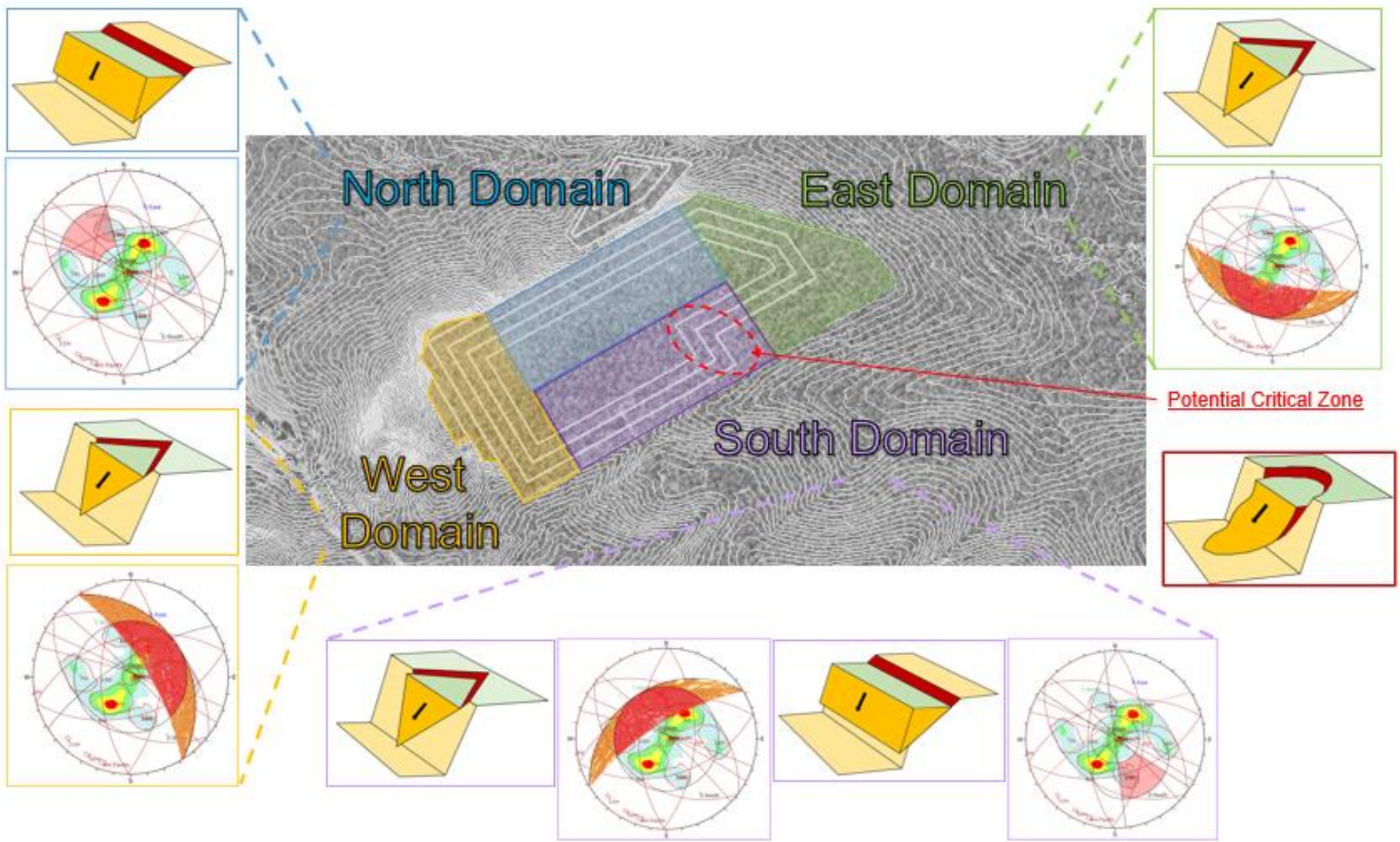

Figure 4.17 Stone Ridge Geotechnical Domain Model

5. Stability Analyses

RocScience's limit equilibrium software suite was used to assess long-term slope stability performance of the proposed Stone Ridge Quarry pit geometry. Stability analyses was undertaken to assess:

– The kinematic (structural) stability at the individual bench scale
– The overall slope scale

Slope stability performance was measured against nominated design acceptance criteria in line with state government guidelines.

Sensitivity analyses were undertaken on slope profiles to assess the potential instability implications associated with:

– Seismic loading events
– Elevated phreatic conditions
– Influence of pit lake level

Further discussion on each of the above sensitivities is provided in Section 5.5.

5.1 Design Acceptance Criteria

Prior to undertaking stability analyses, the design acceptance criteria (DAC) are nominated which defines the minimum requirements and limits for 'acceptable' risk and consequence levels with respect to the Factor of Safety (FoS). The DAC provides a metric for which stability performance can be assessed, and it should be noted that any slope design for open cut extraction necessitates finding a compromise between the risks associated with slope failure and the economics of mining.

– Design acceptance criteria for the proposed Stone Ridge Quarry have been nominated in line with accepted industry practice as outlined in 'Table 5' of the NSW Resource Regulator's '*Guide – Health and Safety at Quarries*' (2018). For the purpose of this assessment, a design FoS associated to:
    - Slope category 1 (i.e., moderately serious consequence on failure) was adopted for the kinematic stability analyses at the individual bench scale
    - Slope category 2 (i.e., serious consequence of failure) was adopted for the overall slope scale

Table 5.1 Design Acceptance Criteria (extracted from NSW Resource Regulator, 2018)

Wall Class	Consequence of Failure	Design FoS	Design PoF	Examples
1	Moderately serious	1.2	10%	Highwalls not carrying major infrastructure
2	Serious	1.5	1%	Highwalls carrying major infrastructure (e.g., treatment plant, ROM pad, tailings structures, crushing structures)
3	Serious*	2.0	0.3%	Permanent highwalls near public infrastructure and adjoining leases

*Where a mutually acceptable agreement to allow excavation cannot be made between the quarry or mine owner and the "owner" of the adjoining structure or plot of land. Note a higher standard of geotechnical data is required for the design of category 3 slopes compared to category 1 and 2 slopes.

5.2 Nominated Stability Sections

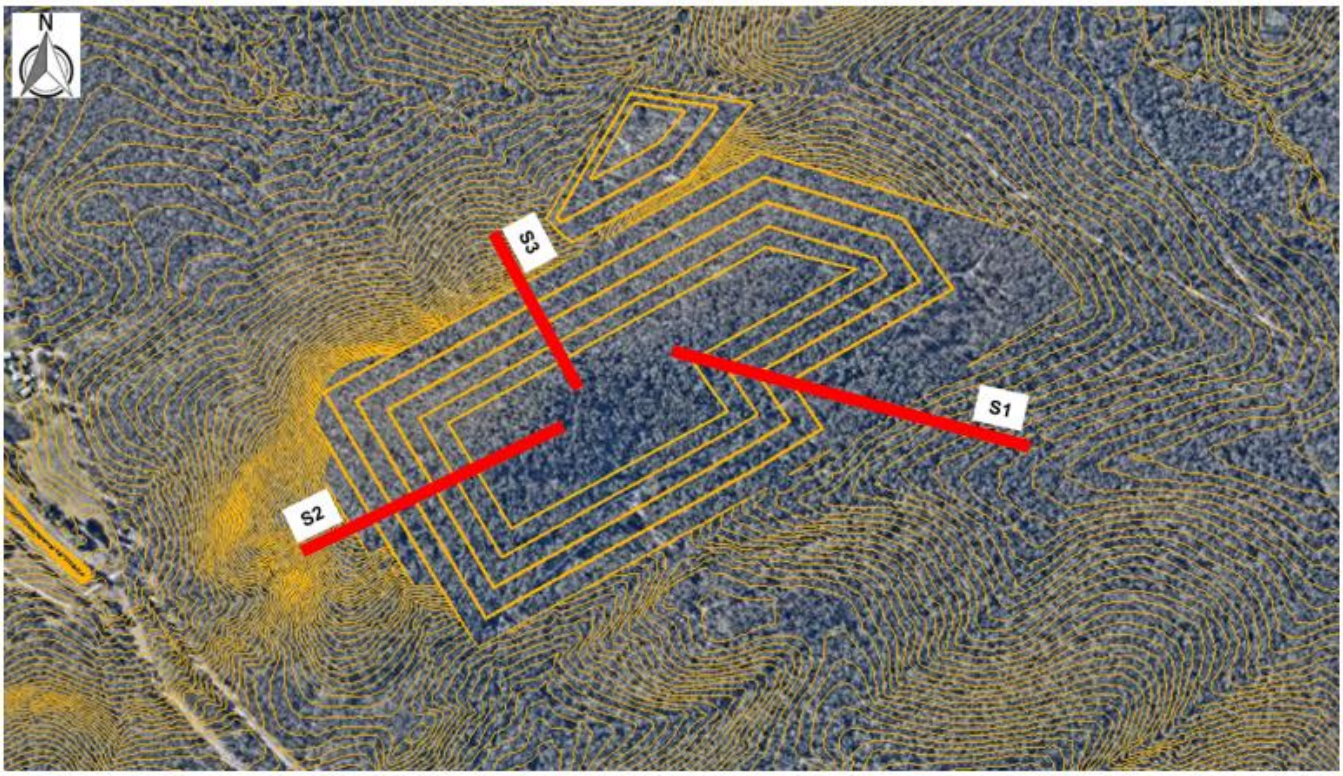

Figure 5.1 Plan View of Proposed Stone Ridge Pit Depicting Nominated Stability Sections

Three critical stability sections for the proposed quarry pit have been chosen for stability analyses. The bases for nomination are as follows:

- **Section S1** – Represents the critical convex vertex (bullnose) and potential interference with Faults ML1, ML2 and ML3
- **Section S2** – Represents the maximum overall slope height of the proposed quarry design
- **Section S3** – Represents the typical geometry along the north wall, which is the longest wall of the pit

5.2.1 Slope Stability Model Construction

The construction of a stability model incorporates and combines the elements of the subsurface geology, hydrogeology, material properties and slope design geometry as defined by the geotechnical model. Example cross-sections depicting a constructed stability model utilised in the assessment of slope stability is presented in Figure 5.2 to Figure 5.4.

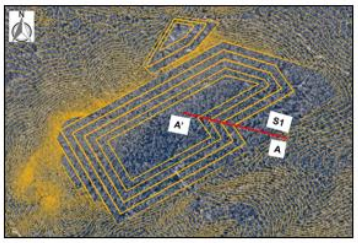

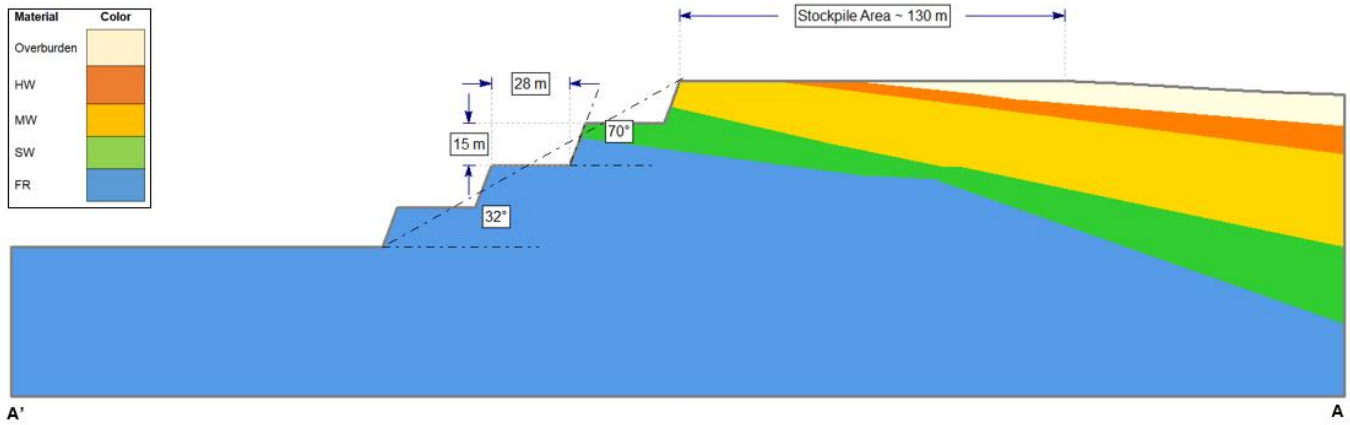

Figure 5.2 Example of Slope Stability Model – Section S1

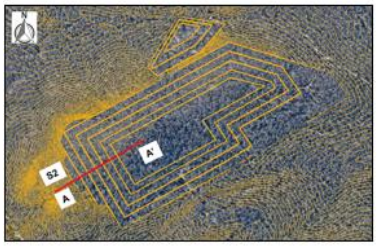

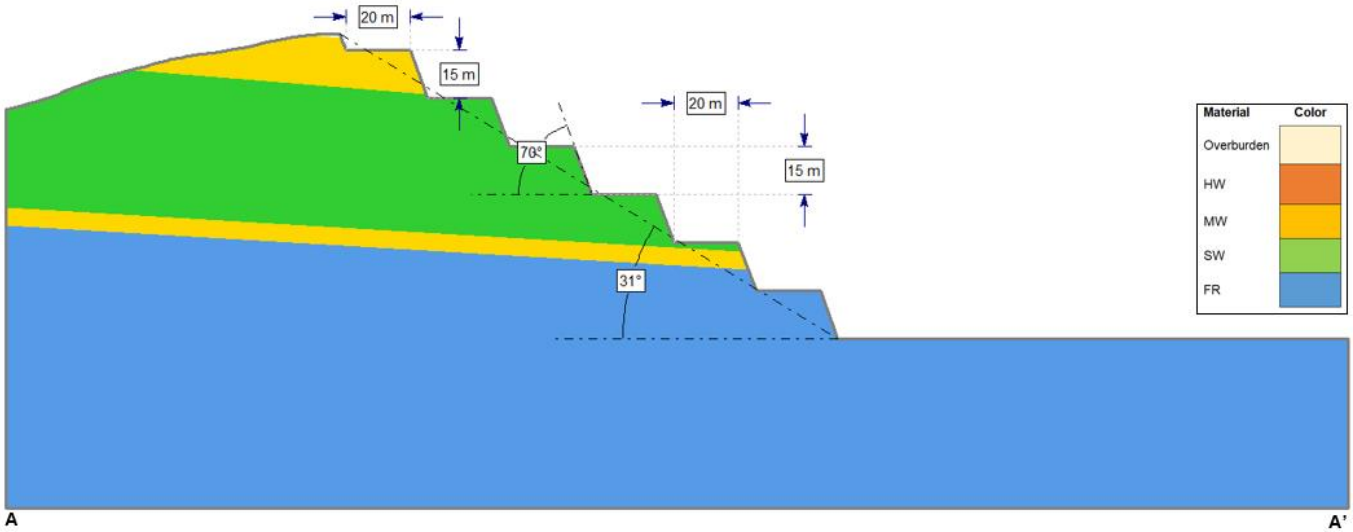

Figure 5.3 Example of Slope Stability Model – Section S2

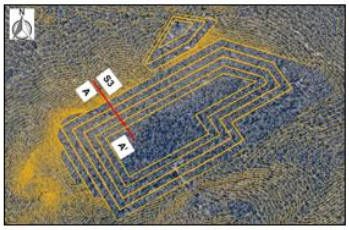

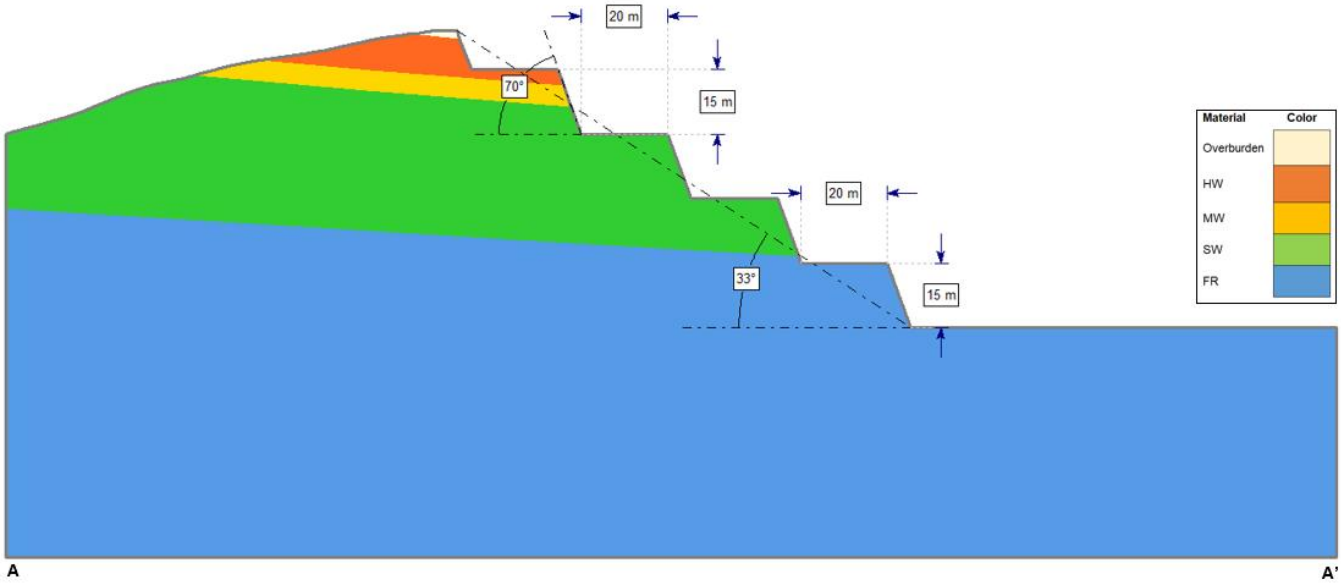

Figure 5.4 Example of Slope Stability Model – Section S3

5.3 Kinematic Analyses

When designing slopes in structurally controlled deposits, such is the case at Stone Ridge Quarry, it is crucial to ensure that the adopted batter-bench configuration is able to sufficiently catch and retain structural instability, where structural instability is inevitable and must be accounted for in the design process.

Kinematic stability analyses were undertaken to assess the stability performance of the proposed batter-bench configuration using 3D Limited Equilibrium (LE) modelling methods, which takes into account the orientation and design geometry of the slope relative to mapped structural defects. For a given defect set the entire range of possible orientations (i.e., angular deviation), can be accounted for to facilitate probabilistic analyses. Adopting such an approach allows for both the Factor of Safety (FoS) and Probability of Failure (PoF) to be calculated. Kinematic analyses were undertaken for each stratigraphic unit that has discernible structure (i.e., Units 2 to 5).

The following Rocscience LE software was utilised for undertaking individual batter scale assessments:

– RocPlane v 4.007 – Planar sliding
– Swedge v7.009 – Wedge sliding
– RocTopple v 2.004– Rock Toppling

Instability surfaces calculated as part of the kinematic assessment were used to define the critical structure orientations, i.e., dip angle and dip direction, which provide the requisite information to assess minimum bench width requirements, and thus assess the adequacy of the proposed pit geometry.

5.3.1 Planar Sliding

Planar sliding was identified to be a kinematically feasible structural instability mechanism for all wall orientations. Kinematic analyses considering the planar sliding mechanism was undertaken conservatively, where it was assumed that defect planes are orientated in the same direction as the slope face. Where multiple blocks were calculated to fall below unity (i.e., FoS < 1), only the critical block formation, i.e., minimum FoS, is reported along with the minimum bench width requirements.

Presented in Figure 5.5 is an example stability model output for the slopes in South Domain and depicted in Figure 5.6 is the corresponding minimum berm with plot.

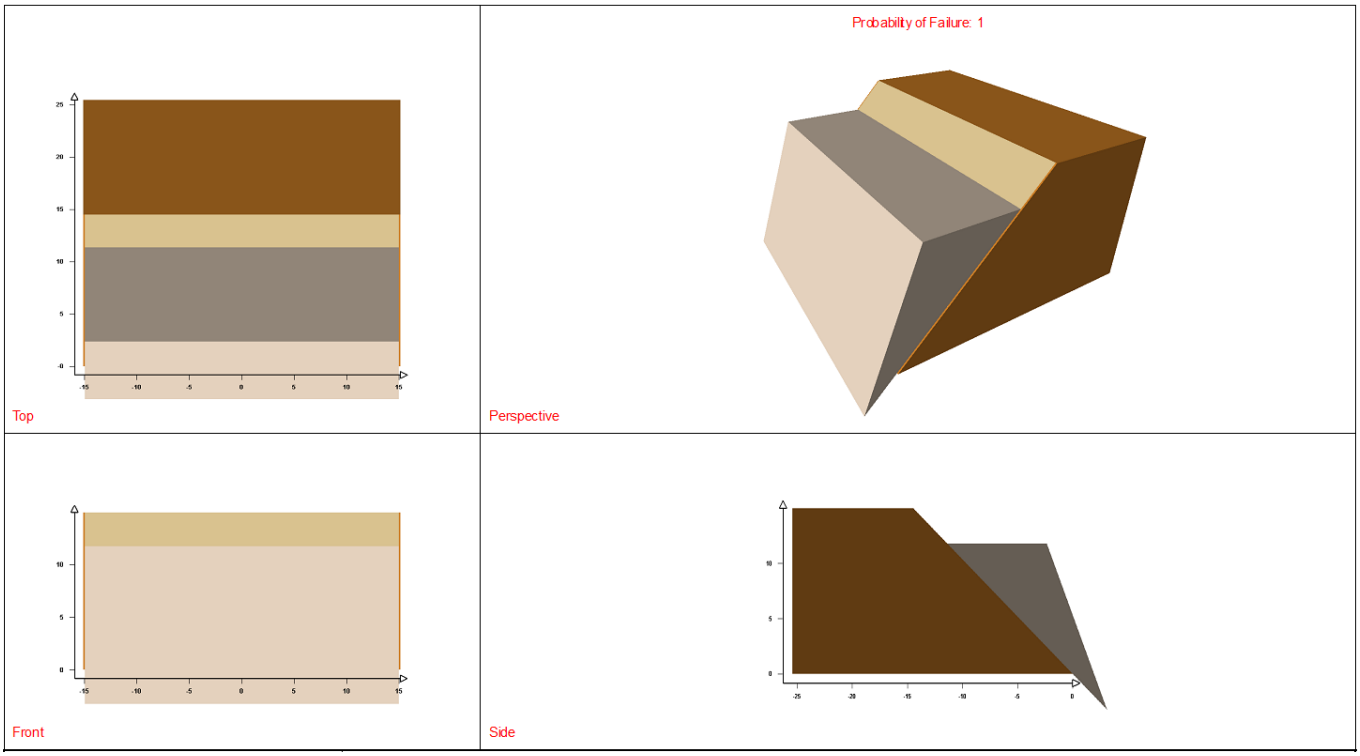

Figure 5.5 Example Stability Model Output for Planar Sliding – South Domain – Defect Set 6

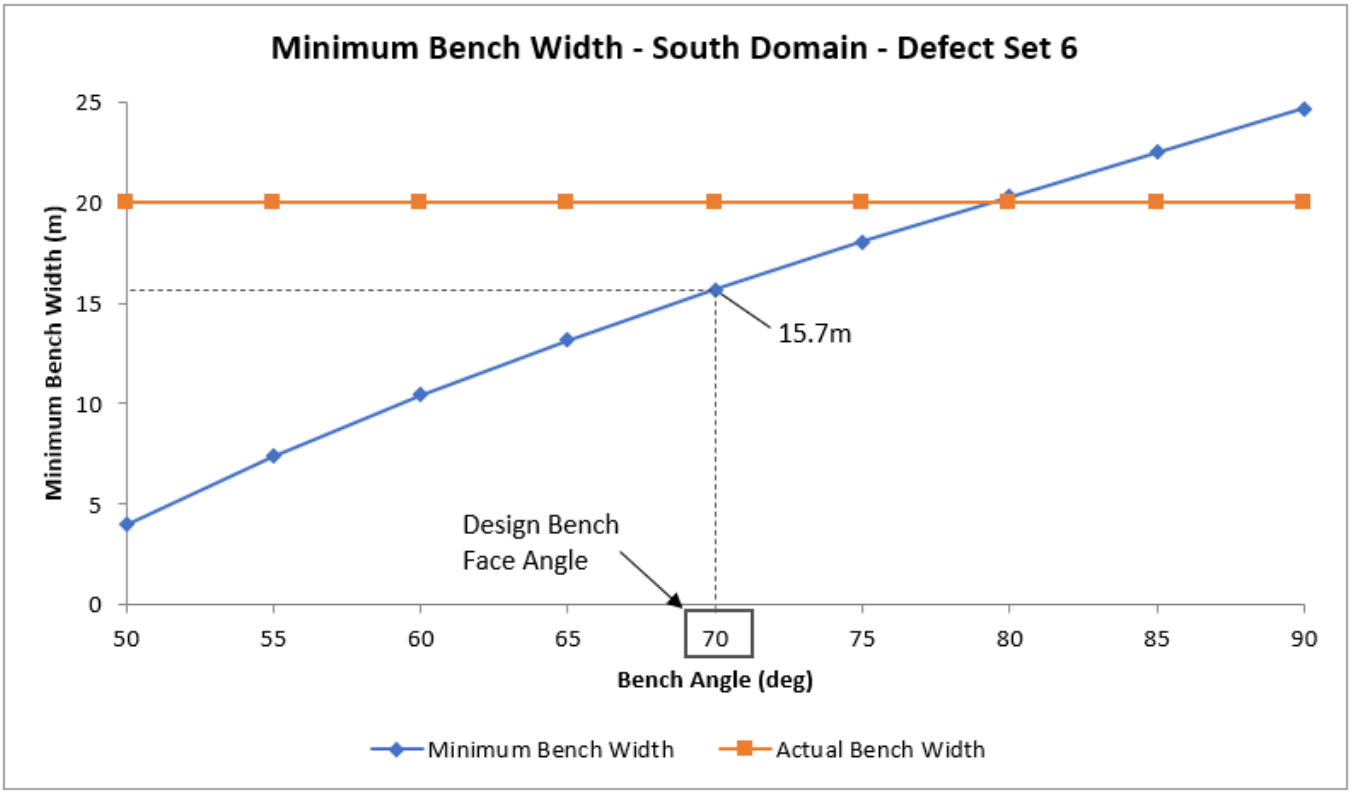

Figure 5.6 Example Minimum Bench Width Plot – South Domain – Defect Set 6

The results of the planar sliding analyses undertaken to assess the stability performance of the proposed batter-bench design configuration are presented below in Table 5.2.

Table 5.2 Summary of Planar Sliding Analyses Results

Domain	Critical Set ID	Weathering Grade	Min. FoS	PoF	Min. Bench Width (m)	Vol. of Instability (m^3/m)
North	Set 7	HW	0.82	100.0%	14.8	67
		MW	0.86	100.0%	14.8	
		SW	0.90	100.0%	14.8	
		Fr	0.93	100.0%	14.8	
East	Set 2	HW	1.23	< 0.1 %	<1	>100
		MW	1.28	< 0.1 %	<1	
		SW	1.34	< 0.1 %	<1	
		Fr	1.39	< 0.1 %	<1	
	Set 7	HW	0.82	100.0%	14.8	67
		MW	0.86	100.0%	14.8	
		SW	0.90	100.0%	14.8	
		Fr	0.93	100.0%	14.8	
South	Set 6	HW	0.85	100.0%	15.7	71
		MW	0.89	100.0%	15.7	
		SW	0.93	99.5%	15.7	
		Fr	0.96	98.5%	15.7	
West	Set 3	HW	0.62	100.0%	9.15	37
		MW	0.65	100.0%	9.15	
		SW	0.68	100.0%	9.15	
		Fr	0.70	100.0%	9.15	
	Set 4	HW	1.23	< 0.1 %	<1	>100
		MW	1.28	< 0.1 %	<1	
		SW	1.34	< 0.1 %	<1	
		Fr	1.39	< 0.1 %	<1	

The results of the planar sliding analyses indicate that:

– Under expected conditions, north, east, and south walls (i.e., excavations within the northern, eastern and southern domains), are more sensitive to planar sliding than the western wall.
– The minimum calculated bench width with respect to critical sets and weathering grade was calculated (to the nearest metre) to be 16 m.
– In general, the FoS increases and the PoF decreases where the degree of weathering decreases.
– Note that potentially larger volumes are calculated along the east wall.

5.3.2 Tetrahedral Wedge Analysis

Tetrahedral wedge sliding was identified to be a kinematically feasible instability mechanism for all wall orientations. The potential for wedge instabilities to occur along excavated faces was assessed for ‘representative’ batter orientations, which is conceptually nominated based on the wall extent, (e.g., maximum height and length), and the orientation most susceptible to kinematic instability within each domain.

The tetrahedral wedge sliding analyses presented in this section is considered conservative given that:

– Discontinuity systems are ubiquitous.
– Bedding planes are assumed to be infinitely long and linear i.e., does not account for defect waviness (undulations) or significant changes in defect orientation.
– Tertiary discontinuity systems (e.g., rock mass fracturing), that can form release planes are assumed to not be present.

It is noted that this analysis assumes that good blasting and scaling practices are employed.

Presented below in Figure 5.7 is an example stability model output for the excavated slopes located within the East Domain and presented in Figure 5.8 is the corresponding minimum bench width plot.

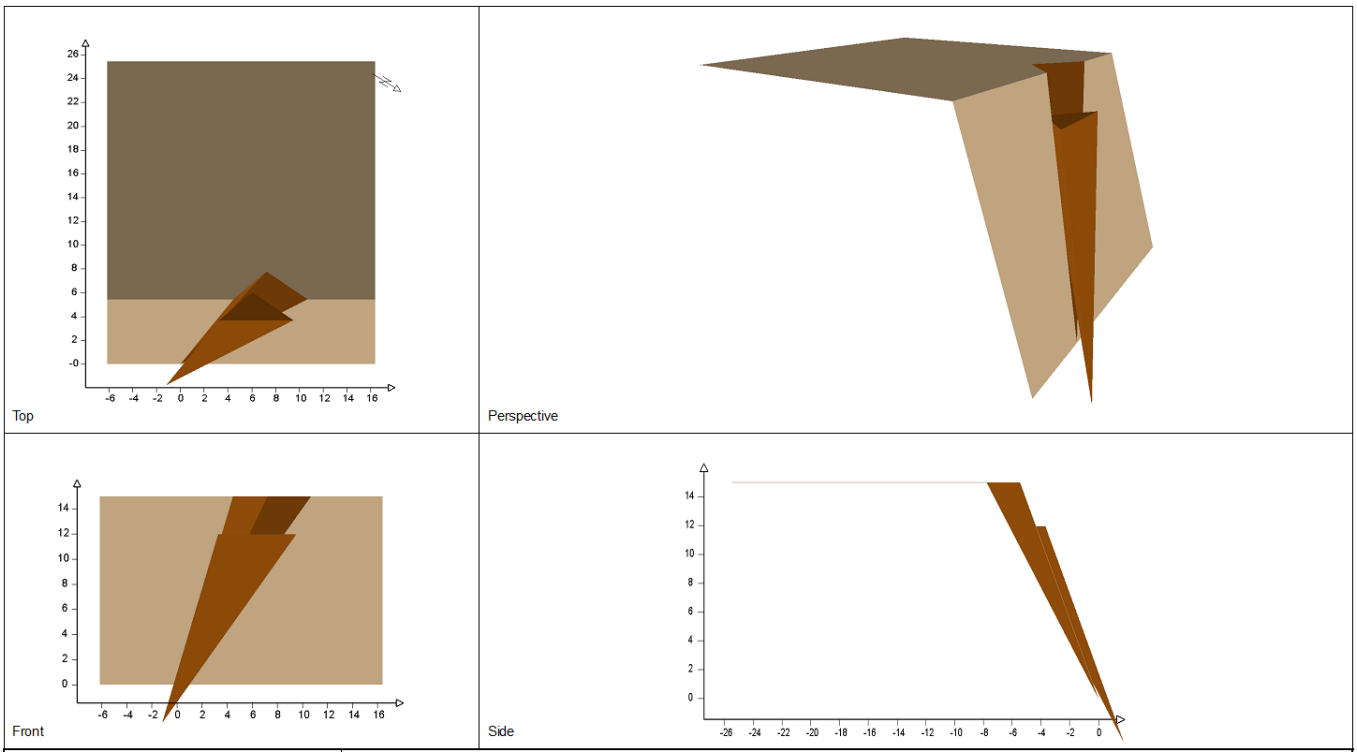

Figure 5.7 Example Stability Model Output for Wedge Sliding – East Domain – Defect Set 2 and Fault ML 4

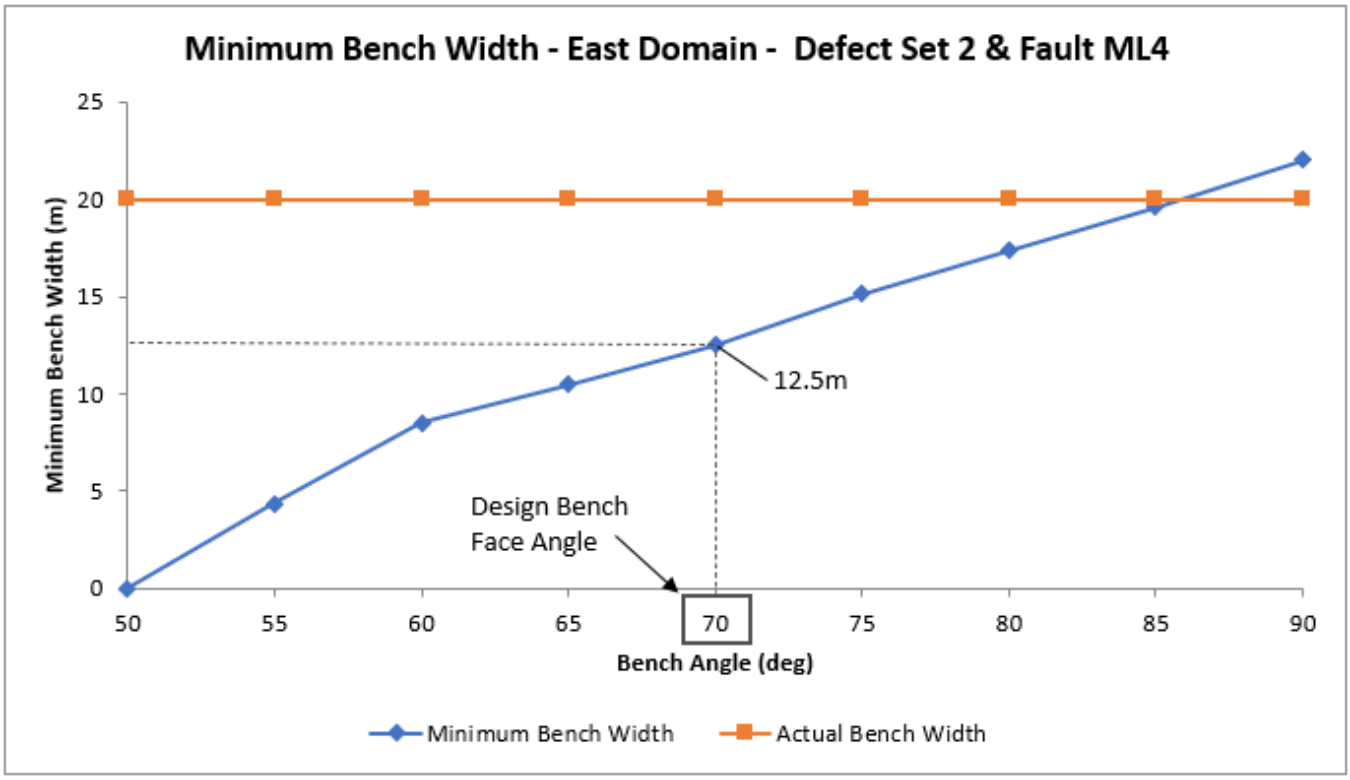

Figure 5.8 *Minimum Bench Width Plot - East Domain – Defect Set 2 and Fault ML 4*

The results of the wedge sliding analyses undertaken to assess the stability performance of the proposed batter-bench design configuration are presented in Table 5.3.

Table 5.3 *Summary of Kinematic Wedge Sliding Results*

Domain	Critical Set ID	Weathering Grade	Min. FoS	PoF	Min. Bench Width (m)	Vol. of Instability (m^3)
North	S2+S7	HW	0.90	43.8%	9.3	112.0
		MW	0.94	38.2%	9.2	
		SW	0.98	32.5%	9.0	
		Fr	1.01	27.0%	8.7	
	S5+S7	HW	0.88	50.0%	8.5	194.0
		MW	0.92	47.0%	8.4	
		SW	0.96	44.0%	8.16	
		Fr	0.99	40.0%	7.9	
	S3+Faults 1&2	HW	0.77	56.0%	4.6	11.9
		MW	0.80	52.0%	4.4	
		SW	0.83	49.0%	4.2	
		Fr	0.86	45.0%	4.0	
East	S2+S7	HW	0.90	49.0%	7.2	56.0
		MW	0.93	42.0%	6.9	
		SW	0.98	32.5%	6.6	
		Fr	1.10	29.0%	6.3	

Domain	Critical Set ID	Weathering Grade	Min. FoS	PoF	Min. Bench Width (m)	Vol. of Instability (m^3)
	S2+Fault 4	HW	0.58	1.0%	12.6	3.3
		MW	0.60	< 0.1 %	12.6	
		SW	0.63	< 0.1 %	12.6	
		Fr	0.65	< 0.1 %	12.5	
	S7+Fault 4	HW	0.68	2.0%	4.7	18.2
		MW	0.70	< 0.1 %	4.6	
		SW	0.74	< 0.1 %	4.6	
		Fr	0.76	< 0.1 %	4.6	
South	S2+S5	HW	0.78	0.3%	5.98	10.2
		MW	0.81	0.2%	5.98	
		SW	0.85	0.2%	5.98	
		Fr	0.88	< 0.1 %	5.98	
	S5 + Faults 1&2	HW	0.86	66.5%	6.1	53.6
		MW	0.89	62.0%	5.8	
		SW	0.92	57.0%	5.55	
		Fr	0.94	53.0%	5.4	
West	S3+S7	HW	0.46	15.0%	6.4	98.7
		MW	0.48	13.8%	6.3	
		SW	0.50	11.8%	6.1	
		Fr	0.52	10.0%	6.0	
	S3 + Faults 1&2	HW	0.65	80.0%	6.1	36.2
		MW	0.68	80.0%	6.0	
		SW	0.71	78.0%	5.8	
		Fr	0.73	75.0%	5..7	

The results of the tetrahedral wedge sliding analyses indicate that:

– Under expected conditions, south and west walls were calculated to be comparatively more sensitive (with PoF > 50%) to tetrahedral wedge sliding compared to the other walls.
– The minimum calculated bench width with respect to critical sets and weathering grade was calculated (to the nearest metre) to be 13 m.
– In general, the FoS increases and the PoF decreases where the degree of weathering decreases.
– The volume of instability was calculated to be of limited scale/volume where good blasting and scaling practices are employed.

5.3.3 Toppling Analysis

Block-flexural toppling was identified to be a kinematically feasible structural instability mechanism for the east wall. The rock toppling analyses presented within this section are considered to be conservative where the critical defect structures are orientated in the same direction as the slope. The results of the toppling analyses are presented as a series of charts which to reflect the stability performance of excavated slopes with respect to the weathering grade, as shown in Figure 5.9.

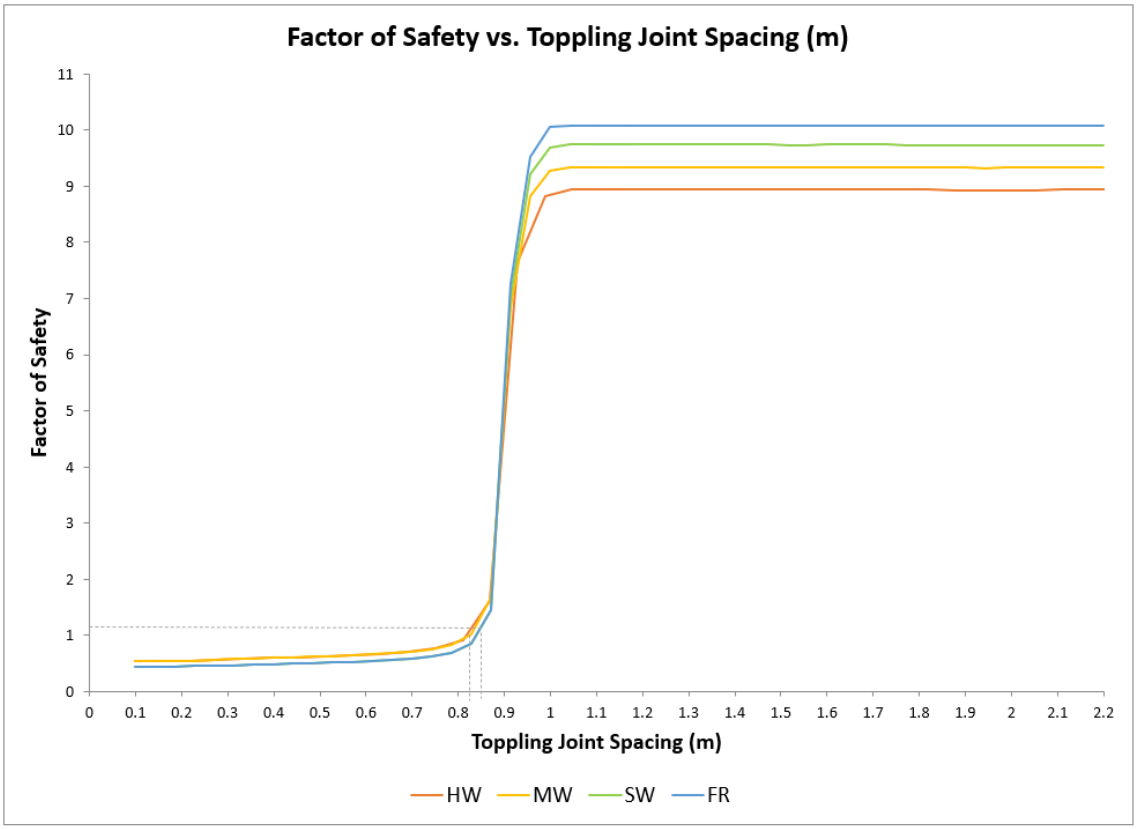

Figure 5.9 Influence of Defect Set Spacing on Stability Performance – Rock Toppling

The results of the rock toppling analyses indicate that:

– Where the spacing of toppling joints occurs in the range of 0.8 m to 0.85 m or less, the likelihood of toppling becomes notably higher as the calculated FoS falls below 1.2 for all stratigraphic units.
– Note that for this mechanism to be kinematically feasible, the sub-vertical joint set needs to be orientated, i.e., have a dip direction of ±10 to 15° of the slope face.

5.3.4 Summary of Kinematic Analyses Results

The results of the kinematic analyses indicate that:

Planar Sliding

– Under expected conditions, north, east and south walls i.e., excavations within the northern, eastern and southern domain, are comparatively more sensitive to planar sliding than the western wall.
– The minimum calculated bench width with respect to critical sets and weathering grade was calculated (to the nearest metre) to be 16 m.
– In general, the FoS increases and the PoF decreases where the degree of weathering decreases.
– Note that potentially larger volumes are calculated along the east wall.

Tetrahedral Wedge Sliding

– Under expected conditions, south and west walls were calculated to be comparatively more sensitive (PoF > 50%) to tetrahedral wedge sliding compared to other walls.
– The minimum calculated bench width with respect to critical sets and weathering grade was calculated (to the nearest metre) to be 13 m.
– In general, the FoS increases and the PoF decreases where the degree of weathering decreases.
– The volume of instability was calculated to be of limited scale/volume where good blasting and scaling practices are employed.

Rock Toppling

– Where the spacing of toppling joints occurs in the range of 0.8 m to 0.85 m or less, the likelihood of toppling becomes notably higher as the calculated FoS falls below 1.2 for all stratigraphic units.

In summary, the outcomes of the kinematic analyses indicates that a minimum bench width of 16 m is required to ensure there is adequate catch capacity to retain potentially dislodged material to a single bench. As outlined in Section3, the proposed Stone Ridge Quarry pit design incorporates 20 to 30 m benches at the individual bench scale, which satisfies the minimum bench width requirements.

5.4 Global Slope Stability Analysis Results

Slope stability analyses has been performed under 'expected' conditions which are the in-situ stress conditions known to, or likely to exist at the time of the 2019 drilling campaigns. The stability performance of slopes at the individual and overall slope scale were assessed and compared against the nominated Design Acceptance Criteria (DAC). The following colour coding has been adopted to denote conformance to the DAC.

– Green – The calculated stability performance satisfies the "Serious Consequence of Failure" DAC (FoS > 1.5, PoF<1%).
– Amber - The calculated stability performance satisfies the "Moderately Consequence of Failure" DAC (FoS > 1.2, PoF<10%).
– Red – The calculated stability performance does not satisfy the "Moderately Consequence of Failure".

The results of the stability analyses on slopes along Section S1, S2 and S3 are summarised in Table 5.4 and the corresponding stability model outputs are presented in Figure 5.10 to Figure 5.12 .

Table 5.4 Summary of Stability Analyses Results – Critical cross sections - Stone Ridge Quarry

Stability Section	DAC	Overall Slope Angle (°)	Scale of Instability	Calculated FoS
S1	FoS > 1.5	32	Individual	1.55
			Overall slope	3.27
S2		31	Individual	2.77
			Overall slope	5.08
S3		33	Individual	3.69
			Overall slope	6.66

The results of the stability analyses undertaken under 'expected' condtions indicate that:

– The stability performance at the individual and overall slopes scales satisfy the nominated design acceptance criteria for all asessed stability sections (i.e., Sections S1, S2, and S3).

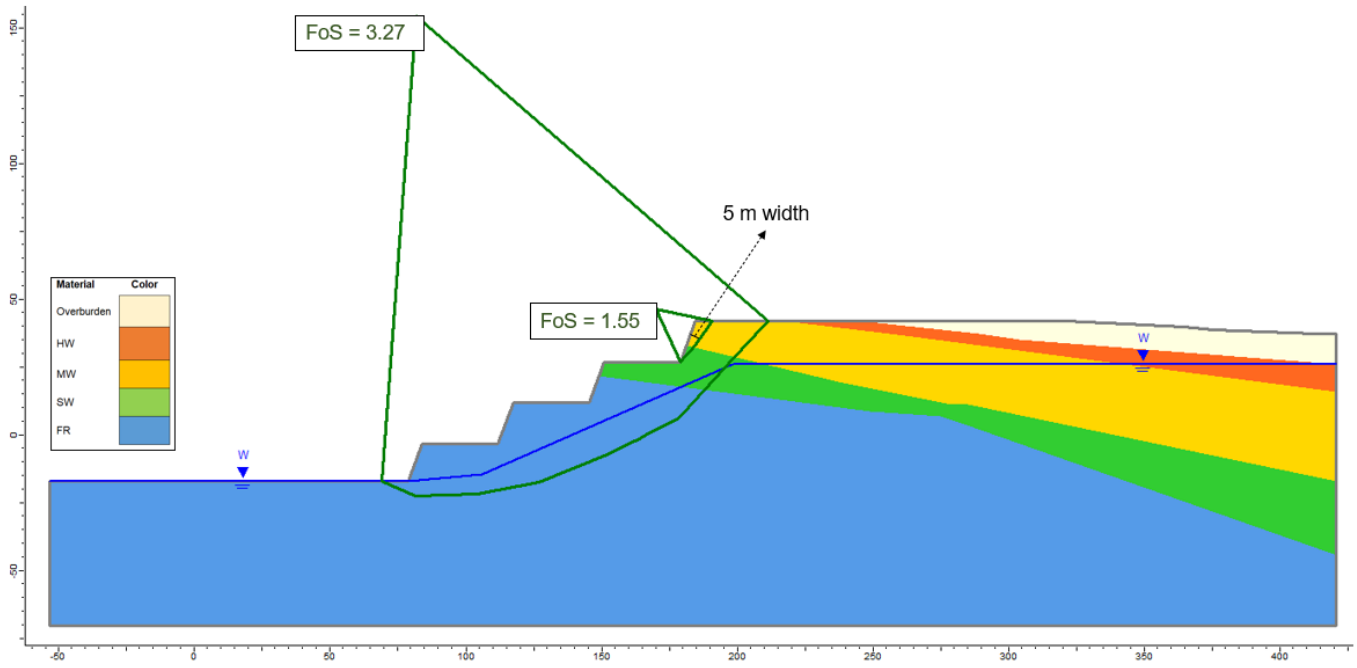

Figure 5.10 Stability Model Output – Stability Section S1

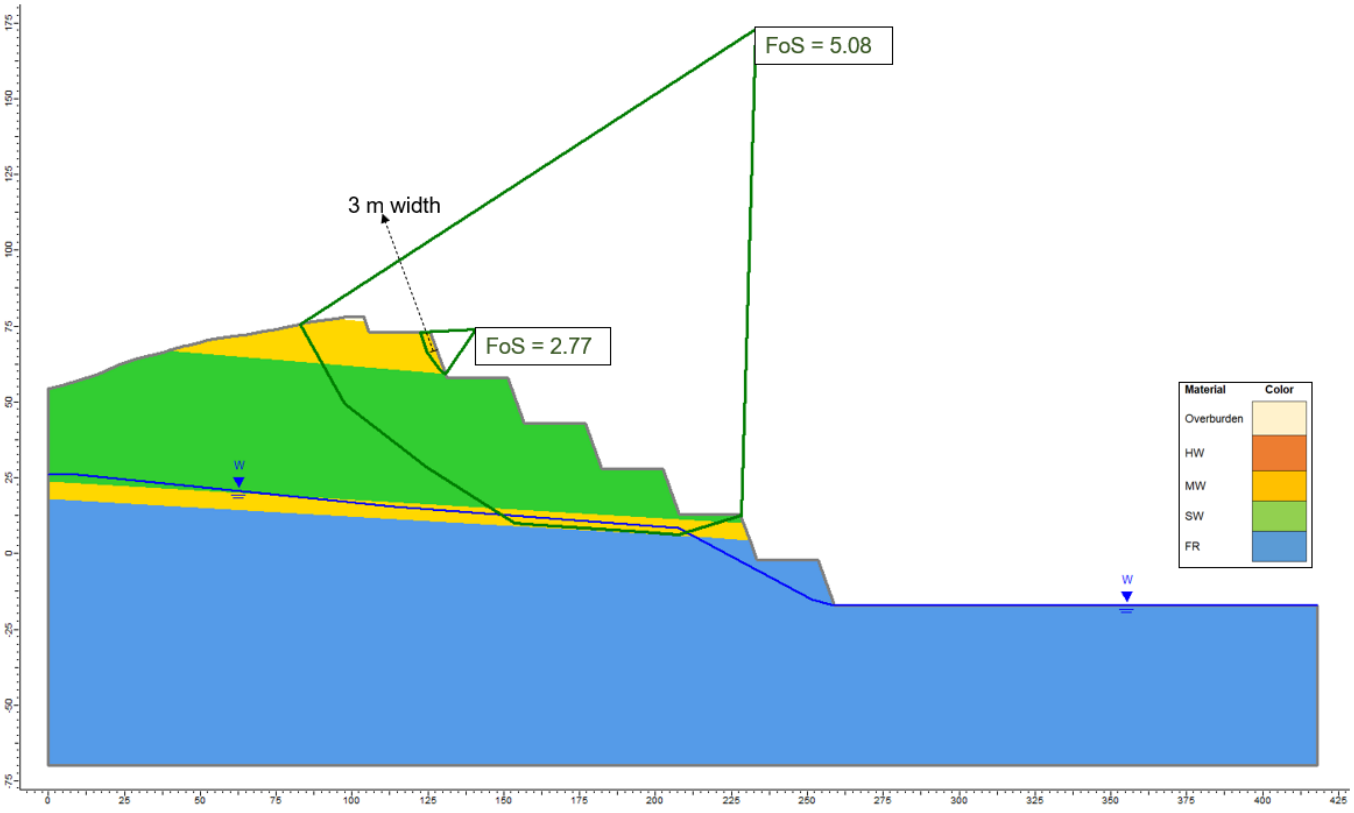

Figure 5.11 Stability Model Output – Stability Section S2

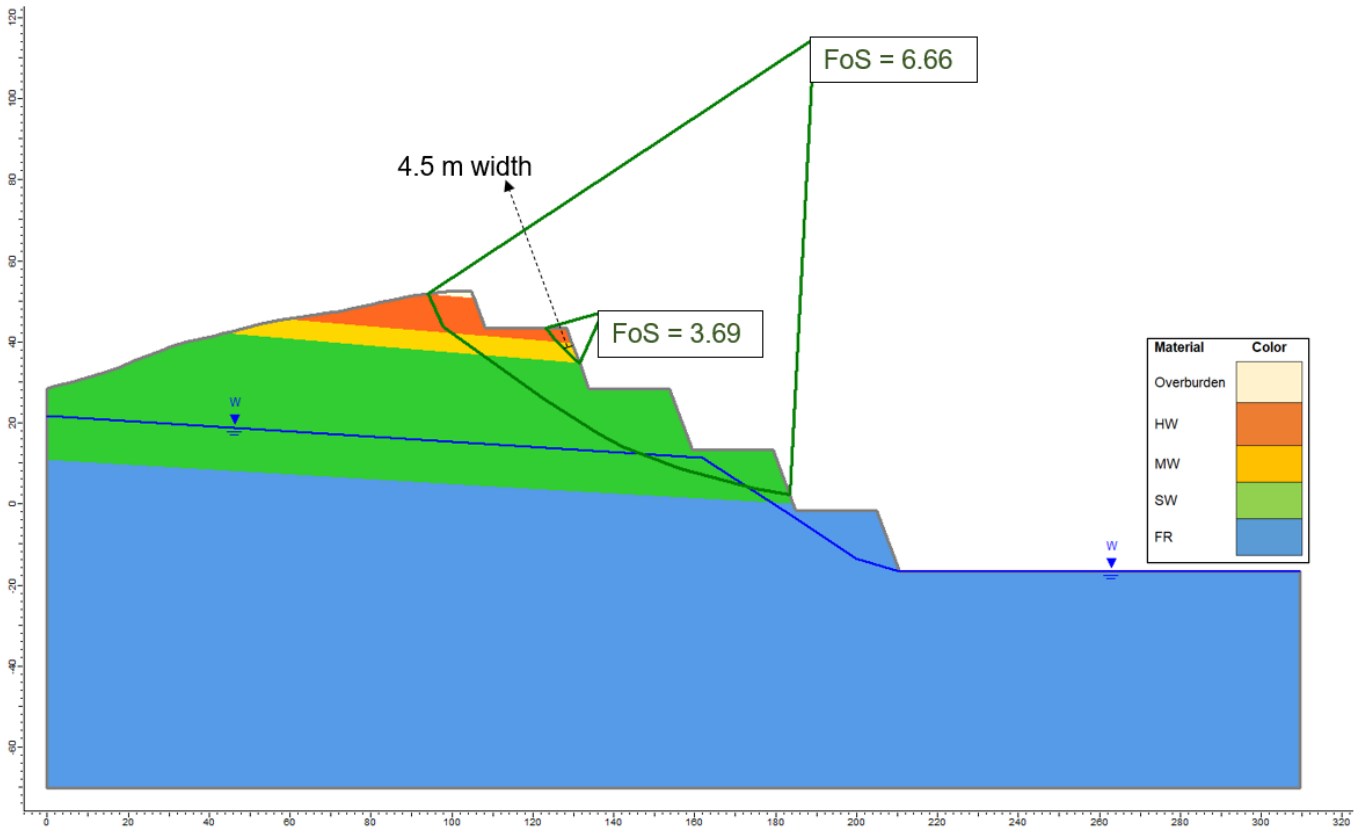

Figure 5.12 Stability Model Output – Stability Section S3

5.5 Sensitivity Analyses

Sensitivity analyses have been undertaken to assess the potential stability implications associated with:

– Seismic loading events
– Elevated phreatic conditions
– Influence of pit lake level

5.5.1 Seismic Loading

Sensitivity analyses have been undertaken to assess the potential stability implications associated with seismic loading events on the slope stability performance. A 1:500-year return event or 'expected' seismic loading event was considered.

A pseudo-static seismic analysis approach was adopted following the methodology outlined by Hynes-Griffin and Franklin (1984), referred to as the USACE method, which assumes:

– Earthquakes can be modelled as a static force acting on the mass of potential slide
– No dynamic pore water pressures are generated
– Materials show no significant loss of strength as a result of cyclic loading

When undertaking a pseudo-static seismic analyses, Hynes-Griffin and Franklin (1984) recommend using a seismic coefficient equal to half of the Peak Ground Acceleration (PGA). PGA values for a 1:500-year event was obtained from the National Seismic Hazard Assessment (NSHA, 2018) maps. An example of the NSHA (2018) seismic hazard atlas map is depicted in Figure 5.13 for a 1:500-year return event.

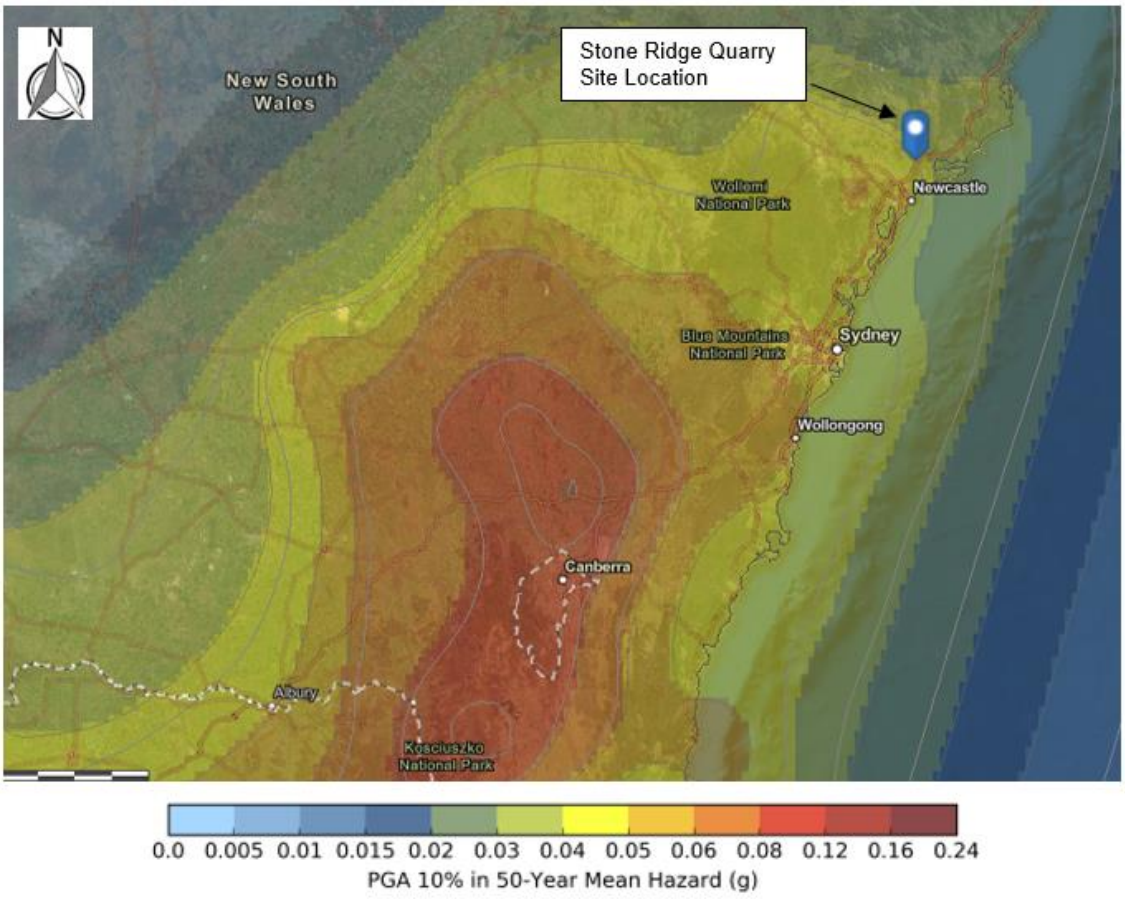

Figure 5.13 Seismic Hazard Atlas Map (1:500-year) Stone Ridge Quarry, after NSHA (2018)

Summarised in Table 5.5 are the PGA and seismic coefficient values adopted for this sensitivity analyses. It should be noted that seismic sensitivity analyses considered the overall scale slope stability performance only.

Table 5.5 Summary of Seismic Input Parameters

Return Interval	Peak Ground Acceleration (g) - PGA	Seismic Coefficient - H_z
1:500	0.044	0.022

The results of the seismic sensitivity analyses are summarised in Table 5.6 below and the corresponding stability model outputs are presented in Figure 5.14 to Figure 5.16.

Table 5.6 Summary of Sensitivity Analyses Results – Seismic Loading

Stability Section	Return Event Period	DAC	Calculated FoS
S1	1:500	FoS > 1.1	3.10
S2			4.81
S3			6.39

The results of the seismic loading sensitivity analsyes indicate that:

– A decrease in the slope stability performance was calculated for all stability sections assessed when comapred to the 'expected' conditions. However, the stability performance was calculated to satisfy the design performance objectives (i.e., FoS > 1.1).

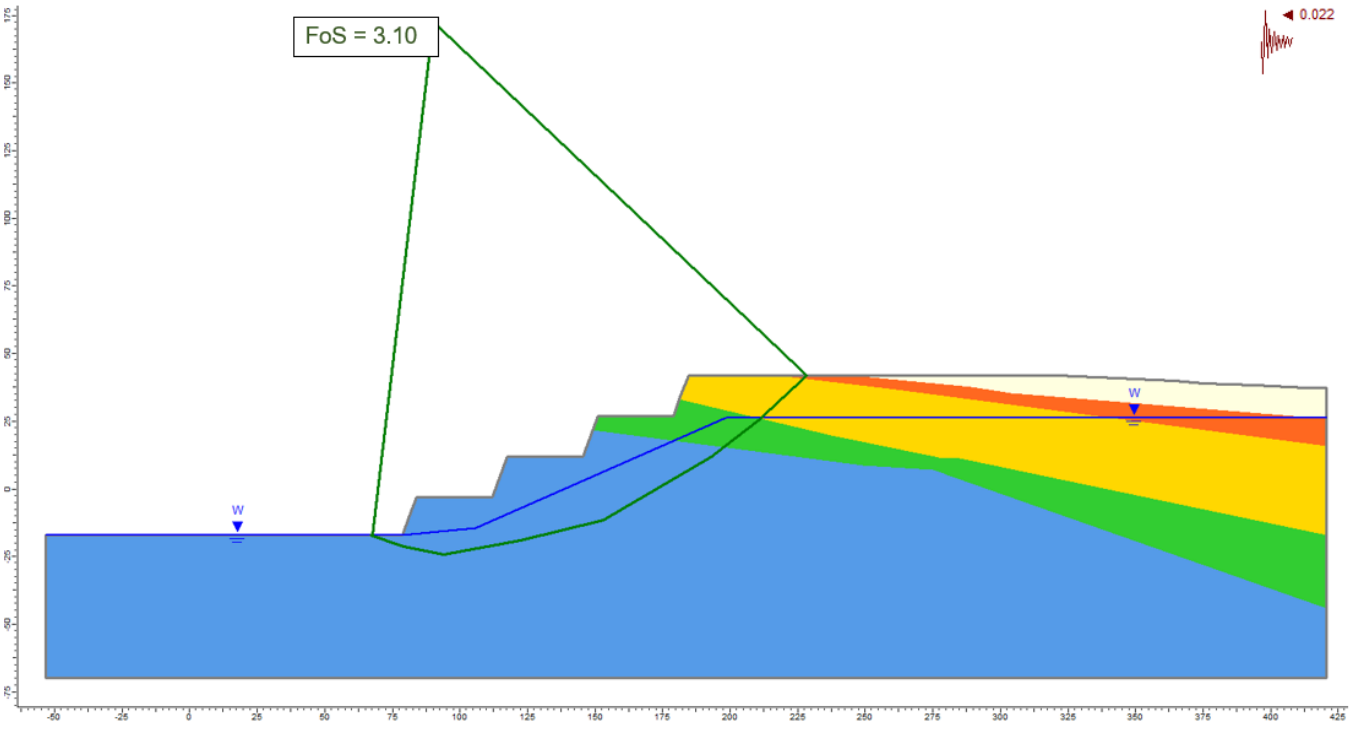

Figure 5.14 Sensitivity Model Output – Seismic Loading (1:500-year) – Section S1

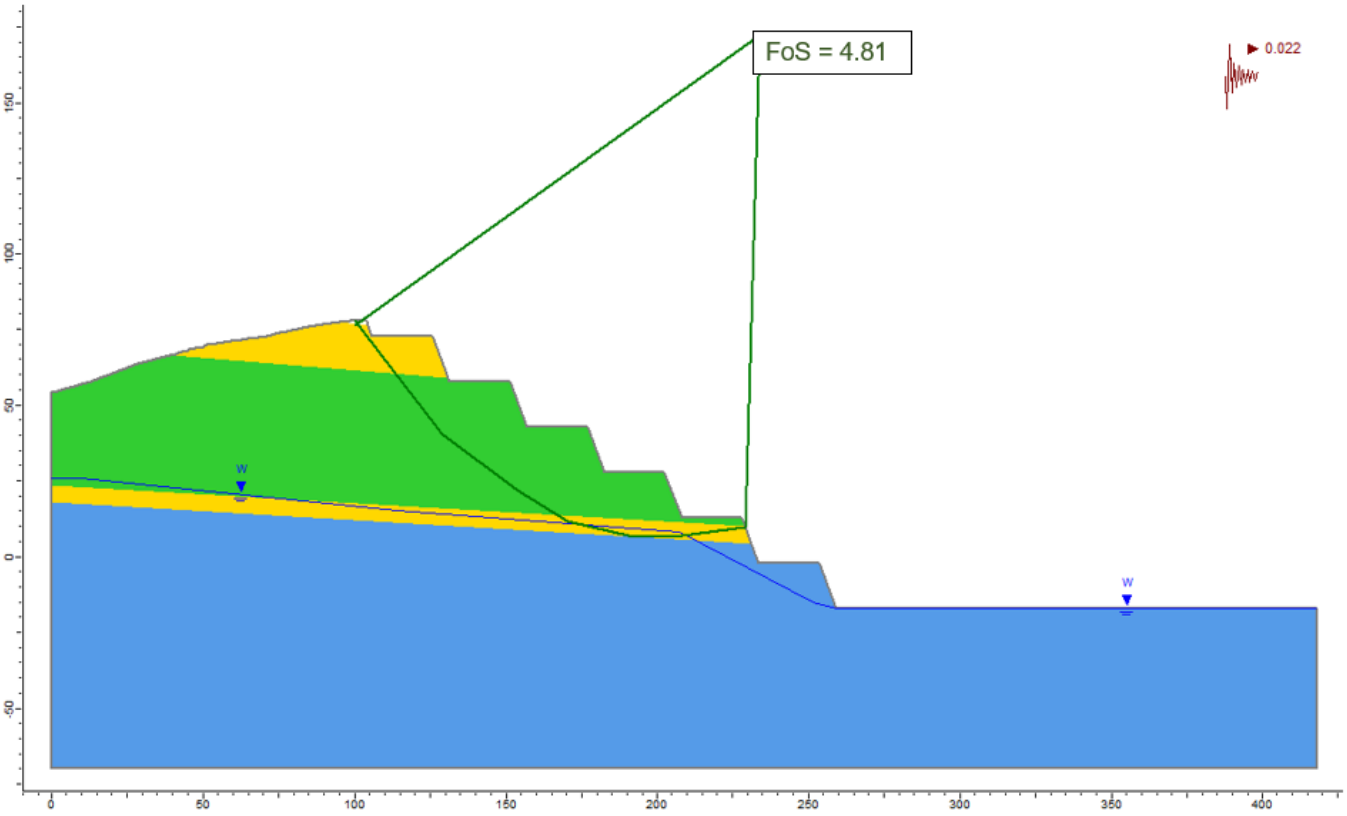

Figure 5.15 Sensitivity Model Output – Seismic Loading (1:500-year) – Section S2

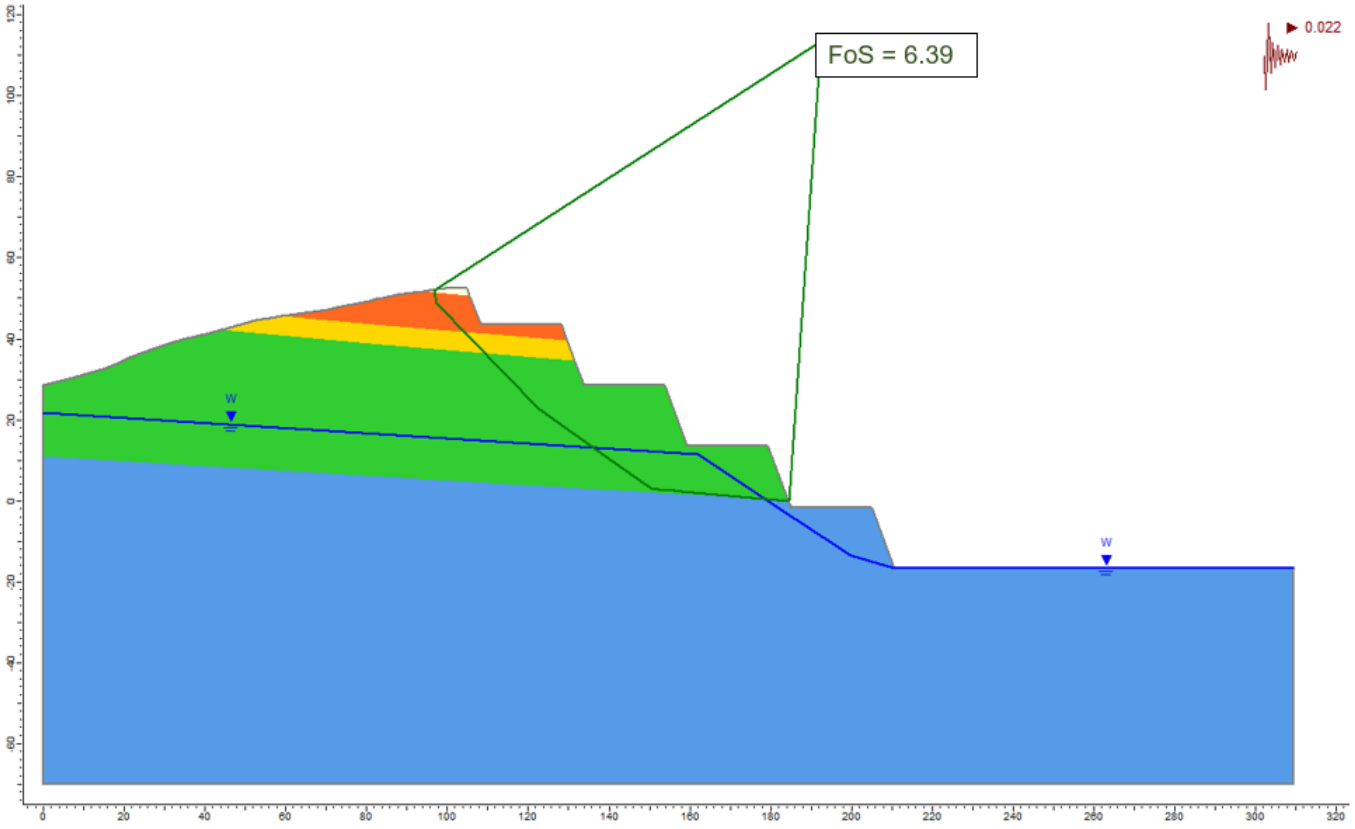

Figure 5.16 Sensitivity Model Output – Seismic Loading (1:500-year) – Section S3

5.5.2 Elevated Phreatic Conditions

Sensitivity analyses have been performed to assess the potential stability implications associated with elevated phreatic conditions, where a fully saturated 'worst case' scenario was adopted. A fully saturated scenario may reflect potential deficiencies in surface and groundwater management protocols during intense and/or prolonged rainfall events.

The results of the elevated phreatic conditions sensitivity analyses are summarised in Table 5.7 and the corresponding stability model outputs are presented in Figure 5.17 to Figure 5.19.

Table 5.7 Summary of Sensitivity Analyses Results – Elevated Phreatic Conditions

Stability Section	Scale of Instability	Calculated FoS*
S1	Overall slope	2.51
S2	Overall slope	3.22
S3	Overall slope	4.70

The results of the elevated phreatic condition sensitivity analyses indicate that:

– A reduction in the slope stability performance was calculated under 'worst case' fully saturated conditions compared to 'expected' conditions for all assessed stability sections.
  - At the overall slope scale the stability performance was calculated to be above unity (FoS > 1) for all stability sections.
  - The results of the elevated phreatic condition sensitivity analyses highlight the importance of implementing and maintaining adequate surface and groundwater management protocols which are integrated into the final landform design.

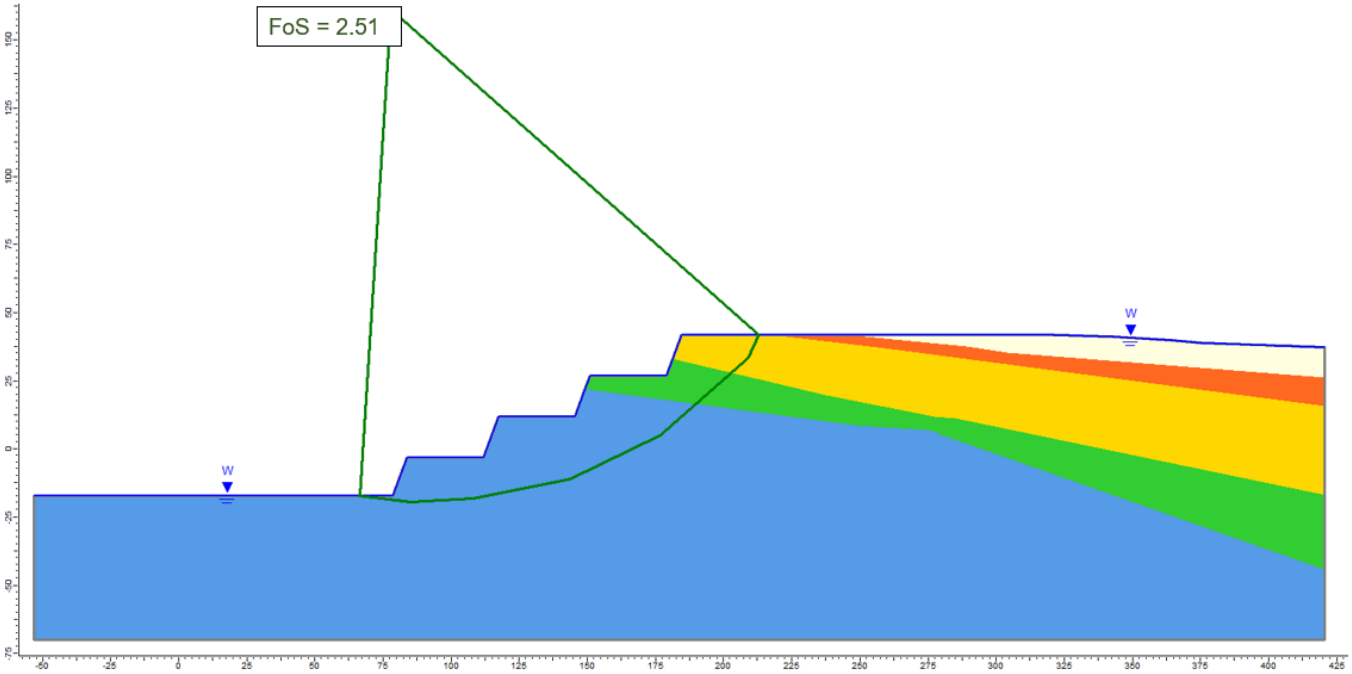

Figure 5.17 Sensitivity Model Output - Elevated Phreatic Conditions – Section S1

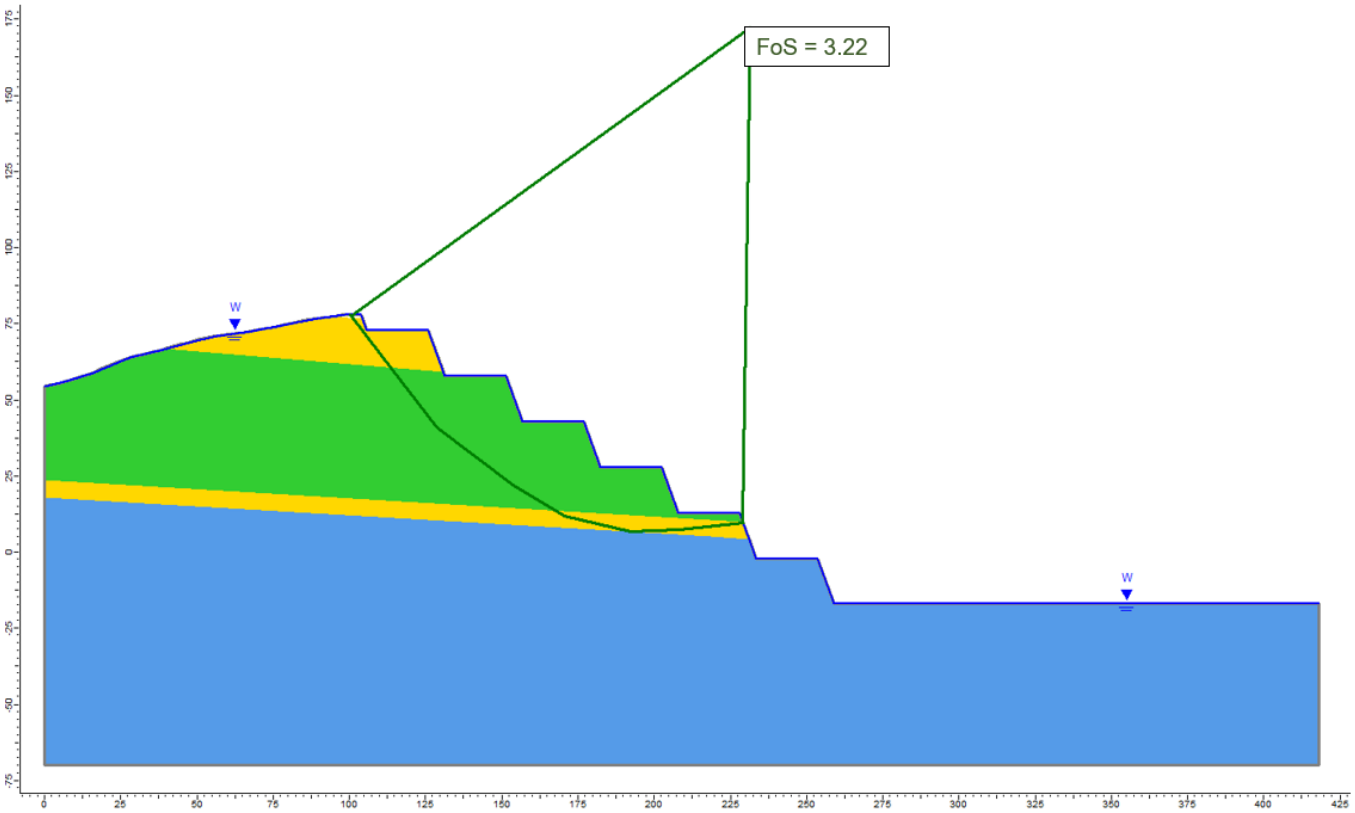

Figure 5.18 Sensitivity Model Output - Elevated Phreatic Conditions – Section S2

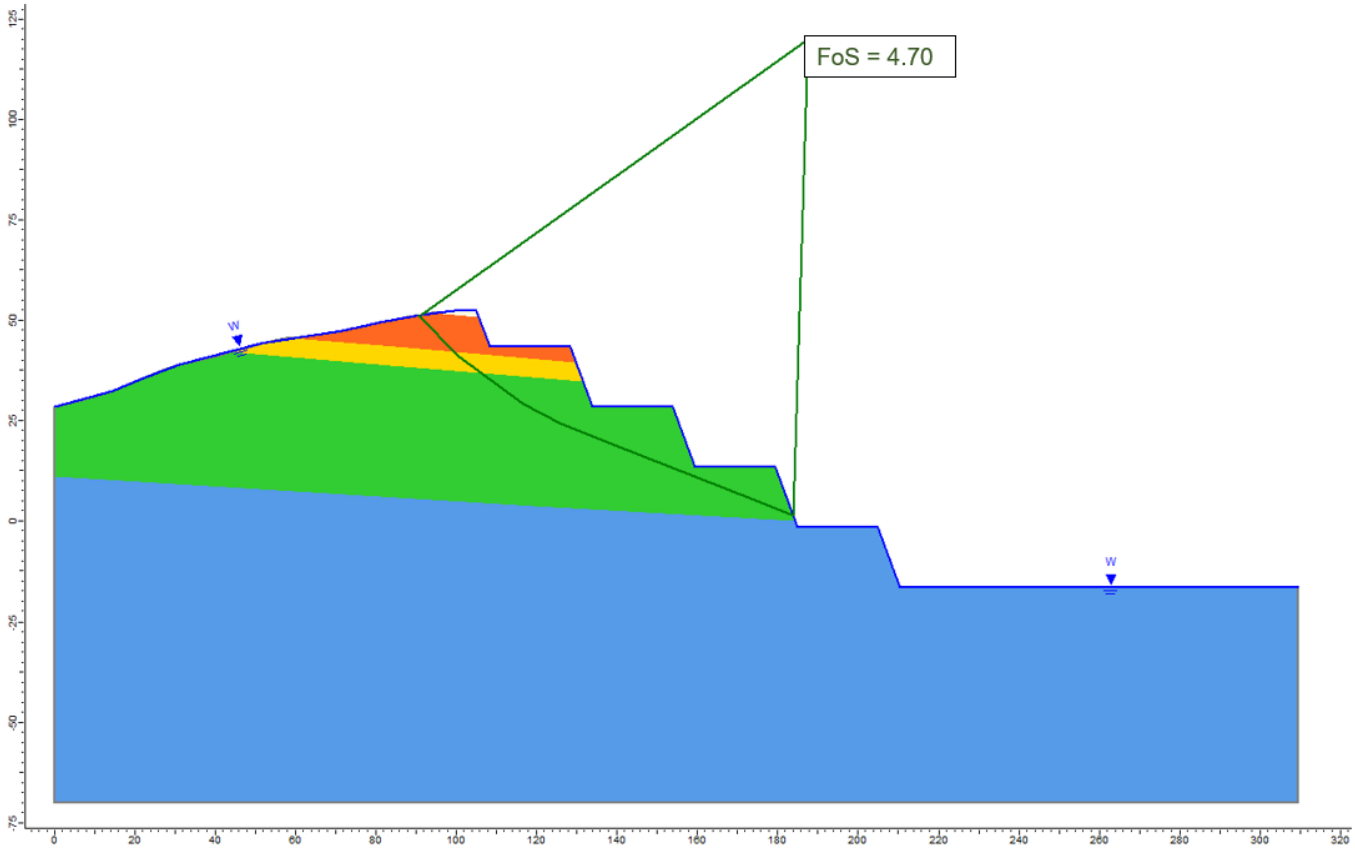

Figure 5.19 Sensitivity Model Output - Elevated Phreatic Conditions – Section S3

5.5.3 Influence of Final Pit Lake Level

It is expected that once mining and active de-watering of the site ceases, groundwater will recover to the pre-mining water level. Outcomes of groundwater monitoring (see Section 2.3) indicate pre-mining groundwater levels in the order of +26 m AHD.

The final pit lake level is expected to vary over time due to seasonal cycles, for example, the pit lake level is expected to be lower in summer periods where evaporation is higher, and rainfall is lower. Accordingly, sensitivity analyses were performed to assess the influence of the final pit lake level on the stability performance of the assessed slopes.

The results of the final pit lake sensitivity analyses are summarised in Table 5.8 and the corresponding stability model outputs are presented in Figure 5.20 to Figure 5.22.

Table 5.8 Summary of Sensitivity Analyses Results- Influence of Final Pit Lake Level

Stability Section	DAC	Final Pit Lake Level	Scale of Instability	Calculated FoS
S1	FoS > 2.0	RL +26	Overall Slope	3.88
S2		RL +26	Overall Slope	4.98
S3		RL +26	Overall Slope	6.08

The results of the sensitivity analyses to assess the influence of the final pit lake on the stability performance of rehabilitated slopes indicate that:

– The stability performance of rehabilitated slopes along Sections S1, S2 and S3 were calculated to satisfy the Design Acceptance Criteria for the “Serious Consequence of Failure” for the overall slope scale, with a FoS greater than 3.0 calculated for all assessed sections.

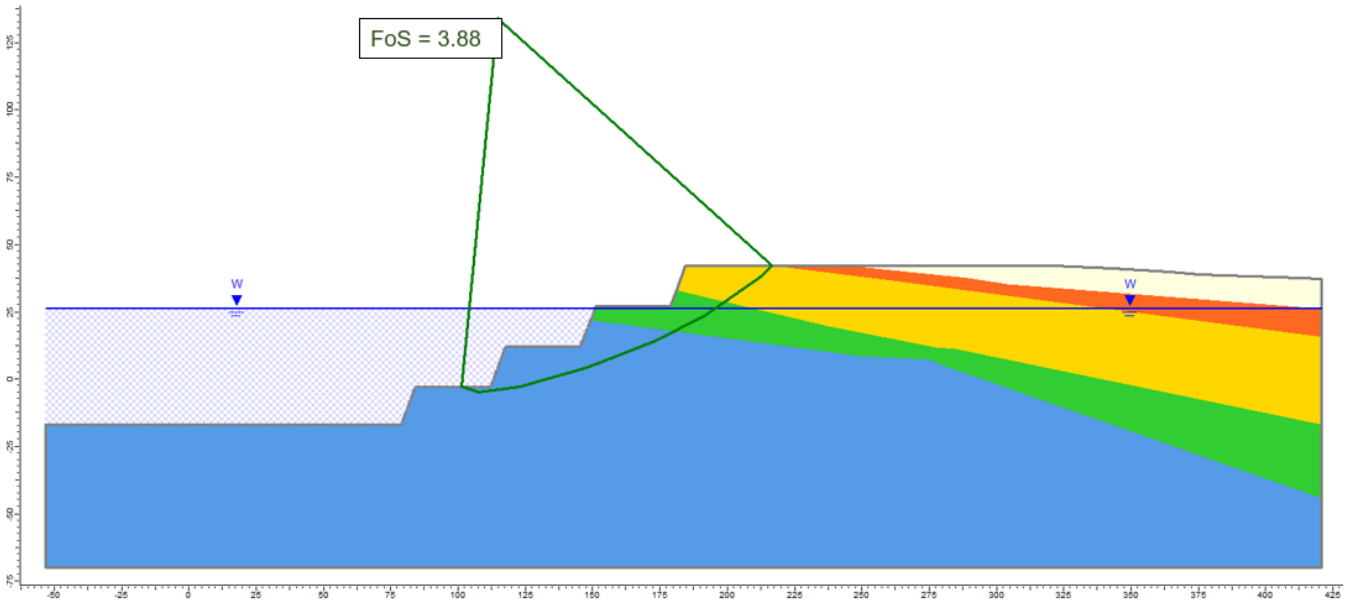

Figure 5.20 Sensitivity Model Output - Pit Lake Level (RL +26m) – Section S1

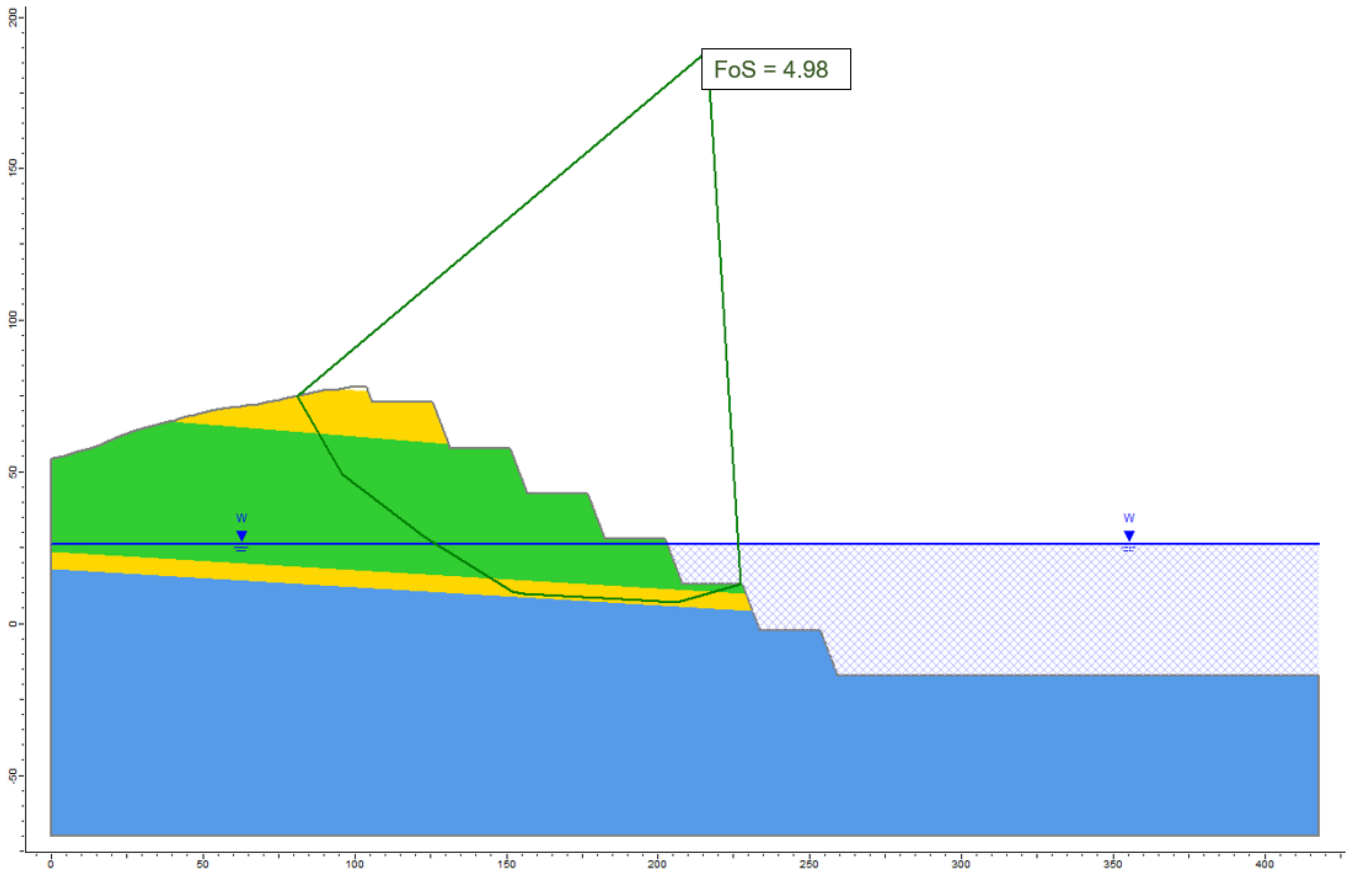

Figure 5.21 Sensitivity Model Output - Pit Lake Level (RL +26m) – Section S2

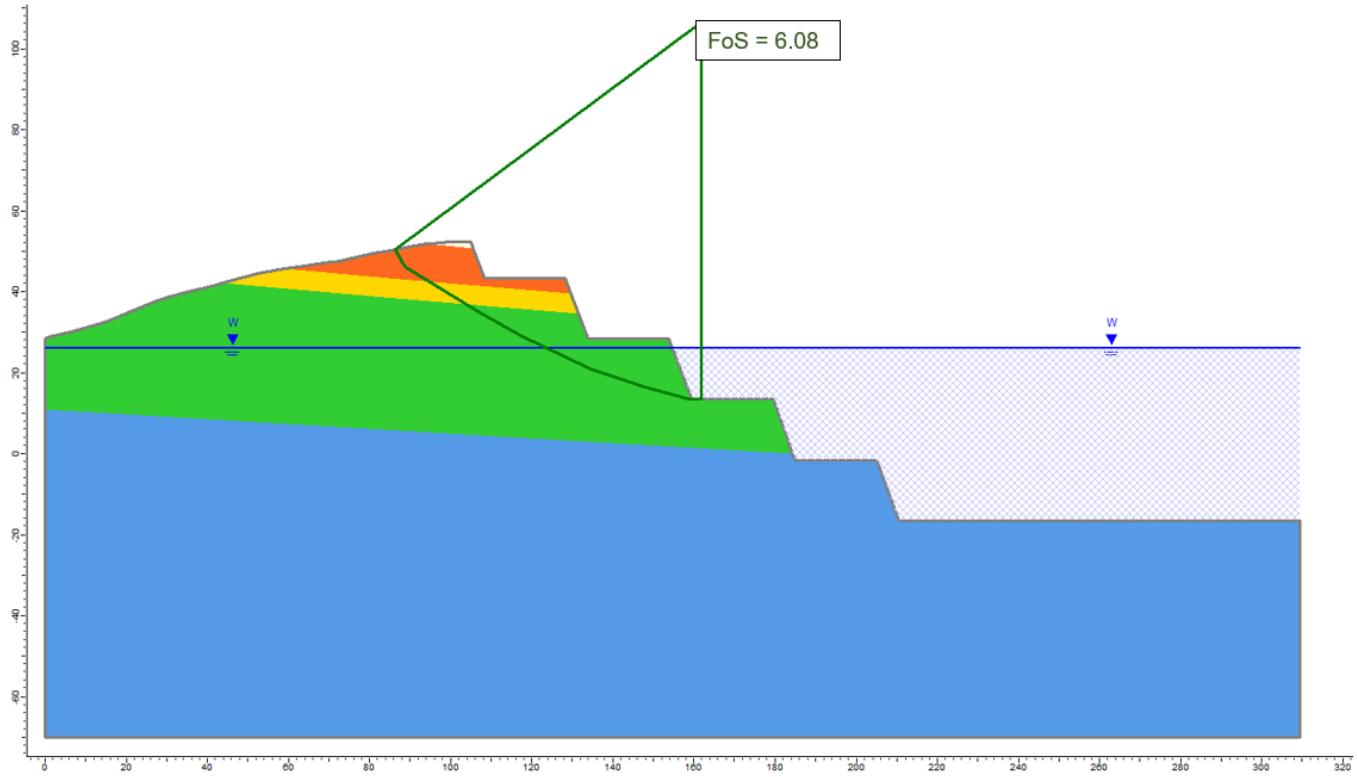

Figure 5.22 Sensitivity Model Output - Pit Lake Level (RL +26m) – Section S3

5.6 Discussion of Stability Analyses Results

The results of the stability modelling indicate the following:

5.6.1 Kinematic Analyses

Planar Sliding

- Under expected conditions, north, east and south walls (i.e., excavations within the northern, eastern and southern domains), are comparatively more sensitive to planar sliding than the western wall.
- The minimum calculated bench width with respect to critical sets and weathering grade was calculated (to the nearest metre) to be 16 m.
- In general, the FoS increases and the PoF decreases where the degree of weathering decreases.
- The volume of instability was calculated to be of limited scale/volume, with larger volumes calculated along the east wall.

Tetrahedral Wedge Sliding

- Under expected conditions, south and west walls were calculated to be comparatively more sensitive (PoF > 50%) to tetrahedral wedge sliding compared to other walls.
- The minimum calculated bench width with respect to critical sets and weathering grade was calculated (to the nearest metre) to be 13 m.
- In general, the FoS increases and the PoF decreases where the degree of weathering decreases.
- The volume of instability was calculated to be of limited scale/volume where good blasting and scaling practices are employed.

Rock Toppling

– Where the spacing of toppling joints occurs in the range of 0.8 m to 0.85 m or less, the likelihood of toppling becomes notably higher as the calculated FoS falls below 1.2 for all stratigraphic units.

In summary, the outcomes of the kinematic analyses indicates that a minimum bench width of 16 m is required to ensure there is adequate catch capacity to retain potentially dislodged material to a single bench. As outlined in Section 3, the proposed Stone Ridge Quarry pit design incorporates 20 to 30 m wide benches at the individual bench scale, which satisfies the minimum bench width requirements.

5.6.2 Slope Stability Analyses

Overall Slope Stability

– Under 'expected' conditions:
  - The stability performance at individual batters and overall slope scales satisfy the nominated DAC for stability Sections S1, S2 and S3 .

Seismic Loading

– Under a 1:500 year seismic loading event, the stability performance was calculated to satisfy the design performance objectives.The results of the seismic loading sensitivity analyses highlight the robustness of the design geometery against increased loading conditions.

Elevated Phreatic Conditions

– A reduction in the slope stability performance was calculated under 'worst case' fully saturated conditions compared to 'expected' condtions.
  - At the overall slope scale the stability performance was calculated to be above unity (FoS > 1) for all stability sections.
  - The results of the elevated phreatic condition sensitivity analyses highlight the importance of implementing and maintaining adequate surface and groundwater management protocols which are intergrated into the final landform design.

Influence of Final Pit Lake Level

– The stability performance of rehabilitated slopes, incorporating a recovered pit lake, along Sections S1, S2 and S3 were calculated to satisfy the Design Acceptance Criteria associated to the "Serious Consequence of Failure" category when considering the overall slope scale.

6. Erosion Assessment

The Revised Universal Soil Loss Equation (RUSLE) equation is a tool used to estimate the potential soil loss due to direct rainfall on an exposed slope and can provide an indication of the general erosion risk of the surface. It is also useful for quantifying the impact of various factors that contribute to erosion when designing batters, under long term conditions. In addition to the above, the area of disturbed land as a result of quarrying activities has been considered.

It is important to note that RUSLE only accounts for soil loss due to direct rainfall on the slope, not concentrated flow from any catchments flowing onto the slope.

6.1.1 Scenarios analysed

The erosion potential of the final landform slopes at the Stone Ridge site has considered the following scenario.

– Erosion of susceptible materials of exposed batters under dry void conditions

With respect to erosion along the excavated slopes, it is assumed that only the 'diggable' units (Unit 1 and 2) are susceptible to erosion and therefore are the only stratigraphic units considered in this assessment. Based on the stratigraphic and geological model, the exposure of Unit 1 (Overburden) is likely to very low with observed thicknesses up to 6 m, and the exposure of Unit 2 (HW) is typically in the order of 5 m, except for in certain areas, where unit thicknesses may increase up to 11 m (i.e, Northern walls).

6.2 Nominated Erosion Potential Criteria

Two conventionally applied erodibility potential criterions have been adopted for this assessment. These design acceptance criterions, as suggested by the Commonwealth of Australia (2016) and by Morse and Rosewell (1996) and Landcom (2004) were adopted to assess the potential volume of soil loss at a site against tolerance levels. In the following subsections, each criterion is discussed in further detail.

Criterion 1

Based on the Erosion Hazard Guidelines (after Morse and Rosewell (1996) and Landcom (2004)), which are summarised in Table 6.1.

Table 6.1 Soil Loss Classes after Morse and Rosewell (1996) and Landcom (2004

Soil loss class	Calculated soil loss (t/ha/yr)	Erosion hazard
1	0 to 150	Very Low
2	151 to 225	Low
3	226 to 350	Low-moderate
4	351 to 550	Moderate
5	501 to 750	High
6	751 to 1500	Very High
7	> 1500	Extremely High

Criterion 2

Criterion 2 is based on the tolerable soil loss tolerances which are cited in 'Mine Rehabilitation, Leading Practice Sustainable Development Program for the Mining Industry' (Commonwealth of Australia, 2016). This design acceptance criteria indicates that the soil loss should not exceed 4.5 tonnes per hectare per year (i.e., 4.5 t/ha/yr).

6.3 Potential Erodibility of Terminal Slopes

The RUSLE equation calculates an annual erosion rate based on the multiplication of five factors, and is expressed as:

$$\boldsymbol{A = R \cdot K \cdot LS \cdot C \cdot P}$$

Where:

A = Estimated average soil loss in tonnes per acre per year

R = Rainfall erosivity factor

K = Soil erodibility factor

LS = Topographic factor that accounts for slope length and slope gradient

C = Erosion practice control

P = Ground cover factor

The above RUSLE factors are outlined in further detail in the following subsections.

6.3.1 Rainfall erosivity factor 'R'

This factor is determined by the intensity of rainfall in the area and is therefore not a design parameter. Using the aforementioned principal, empirical relationships have been established to correlate mean annual precipitation with the Rainfall Erosivity Factor (R). Yu and Roswell (1996) established a relationship to estimate the R-factor based on studies conducted in south-eastern Australia. The relationship had a very good correlation with R^2 = 0.91. The R-Factor and mean annual relationship is expressed as:

$$R = 0.0438 \cdot P^{1.61}$$

Where: P = Mean annual precipitation (mm)

Mean annual precipitation for the proposed Stone Ridge Quarry site were obtained from the Bureau of Meteorology (2022) for the nearby weather station located approximately 8 km away at Clarence Town (Prince St) (station number 061010). The mean annual precipitation for the area is 1067.9 mm, calculated using approximately 128 years of rainfall data. The calculated R-factor is equal to 3291.61.

6.3.2 Soil erodibility factor (K)

The soil erodibility factor (K) accounts for the erodibility of the soil based on its composition (e.g., clay). Nomograph equations (and visual representations) are frequently relied upon for deriving suitable K-factors, which is a simple method that makes use of basic soil properties (e.g., particle size distributions). According to the CSIRO publication after Yang et al. (2017) most of the models used to determine K-factors (e.g., Wishmeier *et al*., 1971) have been developed for American soils and may not be representative of Australian soils. According to Yang et al. (2017) the nomograph developed by Rosewell (1993) referred to as 'K_SOILOSS' yielded comparative results to field measurements and is a preferred method for deriving a suitable K-factor for Australian soils, which contain less than 68% silt content).

The K_SOILOSS nomograph equation is expressed as:

$$K_{SOILOSS} = \left(2.77 \cdot M^{1.14} \cdot 10^{-7} \cdot (12 - OM)\right) + \left(4.28 \cdot 10^{-3} \cdot (SS - 2)\right) + ((3.29 \cdot 10^{-3} \cdot (PP - 3))$$

Where:

M = Particle Size Parameter = (%Silt + %Very Fine Sand) x (100 – %Clay)

OM = Organic Matter (%)

SS = Soil Structure (ranging from; 1-very fine granular; 2-fine granular; 3-medium to coarse grained; and 4-blocky, platy or massive.

PP = Soil Permeability (ranging from; 1-rapid; 2- moderate to rapid; 3-moderate; 4-slow to moderate; 5-slow; and 6-very slow).

Available soil data required for the input into the above nomograph equation was obtained from the publicly available Soil and Landscape Grid of Australia (SGLA, 2017) database. This data access platform enables the user to query soil data based on the site location with a 95% confidence interval and provides the necessary information to estimate a K-factor. Summarised in Table 6.2 are the adopted overburden soil index parameters obtained from SGLA (2017) utilised to calculate the particle size parameter 'M'.

Table 6.2 Summary of Soil Properties (after SGLA, 2017)

%Sand (0.05-0.1 mm)	%Silt (0.002-0.05 mm)	%Clay (< 0.002 mm)	M – Particle size Parameter
15	15	70	900

Summarised in Table 6.3 are the parameters obtained from SGLA (2017) used to calculate the K-Factor for the Stone Ridge Quarry site.

Table 6.3 Summary of K-Factor Parameters after Rosewell (1933)

M	% Organic matter (OM)	Soil structure (SS)	Permeability (PP)	K-factor (Rosewell, 1993)
900	0.5	2 Fine Granular	4 Slow to Moderate	0.0012

Based on the above, a K-factor of 0.0012 has been adopted for this assessment.

6.3.3 Topographic Factor (LS)

The topographic factor (LS) accounts for a slopes height (L) and gradient (S) and is used to represent the effect of topography on erosion rates. The equations for calculating the LS in RUSLE are:

$$LS = L \cdot S$$

$$L = \left(\frac{\lambda}{22.13}\right)^{m}$$

$$m = \frac{\beta}{(1+\beta)}$$

$$\beta = \frac{\sin(\theta)}{[3 \cdot \sin(\theta)^{0.8} + 0.56]}$$

$$S = 16.8 \cdot \sin(\theta) - 0.5 \; ; \quad \theta \geq 9\%$$

Where:

λ= Slope length (m)

m = Variable length-slope component

β = Variable slope gradient component

θ = Slope angle

The calculated topographic factors for the excavated slopes and overburden emplacement areas are summarised in Table 6.4.

Table 6.4 Summary of Topographic Factor Parameters

Geometry	Slope angle (°) - θ	Maximum slope height (m) - L	Topographic factor - LS
Excavated slope (Units 1 and 2)	~70	15	15.00

It should be noted that for this assessment, the rock slope is considered to be a continuous slope and does not consider the potential slope flattening associated with intermediated benches.

6.3.4 Erosion control factor (C)

The erosion control factor (C) is used to measure the effect of vegetation and management practices on erosion rates. This includes the effects of vegetation, soil cover, soil biomass and soil disturbing activities. Typical cover factors are presented in Table 6.5.

Table 6.5 Summary of Typical C-factors

Treatment	Time after application (months)	Assumed grass coverage (%)	C-factor after Landcom (2004)	C-factor after Sprague, (1999)
Untreated	Undefined	0	1.0	1.0
Topsoiled and vegetated	0	0	1.0	0.7
	1 – 3	15	0.55	0.1
	3 – 6	30	0.32	
	6 - 12	45	0.18	0.05
	12 – 18	60	0.1	0.01
	18 – 24	75	0.05	0.01
	> 24	80	0.03	0.01

It is anticipated that rehabilitation of excavated batters and the rock slope will include the application of topsoil and perennial grasses. Accordingly, a temporal overlay to soil erosion has been added, which reflects a reduction in the erosion potential commensurate with increased grass coverage. It should be noted that the correlated C-factors presents a conservative approach to reducing soil erosion over time, (i.e., C-factor reductions may be quicker than those tabulated). It is also assumed that the ongoing and active maintenance is employed until grass covers reach the desired level and have become ‘fully’ established (i.e., can maintain grass coverage without active maintenance).

6.3.5 Ground Cover Factor (P)

The erosion control practice factor (P) measures the effect of practices that reduce flow velocity and tendency for water to flow directly downhill (e.g., track-walking or punching straw into the ground). Table 6.6 presents a summary of typical erosion control practices and the respective P-factor.

Table 6.6 Ground Cover Factor Scenarios

Surface condition	Erosion control practice factor, P
Compacted and Smooth	1.3
Track-walked along contour	1.2
Track-walked up and down the slope	0.9
Punched Straw	0.9
Sacrificial Layer (Loose to 0.3 m in depth)	0.8

Typical 'C' and 'P' factors presented in Table 6.5 and Table 6.6 have been adopted from various sources, including Meyer and Ports (1976), Israelson *et al*. (1980), Goldman *et al.* (1980), URS Greiner Woodward Clyde (1999), the North American Green website (2020) and Sprague (1999).

6.4 Results and discussion

The results of the erodibility potential analyses are based on the assumptions outlined above for the respective input factors. The results are summarised in Table 6.7 and presented graphically in Figure 6.1.

Table 6.7 Summary of Erosion Potential Analyses Results

Scenario	Calculated erosion loss (t/ha/yr)	Erosion criteria	
		Criterion 1	Criterion 2
Excavated slopes	1.12	Very Low (0 to 150 t/ha/yr)	Satisfies the Commonwealth (2016) Guidelines

The results of the analyses indicate that:

– The erosion potential of the excavated batters is considered 'Very Low' (< 150 t/ha/yr- Criterion 1) and satisfies the Commonwealth (2016) guidelines (Criterion 2) after ~20 months of perennial grass coverage.

– The susceptibility to erosion within these units is largely controlled by the topographic factor and ability to apply cover. Erosion in these areas is expected to be ongoing which is likely to result in some minor sloughing of the excavated face. It is anticipated that in the long-term, erosion of these faces would not pose a significant geotechnical risk.

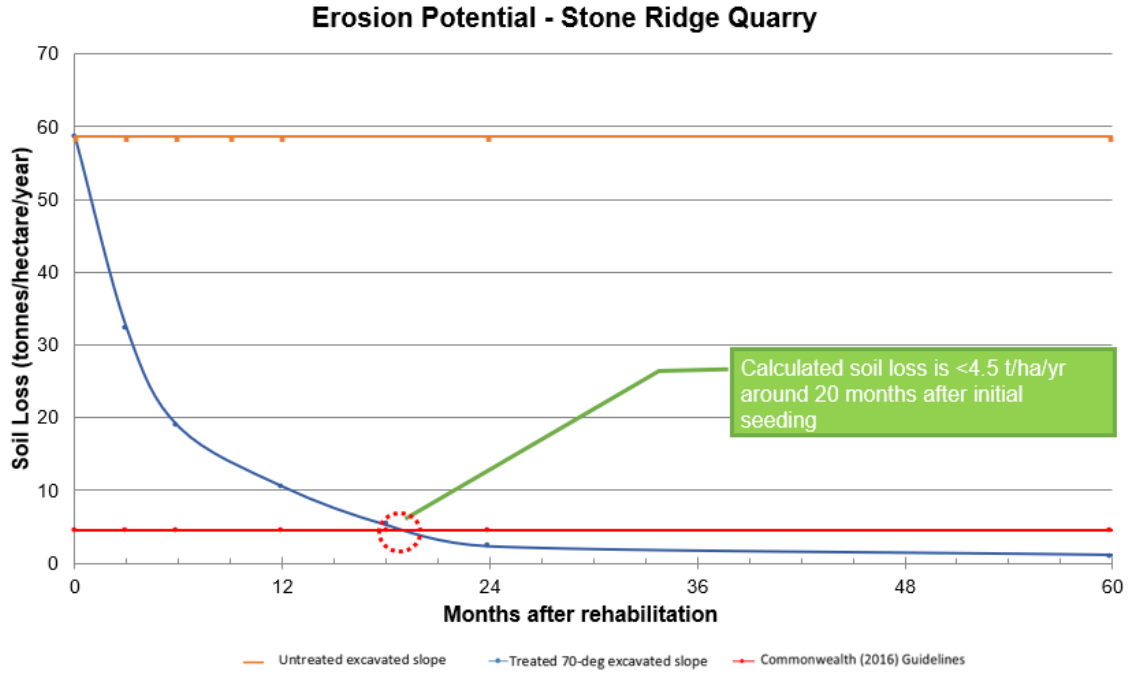

Figure 6.1 Calculated Rate of Soil Loss – Stone Ridge Quarry

7. Conclusions

The results of the stability modelling indicate that:

7.1 Kinematic Analyses

Planar Sliding

– Under expected conditions, north, east and south walls i.e., excavations within the northern, eastern and southern domain, are comparatively more sensitive to planar sliding than the western wall.
– The minimum calculated bench width with respect to critical sets and weathering grade was calculated (to the nearest metre) to be 16 m.
– In general, the FoS increases and the PoF decreases where the degree of weathering decreases.
– Note that potentially larger volumes are calculated along the east wall.

Tetrahedral Wedge Sliding

– Under expected conditions, south and west walls were calculated to be comparatively more sensitive (PoF > 50%) to tetrahedral wedge sliding compared to other walls.
– The minimum calculated bench width with respect to critical sets and weathering grade was calculated (to the nearest metre) to be 13 m.
– In general, the FoS increases and the PoF decreases where the degree of weathering decreases.
– The volume of instability was calculated to be of limited scale/volume where good blasting and scaling practices are employed.

Rock Toppling

– Where the spacing of toppling joints occurs in the range of 0.8 m to 0.85 m or less, the likelihood of toppling becomes notably higher as the calculated FoS falls below 1.2 for all stratigraphic units.

A minimum bench width of 16 m is required to ensure there is adequate catch capacity to retain potentially dislodged material to a single bench. The proposed Stone Ridge Quarry pit design incorporates 20 to 30 m benches at the individual bench scale, which satisfies the minimum bench width requirements.

7.2 Slope Stability Analyses

Overall Slope Stability

– Under ‘expected’ conditions The stability performance at individual batters and overall slope scales satisfy the nominated DAC for stability Sections S1, S2 and S3 .

Seismic Loading

– Under a 1:500 year seismic loading event, the stability performance was calculated to satisfy the design performance objectives.

Elevated Phreatic Conditions

– A reduction in the slope stability performance was calculated under ‘worst case’ fully saturated conditions compared to ‘expected’ condtions.
    - At the overall slope scale the stability performance was calculated to be above unity (FoS > 1) for all stability sections.

Influence of Final Pit Lake Level

– The stability performance of rehabilitated slopes, incorporating a recovered pit lake, along Sections S1, S2 and S3 were calculated to satisfy the Design Acceptance Criteria associated to the “Serious Consequence of Failure” category when considering the overall slope scale.

7.3 Potential Erodibility of Terminal Slopes

– The erosion potential of the excavated batters is considered 'Very Low' (< 150 t/ha/yr) and satisfies the Commonwealth (2016) guidelines after ~20 months of perennial grass coverage.
– The susceptibility to erosion within these units is largely controlled by the topographic factor and ability to apply cover. Erosion in these areas is expected to be ongoing which is likely to result in some minor sloughing of the excavated face. It is anticipated that in the long-term, erosion of these faces would not pose a significant geotechnical risk.

Under 'expected' conditions, the proposed slope design geometry (individual benches with 15 m height, bench widths of 20 to 30 m, nominal face angles of 70 degrees) is sufficient for maintaining stability performance at overall slope scale for the critical sections analysed. At individual batter scale, the proposed slope configuration is sufficient for catching and retaining potential dislodged material of structurally controlled deposits at Stone Ridge Quarry.

8. Recommendations

As part of subsequent stages of design, the following broad scope elements are recommended:

– When quarrying commences, regular site inspections should be undertaken to observe for signs of adverse geotechnical conditions. Furthermore, where site conditions are observed to deviate from those outlined in this report, additional intrusive investigation and / or defect mapping should be undertaken.
    - This may include core sampling of key stratigraphic units, and laboratory testing to confirm the geomechanical properties and strength parameters of the material.
    - Continue ongoing groundwater monitoring of the proposed site area.
– Where deemed required (i.e., notable deviation in site conditions compared to those outlined in this report) a full suite of stability analyses with the benefit of additional data obtained from the intrusive investigation and hydrological studies should be undertaken.

9. References

Legislation and Guidance Documents

Environmental Planning and Assessment Act 1979

Commonwealth of Australia (2016), '*Mine Rehabilitation*, *Leading Practice Sustainable Development Program for the Mining Industry*, Commonwealth of Australia 2016

NSW Resources Regulator. Guide – Health and Safety at Quarries. November 2018.

NSW Department of Planning and Environment. Indicative Secretary's Environmental Assessments Requirements. 2018.

Online Databases

Commonwealth of Australia (2020). Climate Data Online, Bureau of Meteorology, URL: **http://www.bom.gov.au/climate/data/index.shtml**, accessed on 3 October 2022

Soil and Landscape Grid of Australia (2017). Soil and Landscape Grid of Australia. Available at **http://www.clw.csiro.au/aclep/soilandlandscapegrid/index.html**, accessed on 8 September 2022

Relevant Site Documentation/Studies

Information provided by the Client Included:

- Maps for Local and Regional Geology. Figures and Plans for Stone Ridge Quarry Project
- Report on Quarry Resource Assessment Investigations for Stone Ridge Quarry Project January 2020
- Figures and Plans – Geophysics and Ground Magnetics for Stone Ridge Quarry Project
- Figures and Plans - Drilling for Stone Ridge Quarry Project. Including Collar File, Core Photographs, Downhole Data, Downhole Geophysics
- Site Layout Features and Quarry Design
- Groundwater and Surface Water monitoring Information
- Hunter District Water Board (1957). Report on Geology of Balickera Tunnel Site
- Rattigan (1966). The Balickera Section of the Carboniferous Kuttung Facies, New South Wales
- Pells Consulting (2015). Balickera Tunnel Remediation
- JBA (2017) Report titled "State Significant Development Application – Environmental Impact Statement – Eagleton Quarry – Barleigh Ranch Way"
- Australian Resource Development Group Pty Limited (2020). Proposed Stone Ridge Quarry Project – Scoping Report. Wallaroo State Forest No. 781

Published Literature

Erosion Control Technology Council or ECTC. (2003). Guidelines for rolled erosion control products, Erosion Control Technology Council, St. Paul, MN

Goldman, S.J., Jackson, K. and Bursztynsky, T.A. (1986). Erosion and Sediment Control Handbook. McGraw-Hill, New York

Goodman, R. E (1980) '*Introduction to Rock Mechanics'*, Wiley, New York, N.Y.

Hoek, E. (1994) '*Strength of Rock and Rock Masses*', ISRM News Journal

Hoek, E. & Brown, E.T. (2019). '*The Hoek-Brown Failure Criterion and GSI – 2018 Edition',* Journal of Rock Mechanics & Mining Science, Vol 11, Issue 3, pp 445-463

Israelson C.E., Clyde, C.G., Fletcher, J.E., Israelsen, E.K., Haws, F.W., Packer, P.E. and Farmer, E.E. (1980). *Erosion control during highway construction, Manual on Principles and practices*. National Cooperative Highway Research Program Report 221. Transportation Research Board, National Research Council, Washington, DC

ISRM, (1981). '*Rock Characterization Testing and Monitoring*', ISRM suggested method. Int. Soc. Rock Mech

Landcom, (2004). Soils and Construction: managing urban stormwater, Sydney

Mark. L., Burbidge, D. R., Edwards, M., 2013. Atlas of Seismic Hazard Maps of Australia: Seismic Hazard Maps and Hazard Spectra. *Record 2013/41:* Geoscience Australia: Canberra

Meyer, L.D. and Ports, M.A. (1976). "Prediction and Control of Urban Erosion and Sedimentation" in Proceedings from the National Symposium on Urban Hydrology, Hydraulics and Sediment Control – a mini-course held at the University of Kentucky, Lexington, Kentucky, 26-29 July 1976: 323-331

Mitchell J.K. and G.D. Bubenzer. (1980). *Soil loss estimation, soil erosion*. (M.J. Kirby and R.P.C. Morgan, Eds.) John Wiley and Sons, pp. 17-62

Morse, R.J and Rosewell, C.J. (1996). Use of the Universal Soil Loss Equation as a tool in the Management of Urban Lands, *Proceedings of the Annual International Erosion Association (Australasia) and Stormwater Industry Association Conference on Soil and Water Management for Urban Development*, 9 - 13th September 1996, Sydney

Rosewell, C.J. (1993a). Estimation of rainfall erosivity. *Erosion Research Newsletter No. 11*. Department of Infrastructure Planning and Natural Resources, Sydney

Rosewell, C.J. (1993b). "SOILOSS-A program to assist in the selection of management practices to reduce erosion" (Second Edition). *Technical Handbook No. 11*. Department of Infrastructure Planning and Natural Resources, Sydney

Rosewell CJ, Loch RJ (2002). Estimation of the RUSLE soil erodibility factor. In 'Soil physical measurement and interpretation for land evaluation'. (Eds N. McKenzie, K. Coughlan, H. Cresswell) pp. 361–369. (CSIRO Publishing: Melbourne, Vic.)

Soil Conservation Service or SCS. (1986). Urban hydrology for small watersheds, SCS, Technical Release 55, Soil Conservation Service, U.S. Dept. of Agriculture, Washington, D.C.

Sprague, C.J. 1999. Green engineering design principles and applications using rolled erosion control products. Civil Engineering News, March. p.8

Troeh, F.R., Hobbs, J.A. and Donahue. R.L. (1999). Soil and Water Conservation: Productivity and environment protection. New Jersey: Prentice-Hall

URS Greiner Woodward Clyde (1999). *Soil Stabilisation for Temporary Slopes*. Report prepared for State of California Business, Transportation and Housing Agency. Contract No. 43A0004C, Task Order No. 17

Wall GJ, Coote DR, Pringle EA, Shelton IJ (1997). RUSLEFAC–revised universal soil loss equation for application in Canada. Centre for land and biological resources research, research branch, agriculture and agri-food, Ottawa, Canada

Wischmeier W.H., Johnson, C.B., and Cross, B.V., (1971). 'A soil erodibility nomograph for farmland and constructions'. *Journal of Soil and Water Conservation*, 26, pp.189-193

Wischmeier, W.H. and Smith, D.D. (1978). '*Predicting Rainfall Erosion Losses – A Guide to Conservation Planning'*. United States Department of Agriculture, Agriculture Handbook No. 537. United States Government Printing Office, Washington, D.C.

Yang Xihua, Gray Jonathan, Chapman Greg, Zhu Qinggaozi, Tulau Mitch, McInnes-Clarke Sally (2017) 'Digital mapping of soil erodibility for water erosion in New South Wales, Australia'. *Soil Research* 56, 158-170

Yu, B. and Rosewell, C.J. (1996a). 'An assessment of a daily rainfall erosivity model for New South Wales'. *Australian Journal of Soil Research* 34: 139-152

Yu, B. and Rosewell, C.J. (1996b). 'Rainfall erosivity estimation using daily rainfall amounts for South Australia'. *Australian Journal of Soil Research*, 34: 721-733

ghd.com

→ The Power of Commitment